SuGAR MADISON 2024
SEARCHING FOR THE SOURCES OF GALACTIC COSMIC RAYS
OCTOBER 14-17

AMS-02 results and perspectives for future measurements with a magnetic spectrometer

Paolo Zuccon

Trento University & INFN TIFPA

UNIVERSITÀ DI TRENTO
TIFPA

AMS-02: Alpha Magnetic Spectrometer

Launch	MAY 2011
Construction	1999-2010
Dimensions	$3 \times 4 \times 5$ m³
Weight	8.5 t
Power	2500 W

AMS will take data at least through 2030

International Space Station

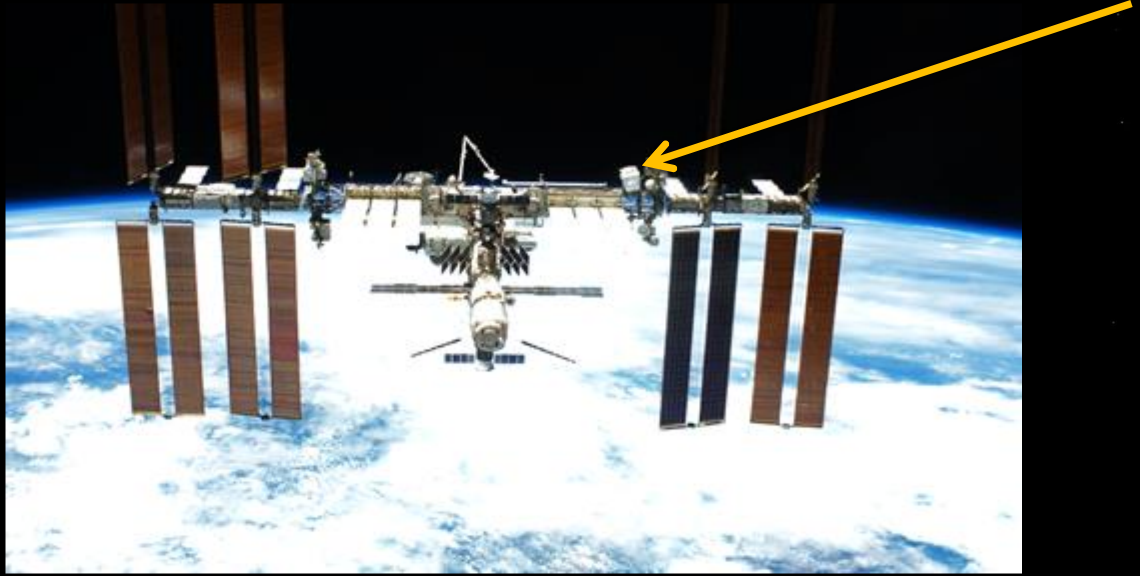

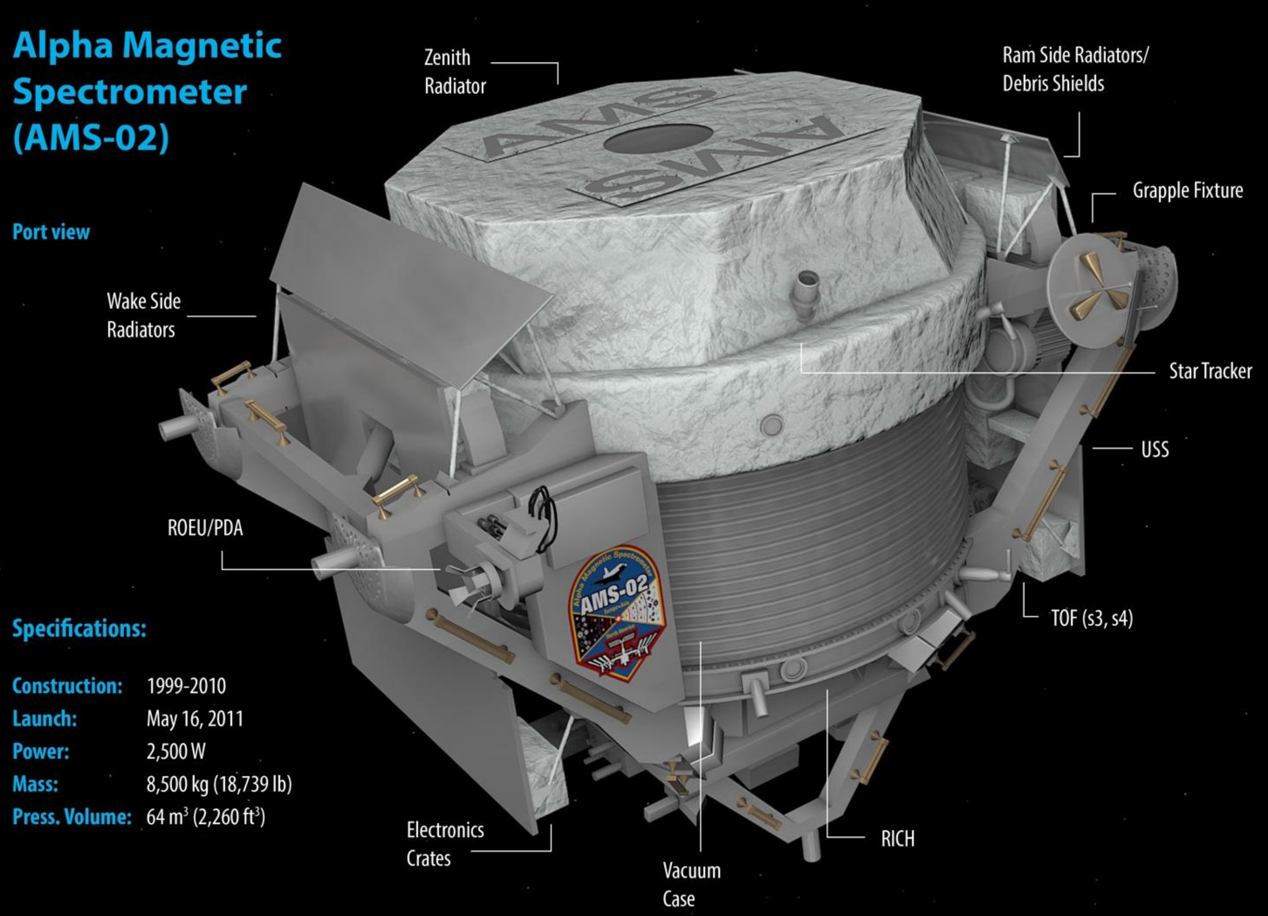

AMS-02 measures charged cosmic rays in the rigidity window from 1 GV to several TV

AMS: A TeV-Precision Spectrometer in Space

Particles and nuclei are defined by their charge (Z) and energy (E) or momentum (P). Rigidity R = P/Z

TRD: Identify e^+, e^-, Z

Silicon Tracker: Z, P

ECAL: E of e^+, e^-

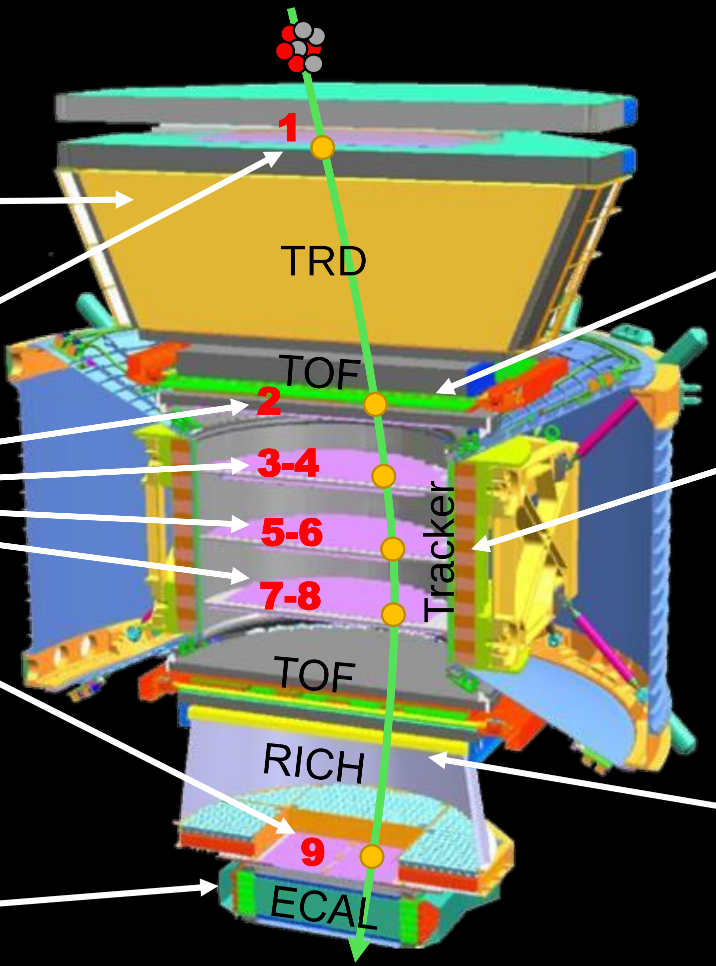

TOF: Z, E

Magnet: ±Z

RICH: Z, E

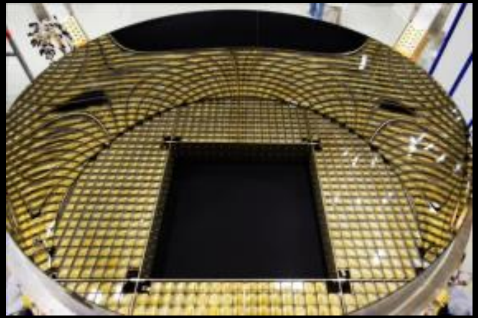

Z and P (or E)

are measured *independently* by the Tracker, RICH, TOF, and ECAL

AMS – Nuclei identification

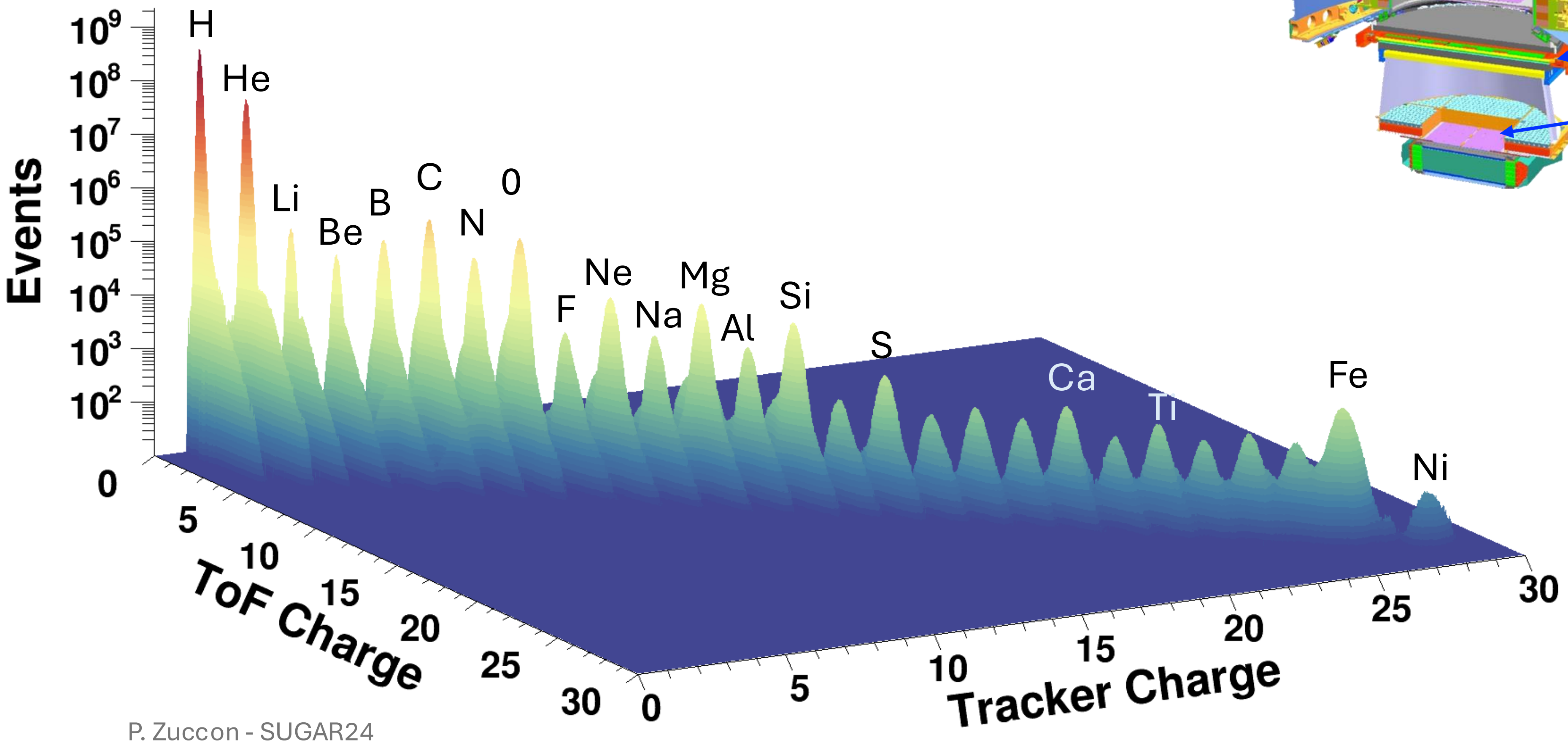

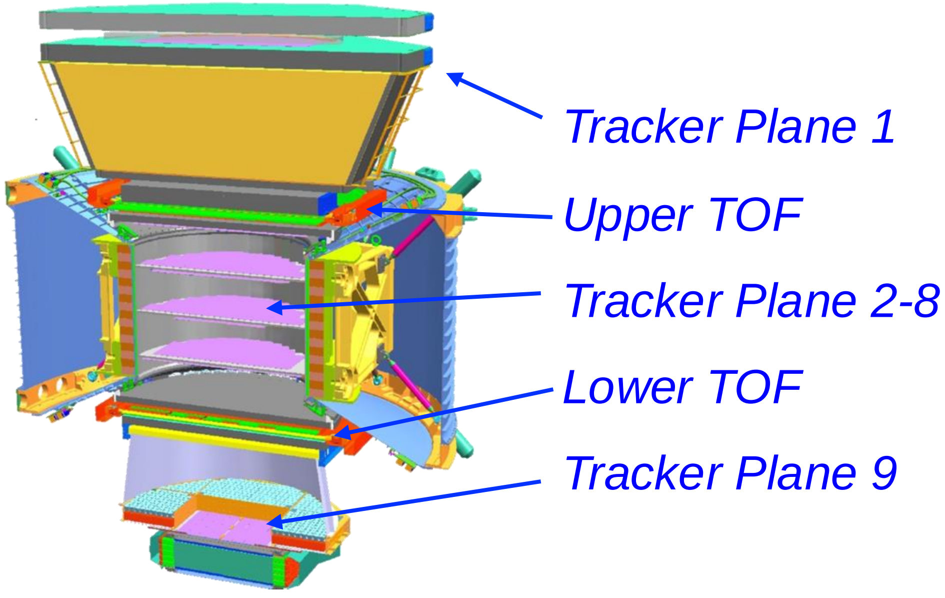

Primary Cosmic Rays

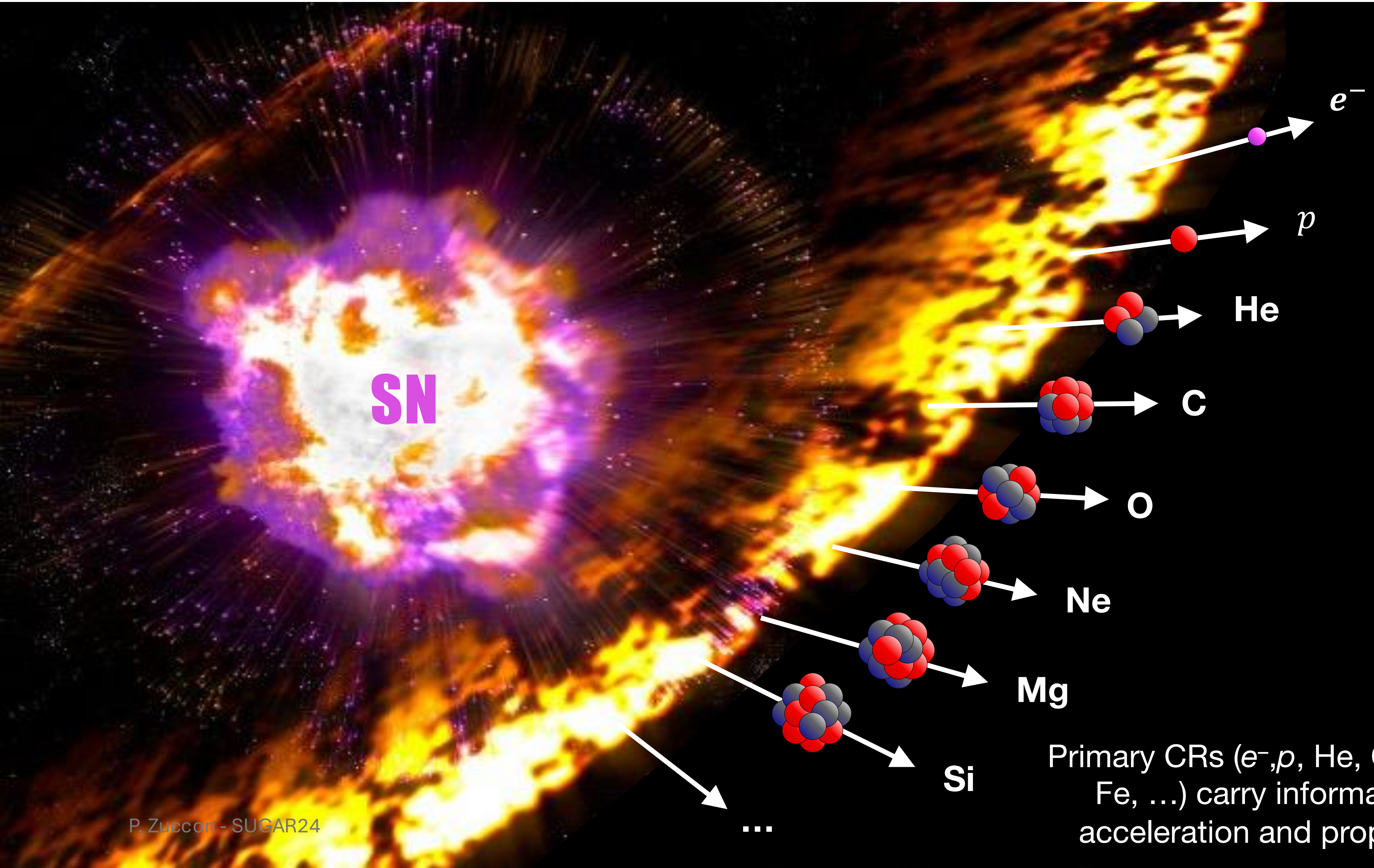

Primary CRs (e^-,p, He, C, O, Ne, Mg, Si, ..., Fe, ...) carry information about sources, acceleration and propagation processes.

Carbon and Oxygen Fluxes

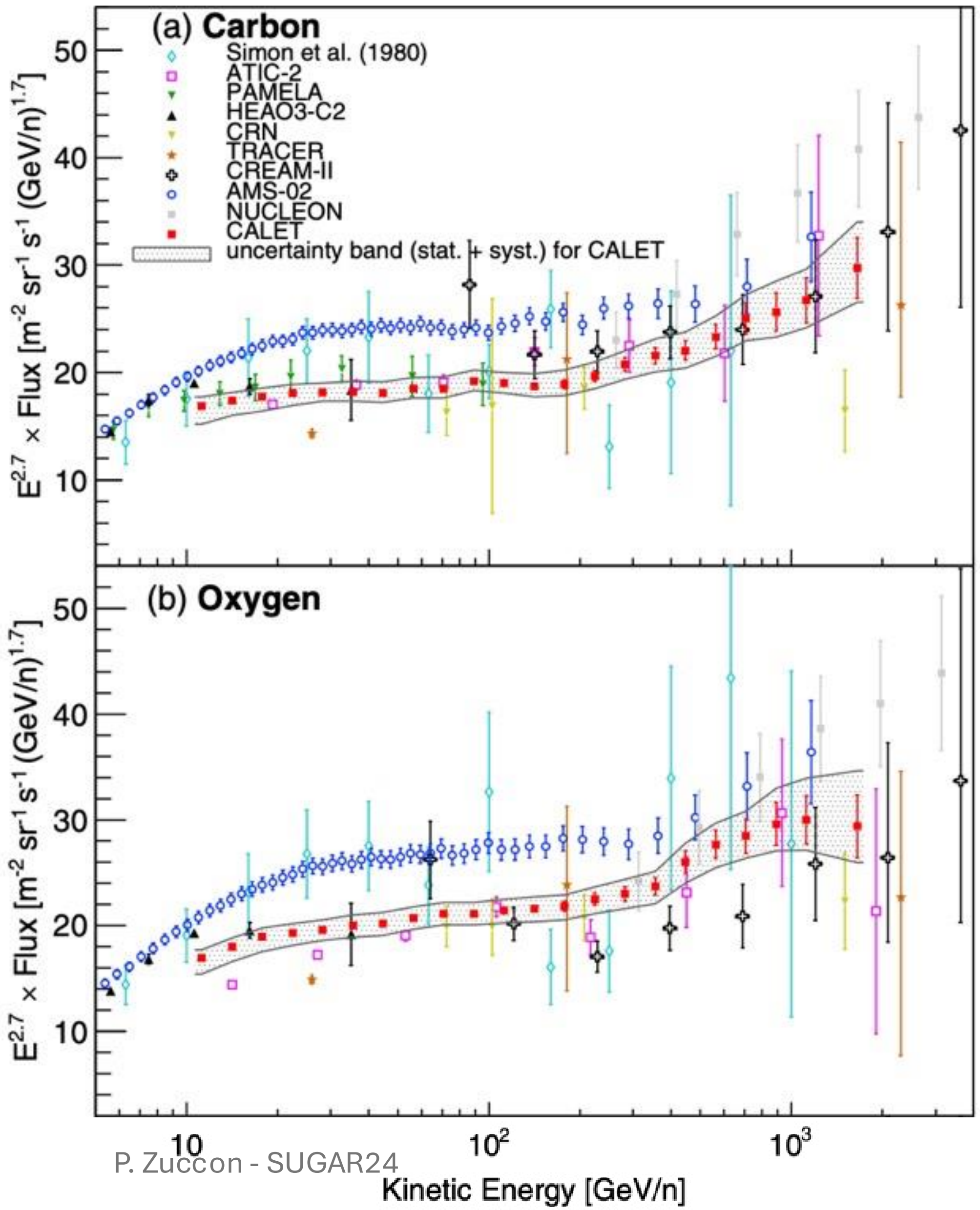

O. Adriani *et al.*, Phys. Rev. Lett. **125** (2020) 251102.

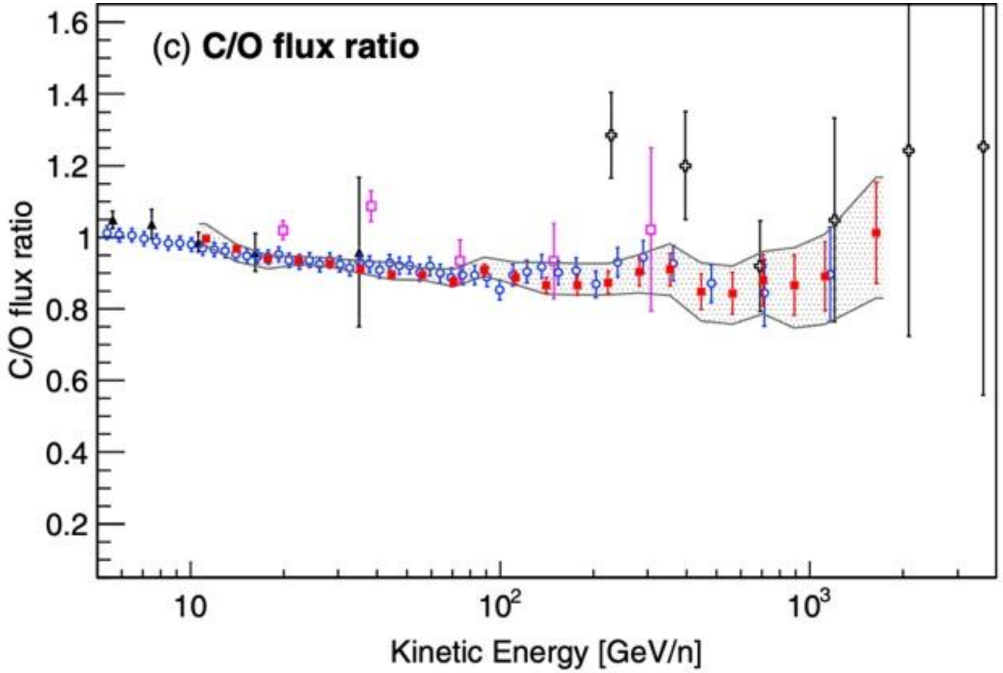

- C and O show a **hardening at hundreds of GeV/n**.
- **Similar energy dependence** observed by AMS-02 and CALET.
- **Difference in flux normalization** between experiments.
- C/O is smooth, meaning that **C and O have similar hardening.**
- All experiments agree in the C/O.

About Flux Normalization: the Nuclear Cross Sections

AMS has made nuclei Interaction cross-section measurements (N+C) in a wide rigidity range from a few GV to TV allowing for the precise control of the flux normalization.

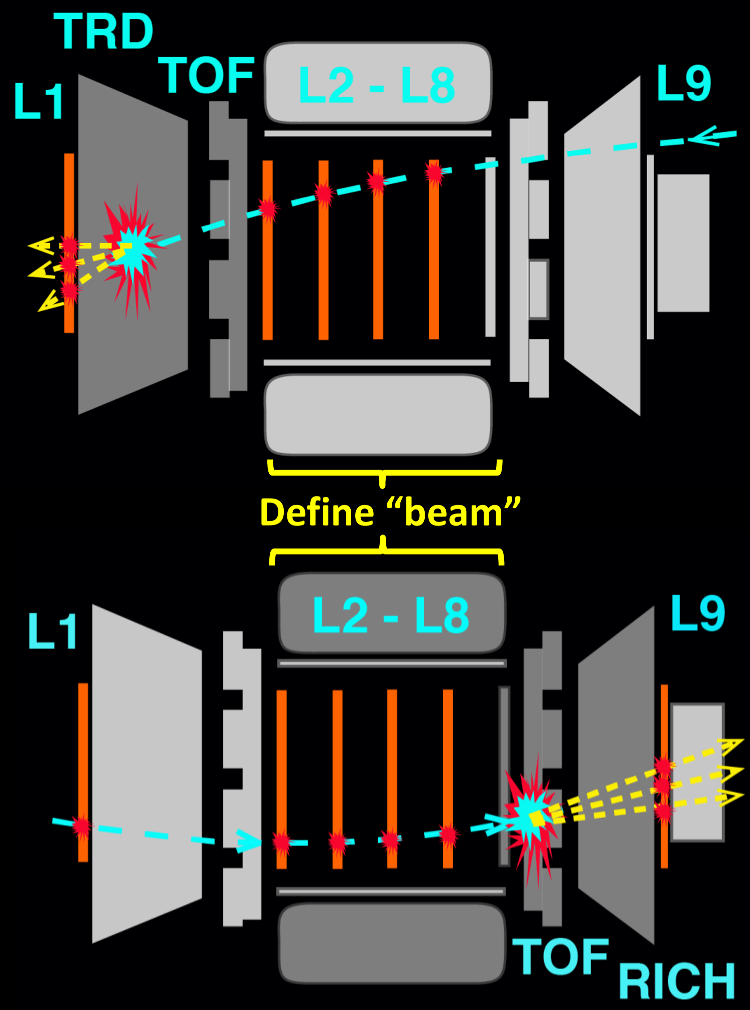

Q. Yan *et al.*, Nucl. Phys. A **996** (2020) 121712.

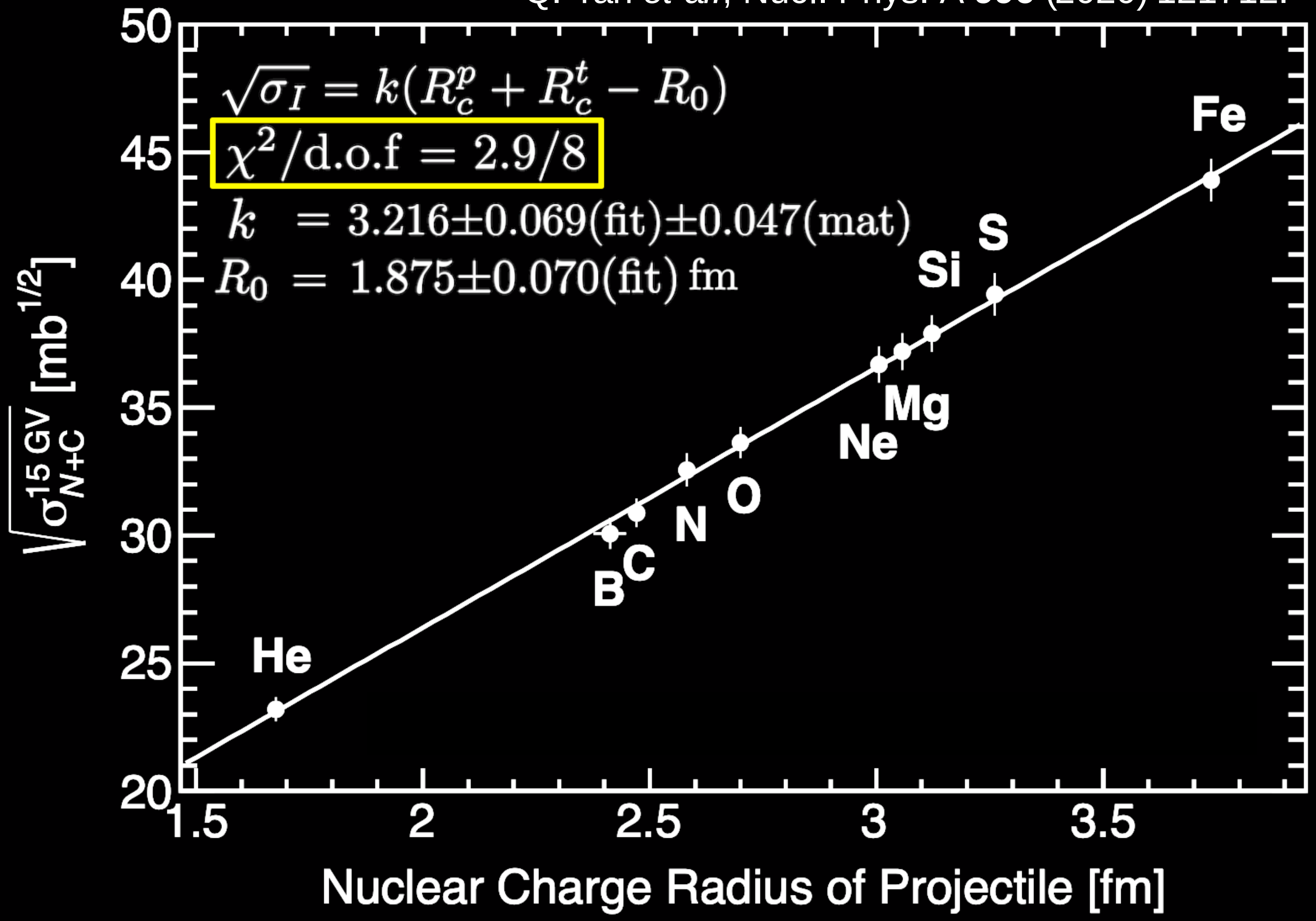

Nuclear inelastic interactions (nuclei over C, Al, Si) are in general **not well known**, and are important for accurate measurement of CRs and to understand the differences between different experimental measurements.

He, C, O, Ne, Mg, and Si

AMS studied with precision the spectral behavior of low-Z He (Z=2), C (Z=6), and O (Z=8) and high-Z Ne (Z=10), Mg (Z=12) and Si (Z=14) primaries.

M. Aguilar et al., Phys. Rep. **894** (2021) 1-116.

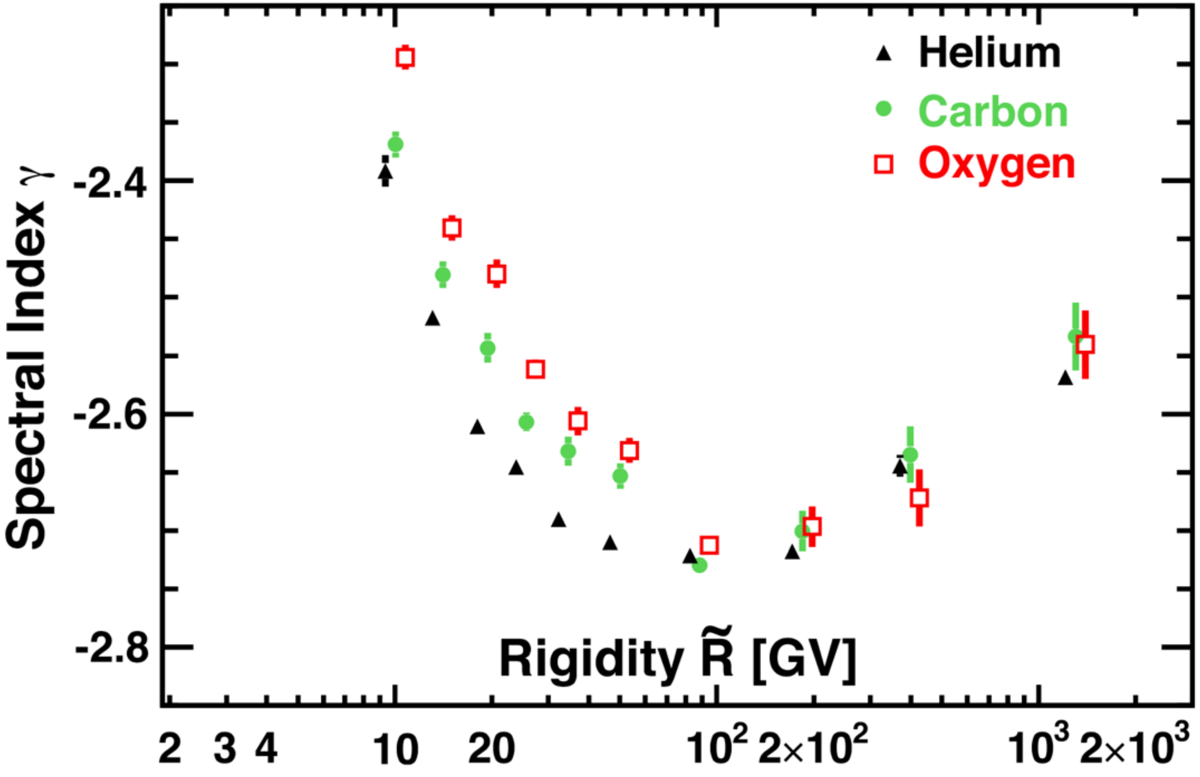

M. Aguilar *et al.*, Phys. Rev. Lett. **124** (2020) 211102.

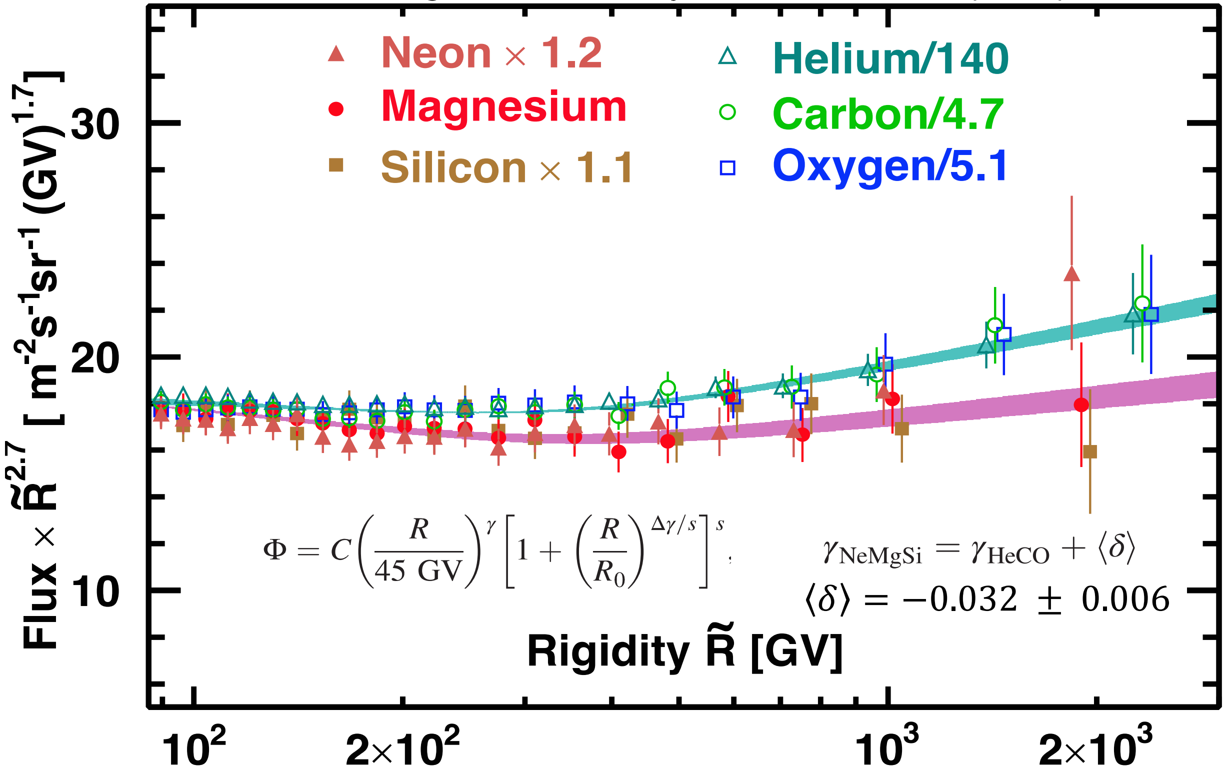

He, C, and O have the same rigidity dependence (i.e. hardening) above 60 GeV.
Above 86.5 GV the Ne, Mg and Si have a different spectral dependence with respect to He, C and O.

Iron and Nickel Fluxes and Their Ratio

O. Adriani *et al.*, Adv. Spa. Res., in press (2024).

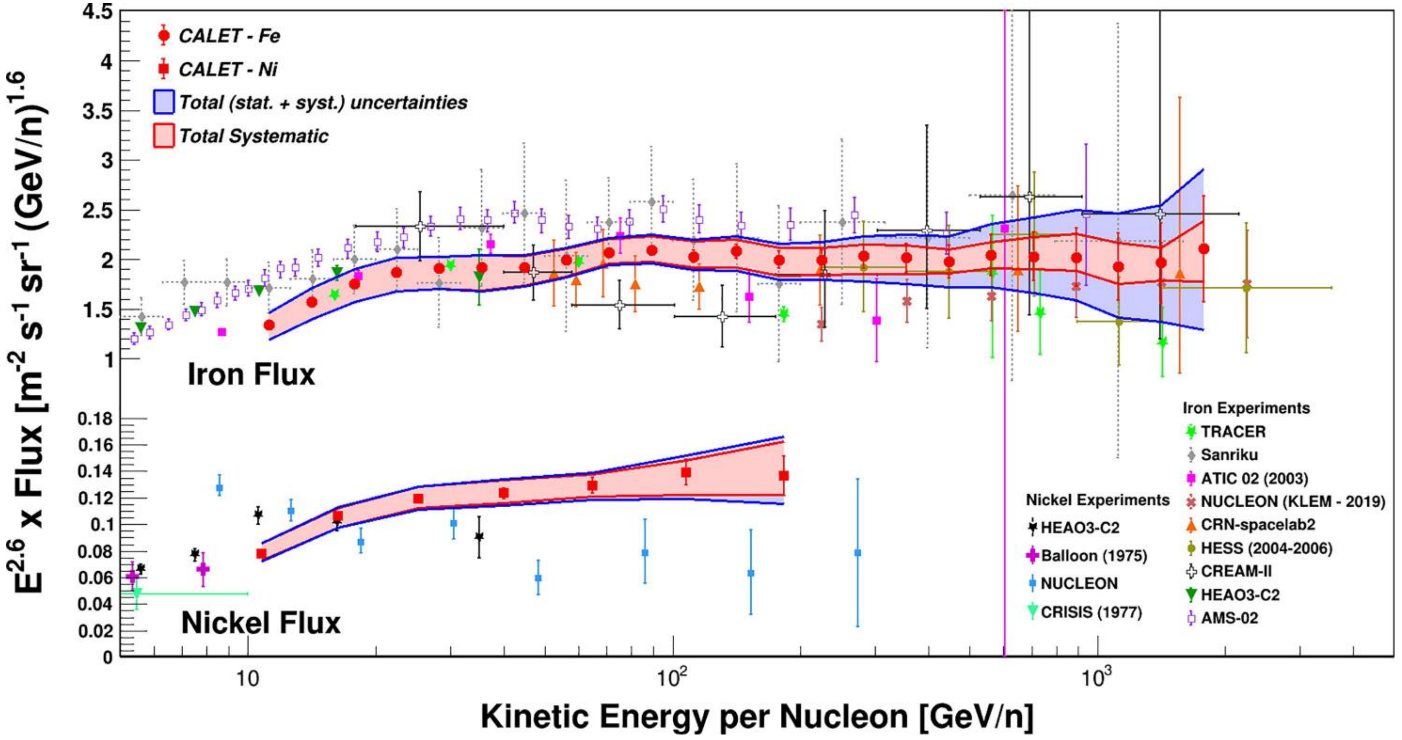

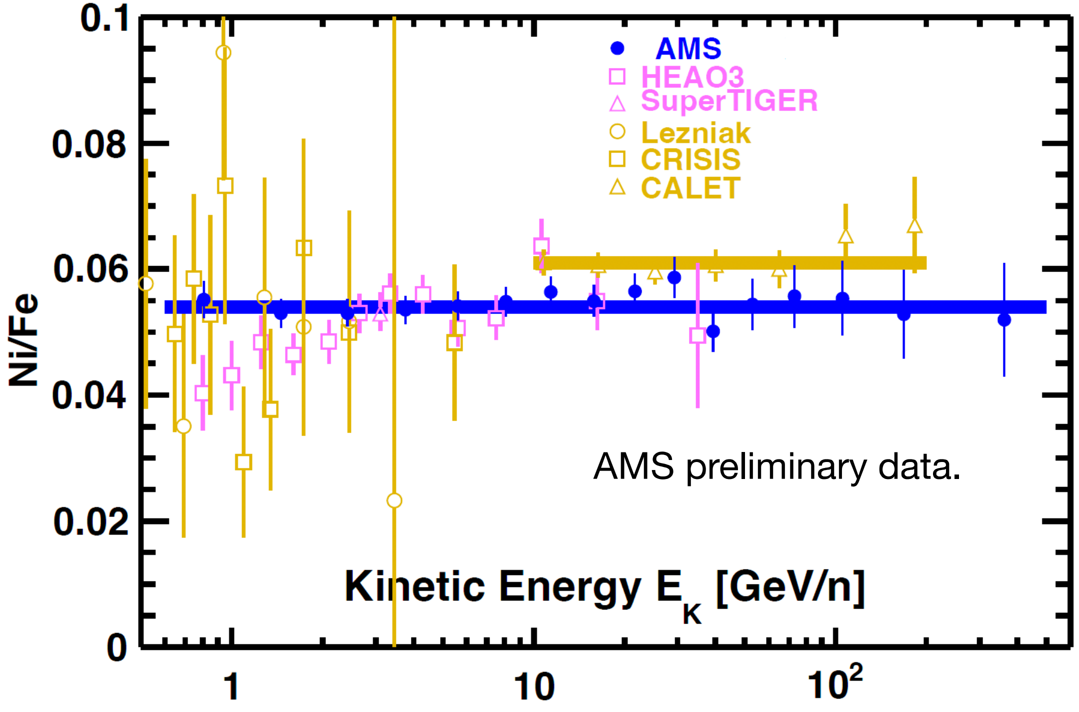

Similar energy dependence observed by recent AMS-02 and CALET data.
Some normalization difference between different experiments.

Secondary Cosmic Rays

While cosmic ray **primaries** are mostly produced at astrophysical sources (ex. e^-, p, He, C, O, …), **secondaries** (ex. Li, Be, B, …) are mostly produced by the collision of cosmic rays with the ISM.

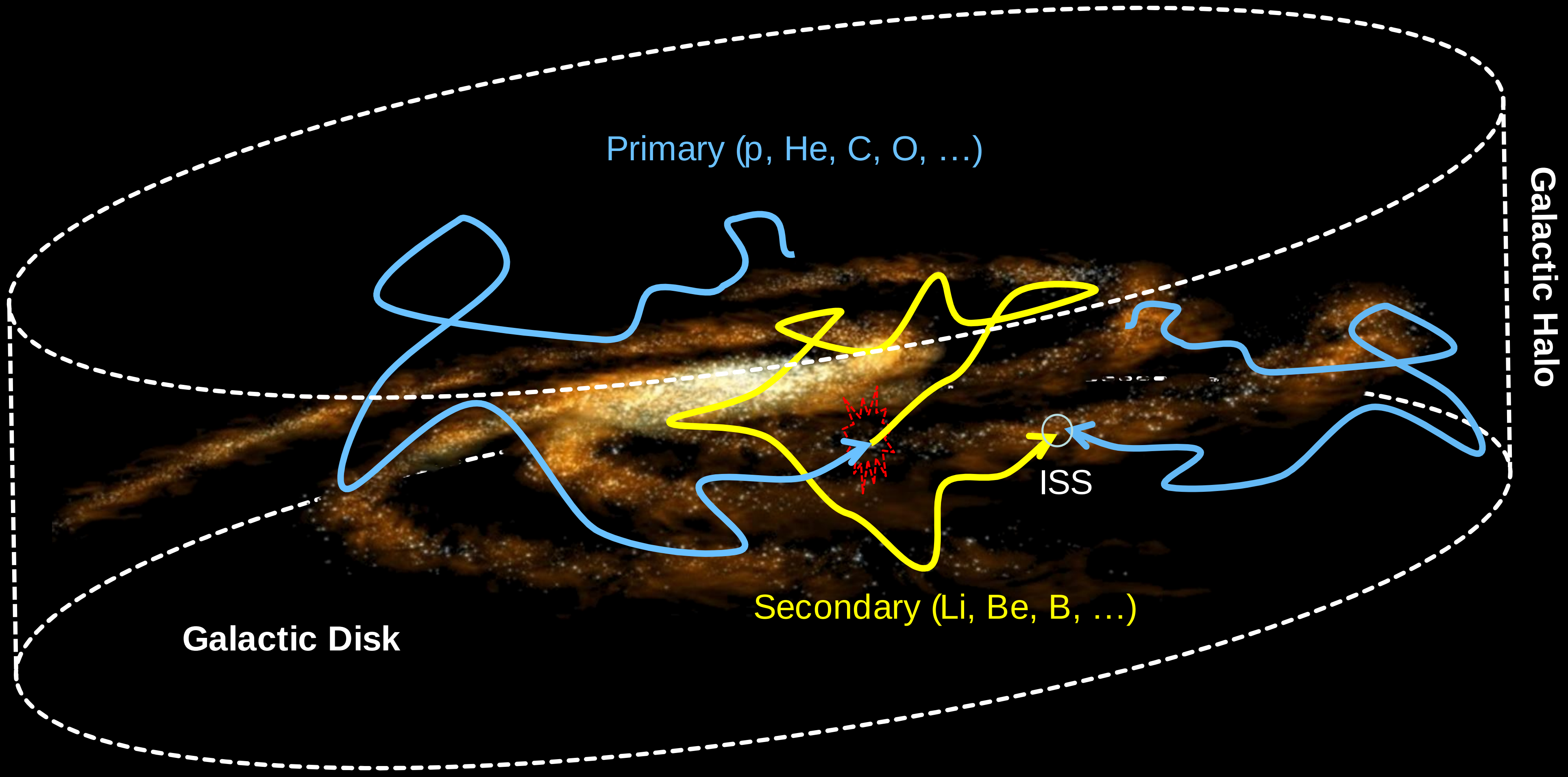

Cosmic rays are commonly modeled as a relativistic gas diffusing into a magnetized plasma.
Basic characteristics of this models are understood studying the **secondary**/**primary** ratios.

Fluxes of Primaries and Secondaries with ≤ ≤

M. Aguilar *et al.*, Phys. Rep. **894** (2021) 1-116.

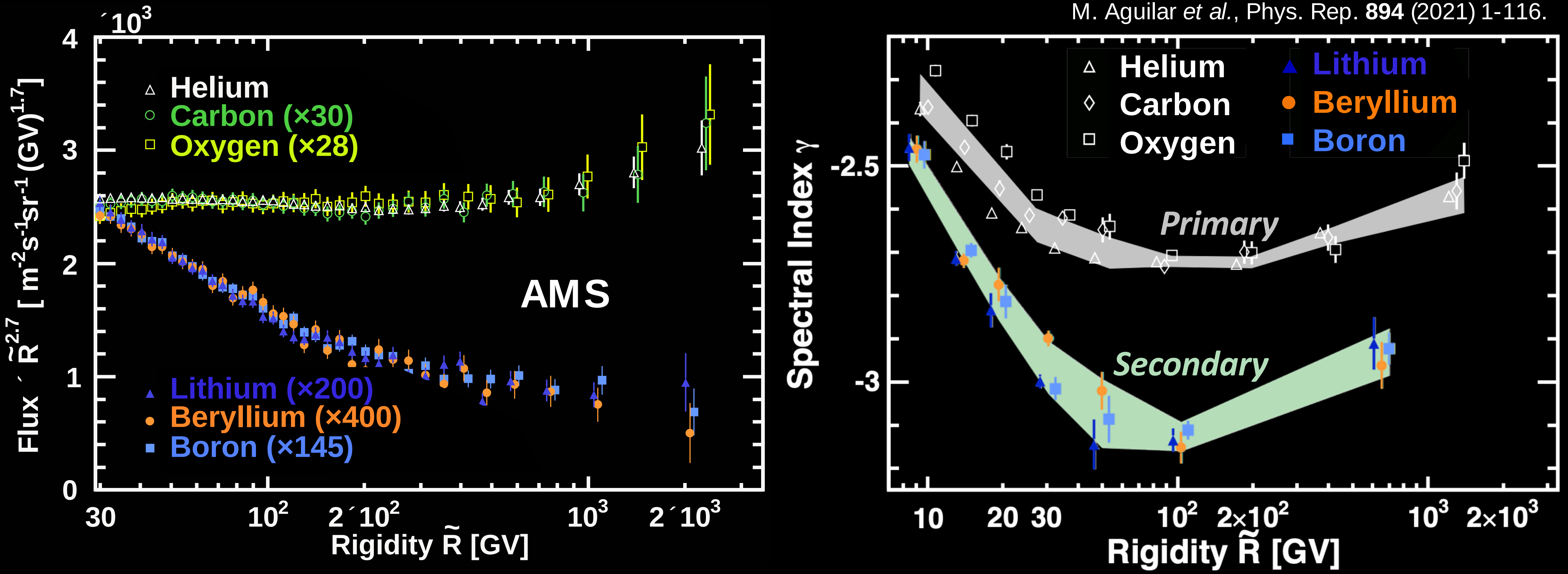

All light nuclei fluxes deviate from single power law above 200 GV.

Secondary hardening is stronger.

This favors the hypothesis that the flux hardening is a **universal propagation effect**.

Secondary/Primary Ratio as a Function of Z

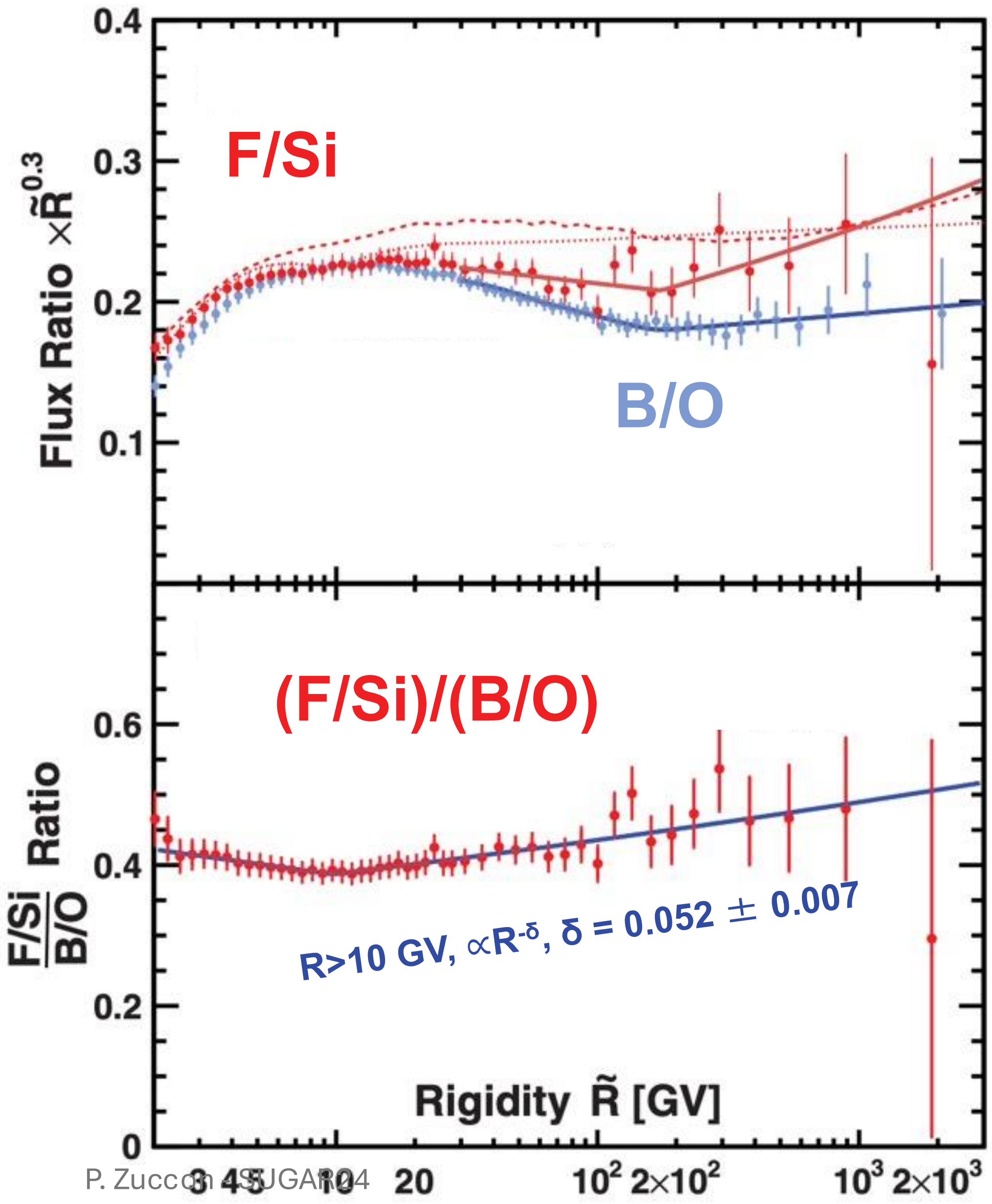

M. Aguilar *et al.*, Phys. Rev. Lett. **126** (2021) 081102.

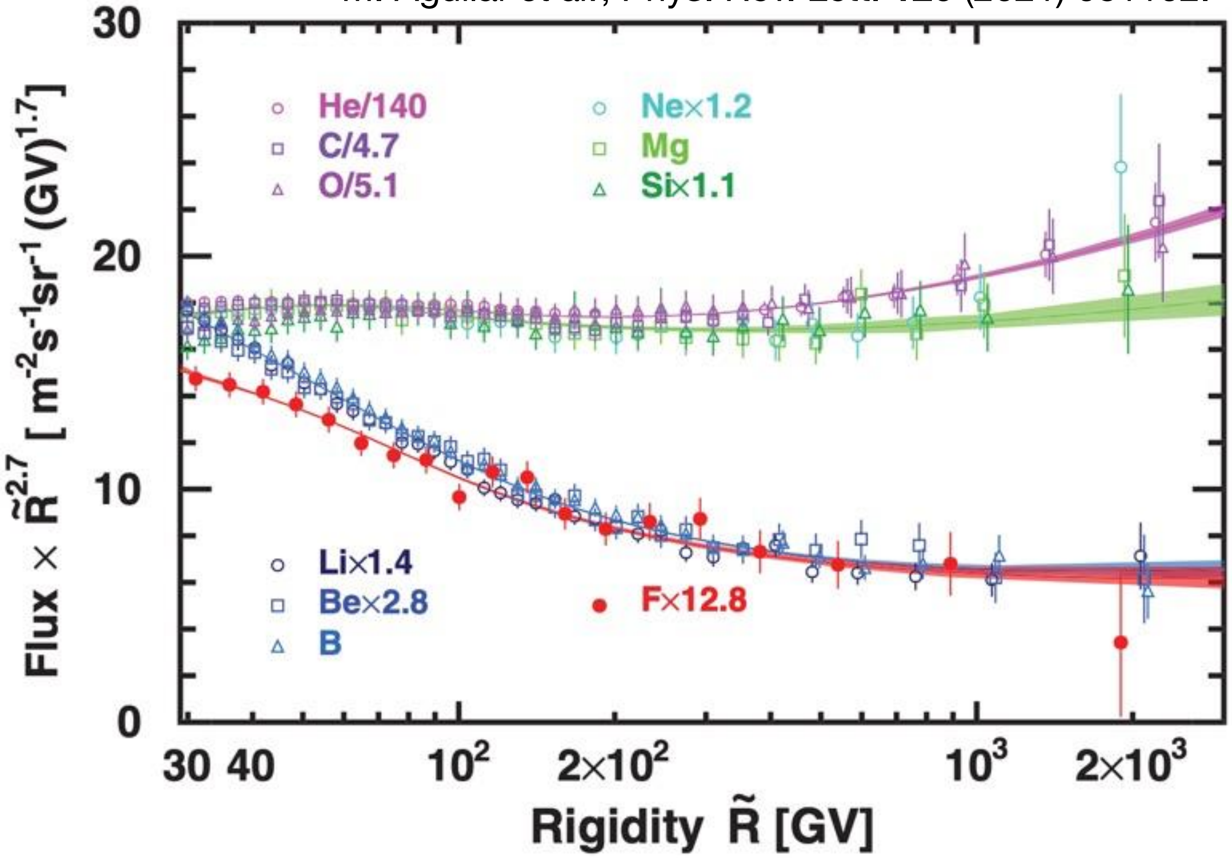

F/Si and B/O have different rigidity dependence, indicating that propagation properties of high-Z CRs, from F to Si, are different from those of low-Z CRs, from He to O.

The rigidity dependence of F is different from Li, Be, B.

Primary/Secondary Composition with AMS

The composition fits are based on assumed pure primary (O, Si) and secondary (B, F) fluxes.

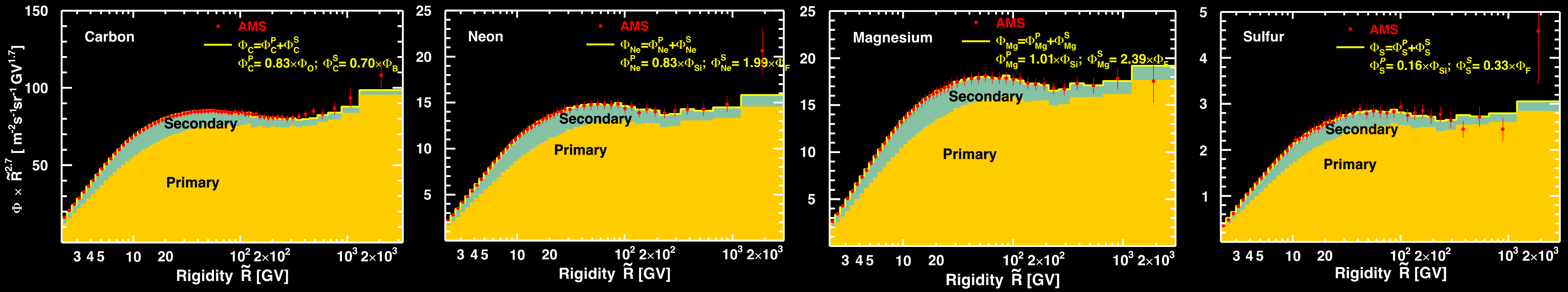

Even-Z nuclei are dominated by primaries

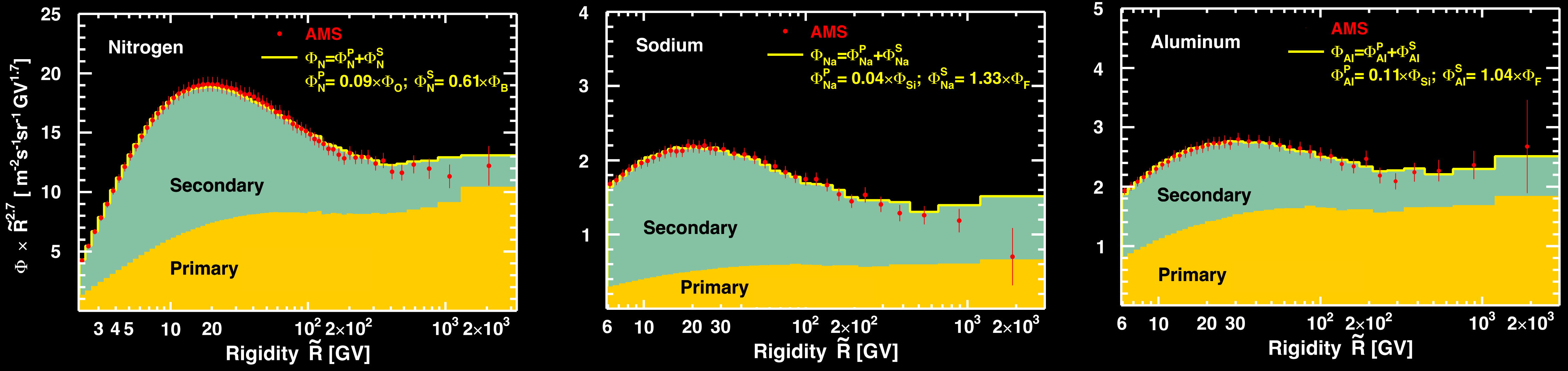

Odd-Z nuclei have more secondaries than even-Z

Hydrogen and Helium ISOTOPES

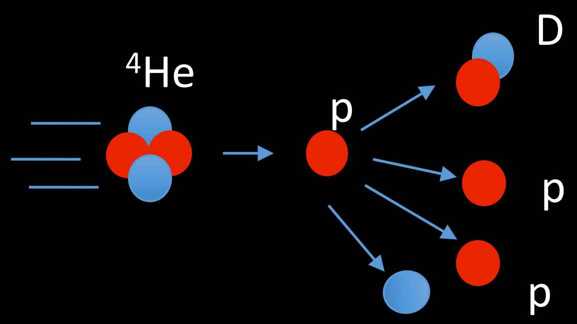

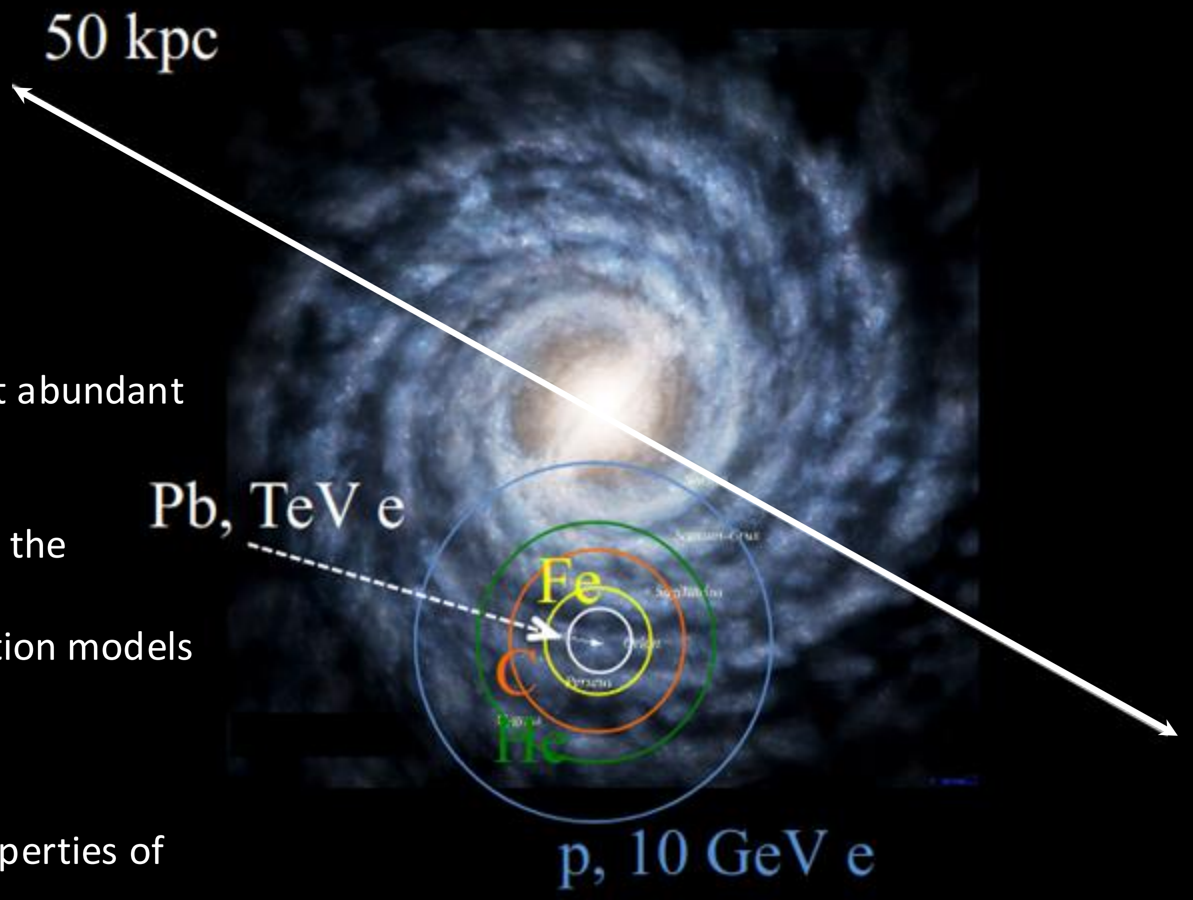

- Helium nuclei are the second most abundant nuclei in cosmic rays.

- D and ^{3}He are mostly produced by the fragmentation of ^{4}He:
  simpler comparison with propagation models wrt heavy nuclei

- Smaller cross section of He:
  $D/^4He$ and $^3He/^4He$ probe the properties of diffusion at larger distances

- Different A/Z ratios of D and ^{3}He allow to disentangle kinetic energy and rigidity dependence of propagation.

Light isotope measurements with AMS02

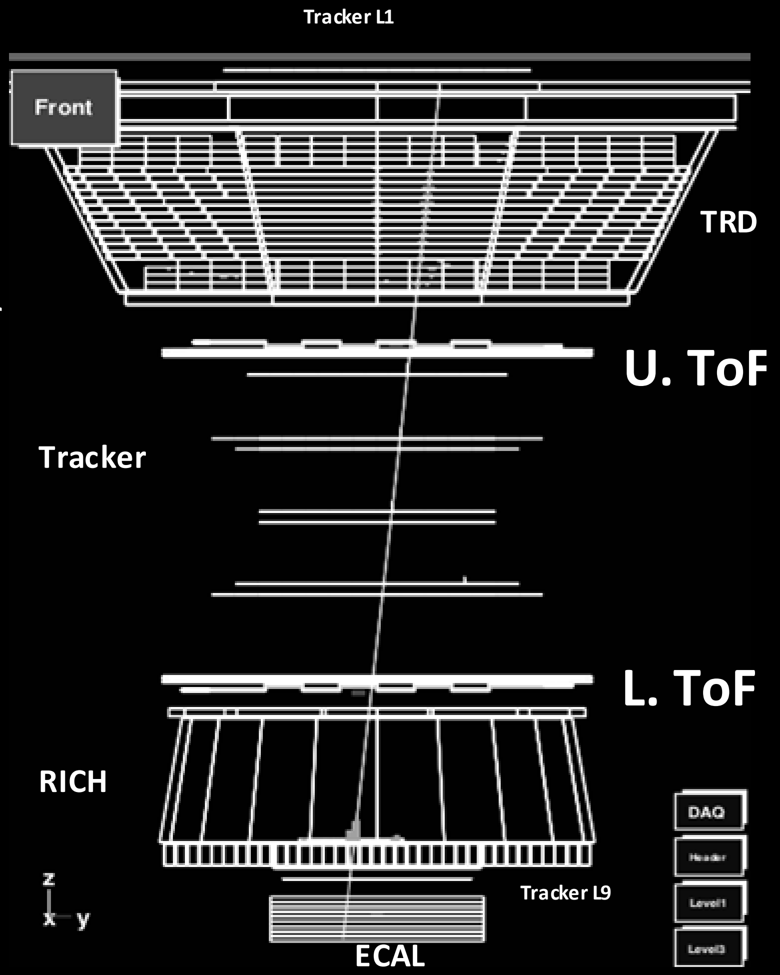

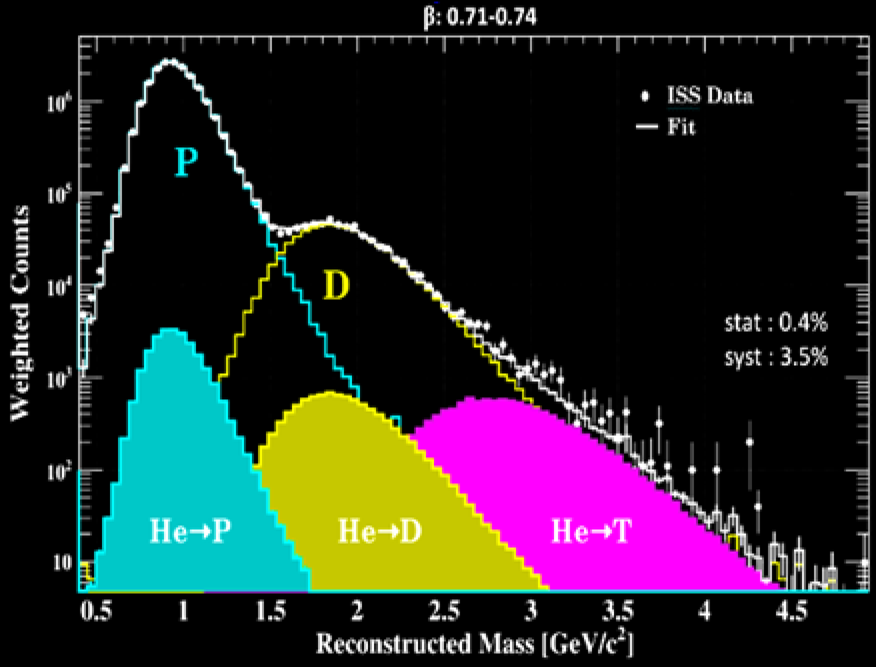

- AMS is composed by different sub-detectors for the redundant ID of the elements in CR
- The **Mass** is identified from the concurrent measurement of **Rigidity, Velocity** and **Charge**
- **Mass resolution** not good enough for event-by-event isotope ID -> Fit of distribution

TOF	σ_β/β ~ 3%	0.2 < E_k< 1.1 GeV/n
RICH NaF	σ_β/β ~ 0.3%	0.7 < E_k < 3.7 GeV/n
RICH AgI	σ_β/β ~ 0.1%	2.6 < E_k< 8.9 GeV/n

3He/4He and D/4He Flux Ratios

Unexpectedly, the D/^{4}He flux ratio spectral index is different from that observed for the ^{3}He/^{4}He flux ratio.

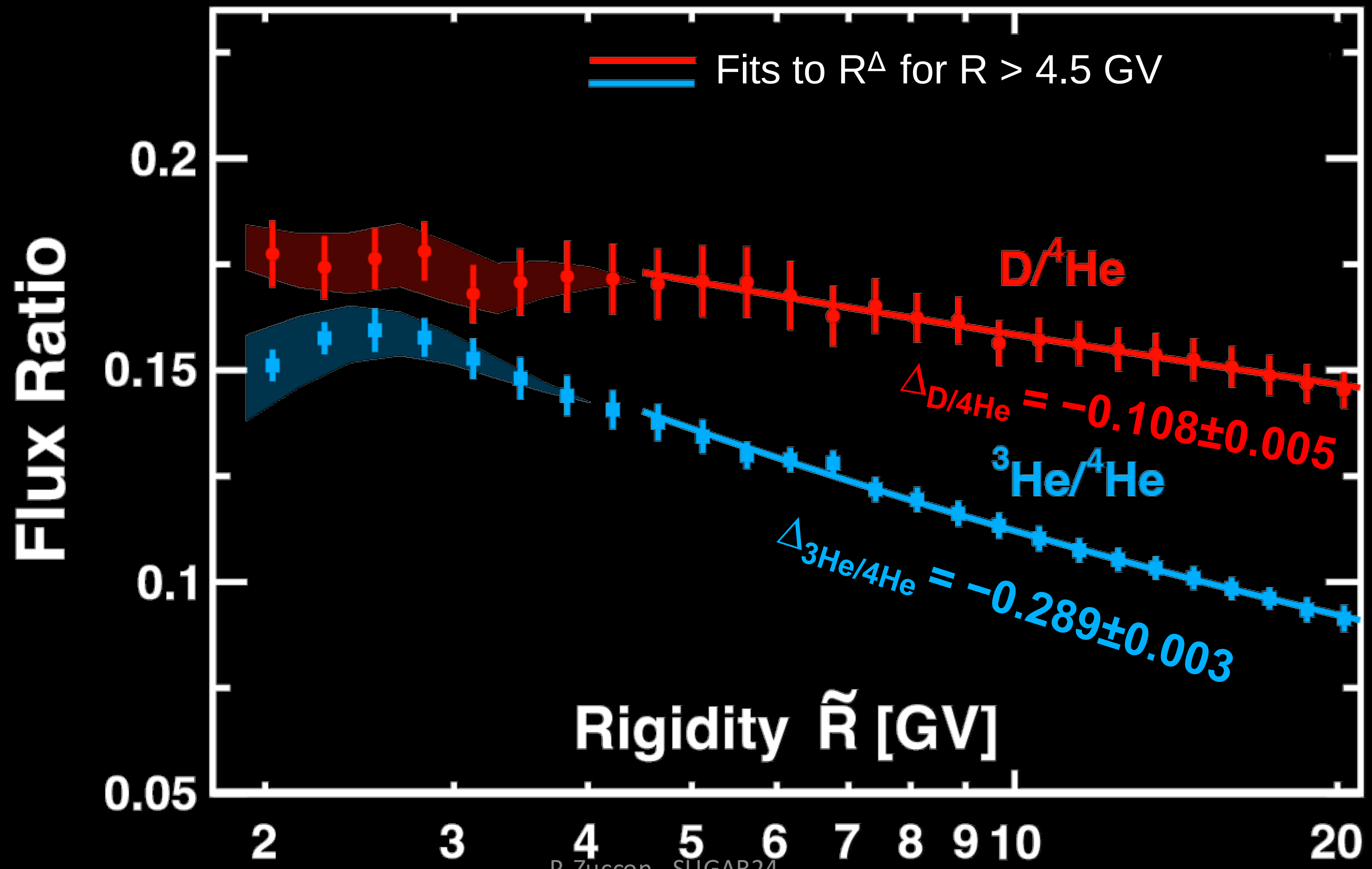

D/p Flux Ratio

D/p flux ratio is increasing with rigidity and flattens out at high rigidities.
This shows that the D and p fluxes have a nearly identical rigidity dependence between 13 and 21 GV

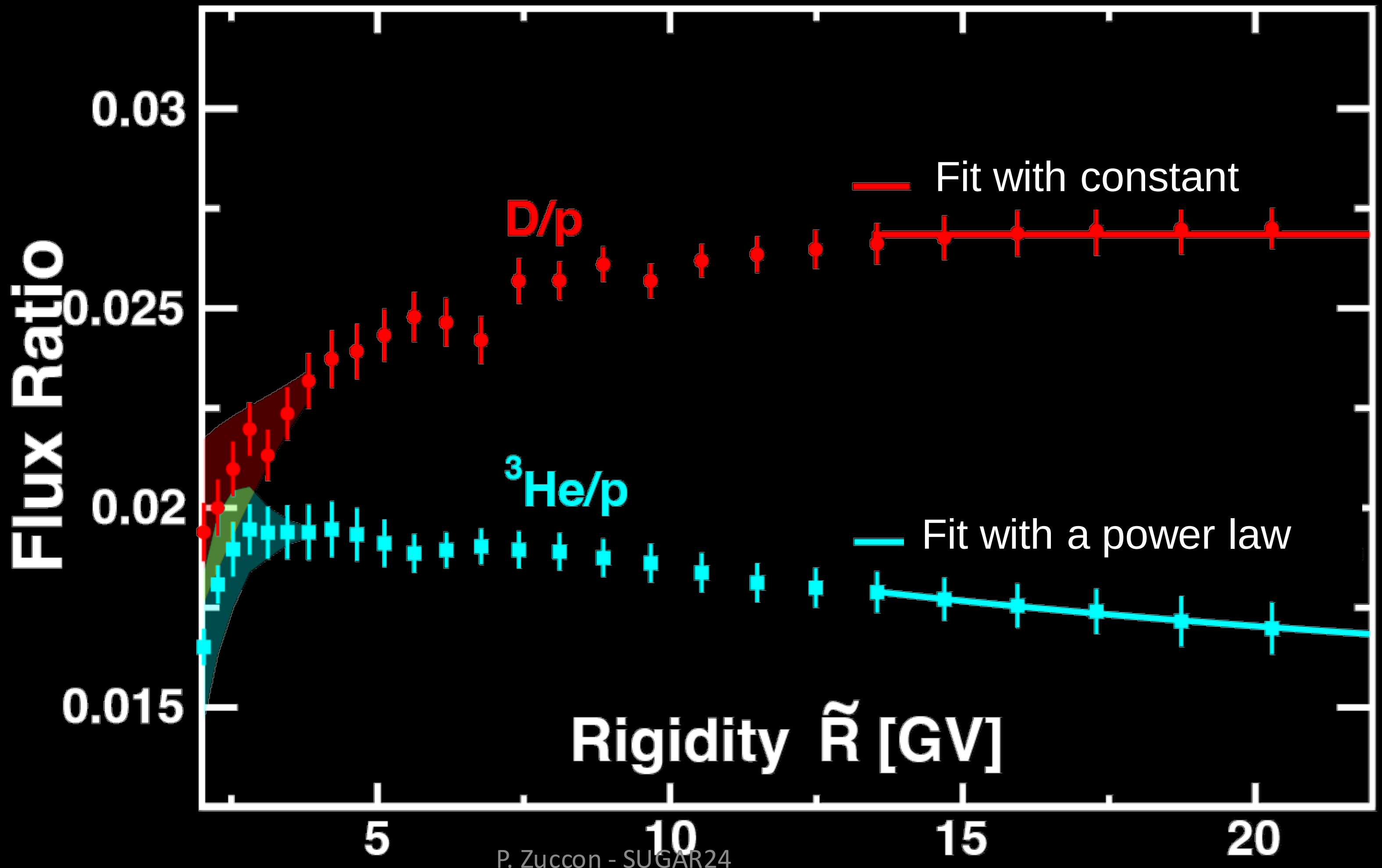

Deuteron as Primary and Secondary like components

To find the primary-like and secondary-like contributions in the D flux we have fitted the D flux as weighted linear combination of primary flux , $\Phi_{^4He}$ and secondary flux, $\Phi_{^3He}$ above 4.5 GV.

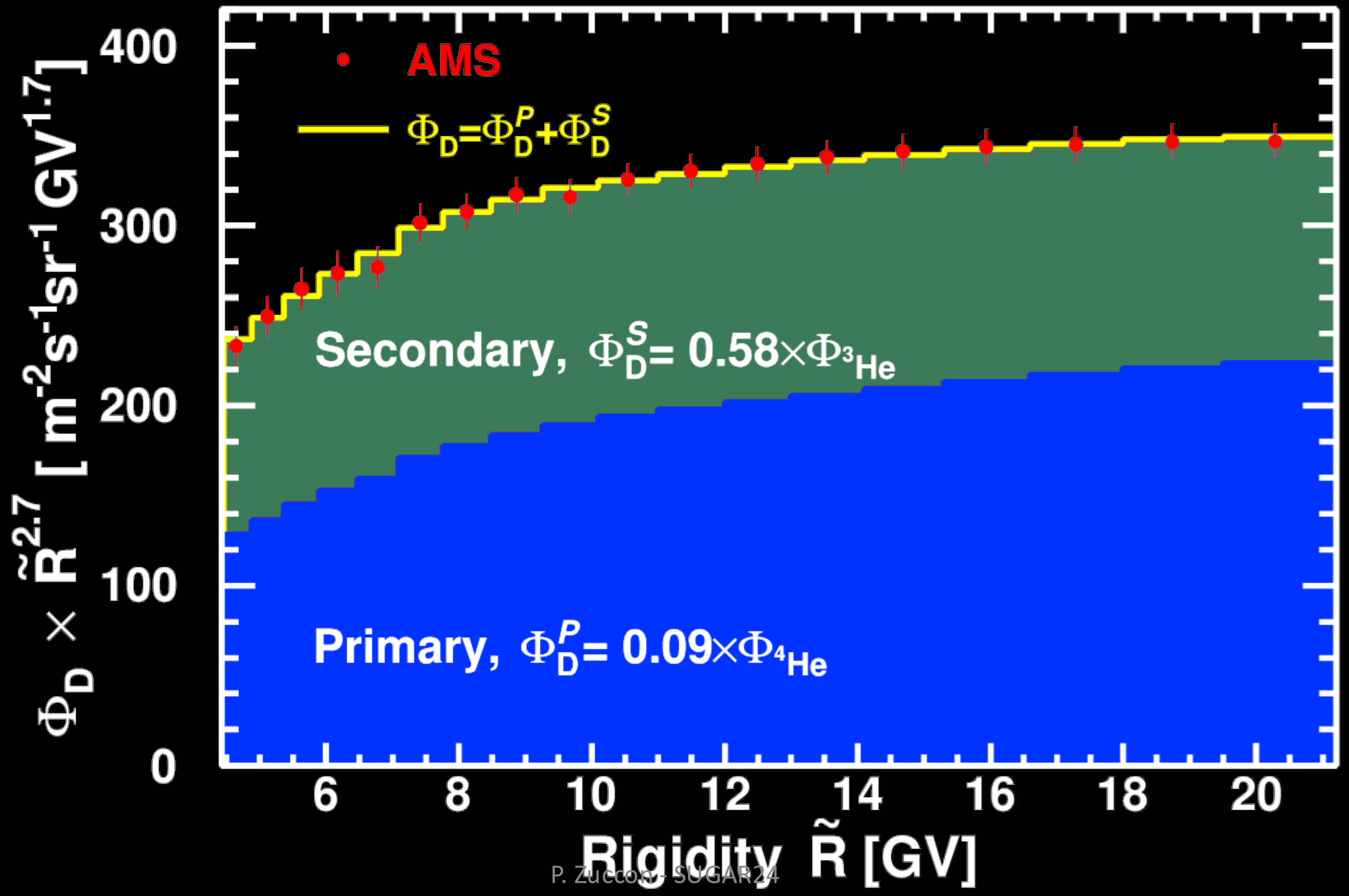

Unstable Secondary Cosmic Rays

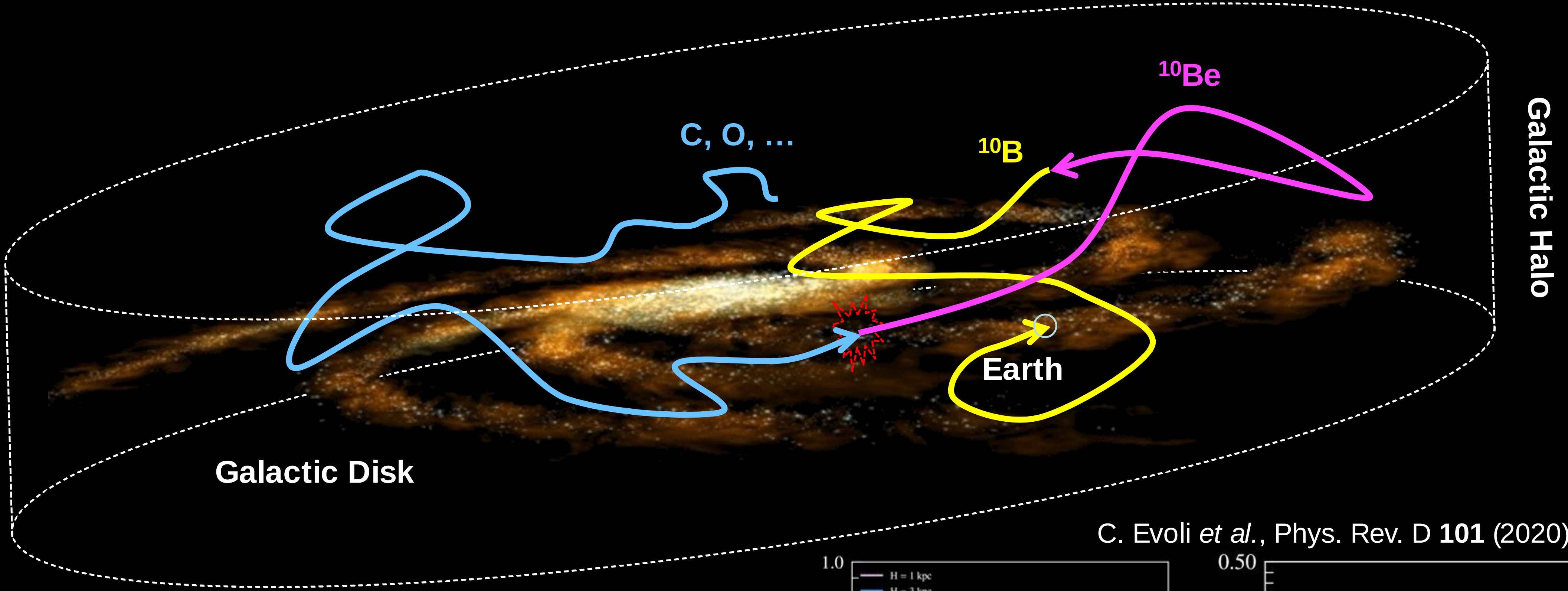

C. Evoli *et al.*, Phys. Rev. D **101** (2020) 023013.

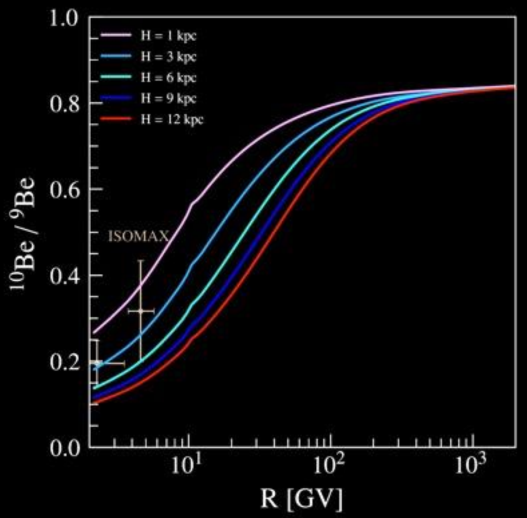

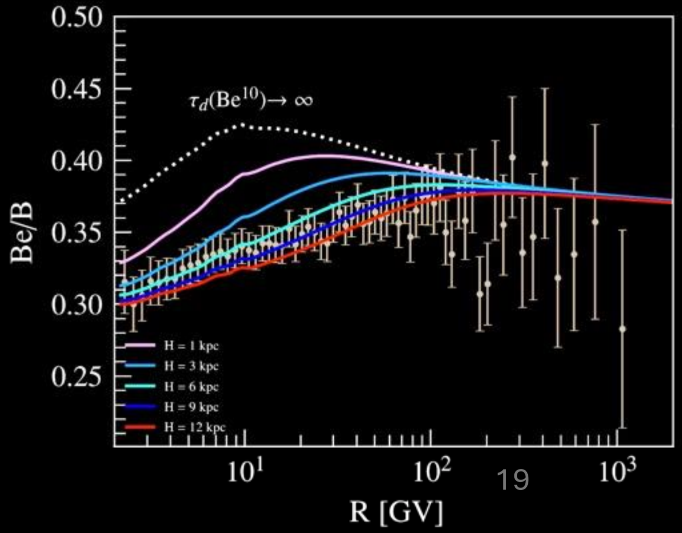

The secondary ^{10}Be β^--decays (^{10}Be → ^{10}B + e^- + $\bar{\nu}_e$)
with a half-life of $t_{1/2}$ = 1.4 My.
Differently from spallation production, happening only on the galactic disk, ^{10}Be may decay anywhere.
Therefore, the amount of ^{10}Be (and ^{10}B) with respect to other secondaries, depends to the **galactic halo size**.

Preliminary Measurement ^{10}Be/^{9}Be with AMS-02

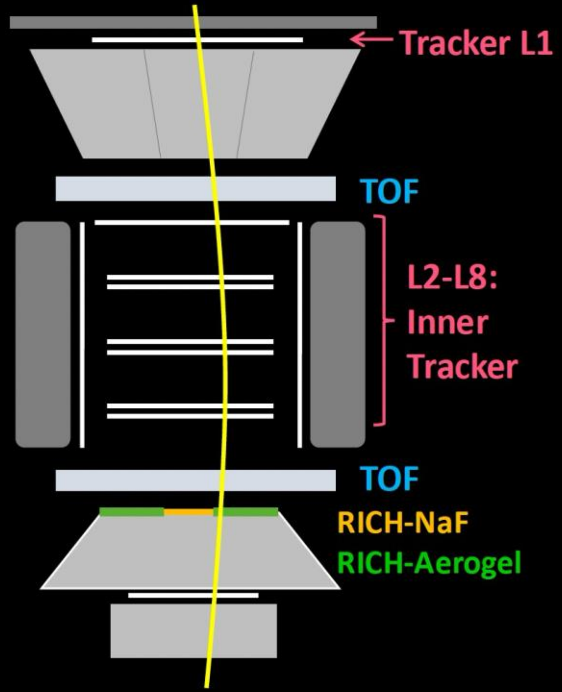

- AMS mass resolution depends on rigidity ($R = P/Z$) and velocity (β) resolutions:

$$\frac{\Delta M}{M} = \sqrt{\left(\frac{\Delta R}{R}\right)^2 + \left(\frac{1}{1-\beta^2}\cdot\frac{\Delta\beta}{\beta}\right)^2}$$

- R measurement :
  - Tracker, $\frac{\Delta R}{R}$ ~9%($Z = 1$), 10%($Z = 4$) below 20 GV
- β measurements:

	E_k/n range (GeV/n)	$\Delta\beta/\beta$ ($Z = 1$)	$\Delta\beta/\beta$ ($Z = 4$)
TOF	(0.4, 1.2)	~4%	~1.5%
RICH-NaF	(0.8, 4.0)	~0.35%	~0.15%
RICH-Aerogel	(3.0, 12)	~0.12%	~0.05%

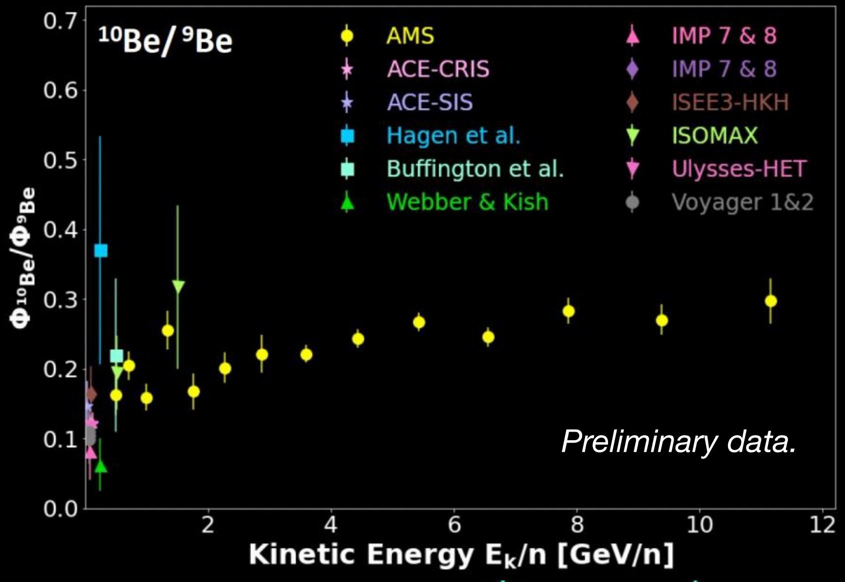

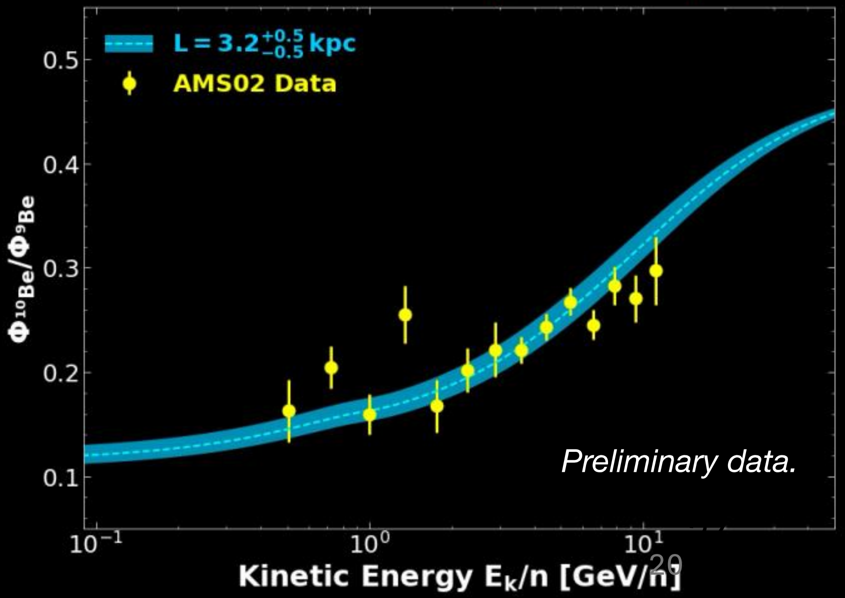

- The precision on the Galactic halo size L from the AMS data is about ~0.5 kpc.
- Error on L is dominated by the **uncertainty on spallation cross-sections** ~1 kpc (D. Maurin *et al.*, A&A **667** (2022) A25).

CR Antimatter as a Probe for New Physics

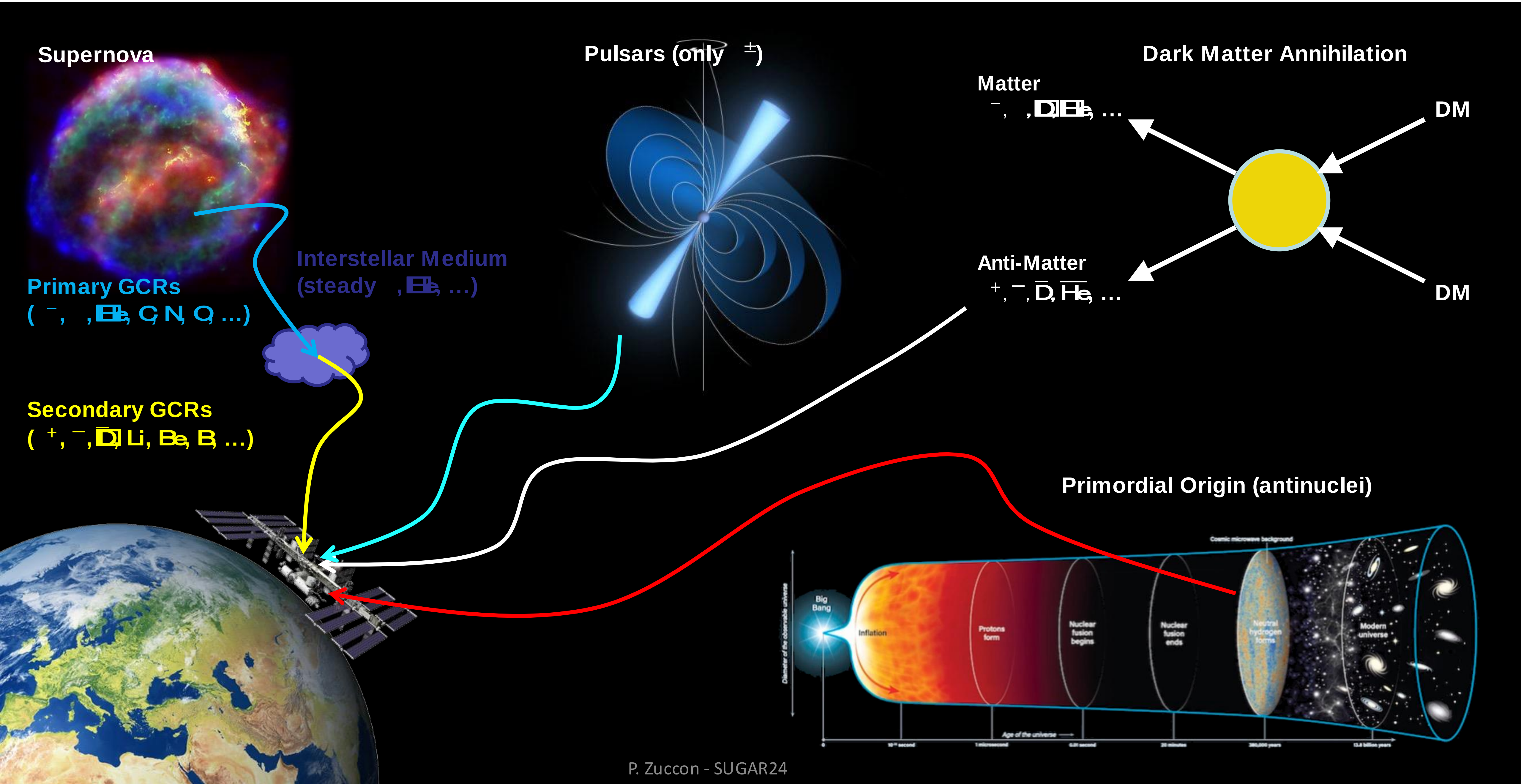

Positron and Electron Fluxes

M. Aguilar *et al.*, Phys. Rep. **894** (2021) 1-116.

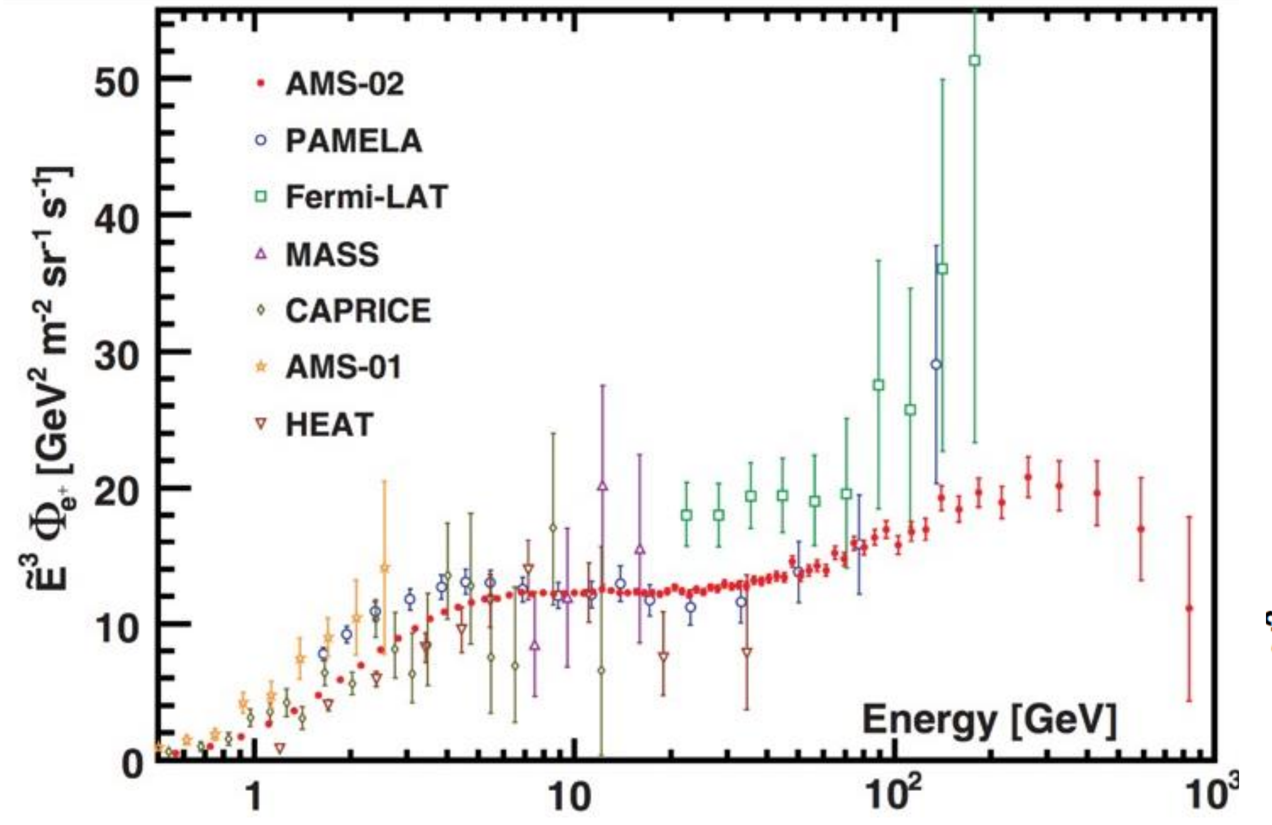

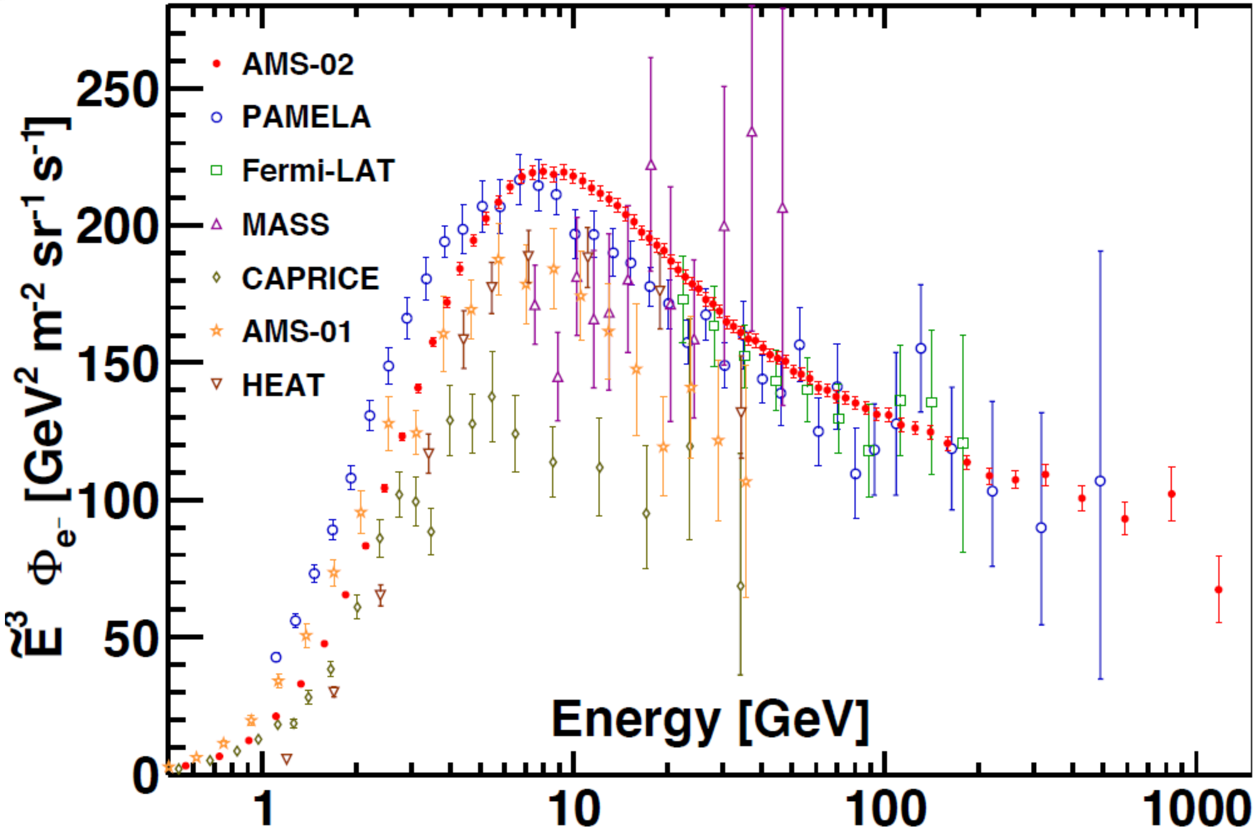

- Spectrometric technique.
- Traditionally the positron excess has been observed and commented on the positron fraction.
- Structures are clearly present on the positron flux.

Positron + Electron Flux

M. Aguilar *et al.*, Phys. Rev. Lett. **122** (2019) 101101.

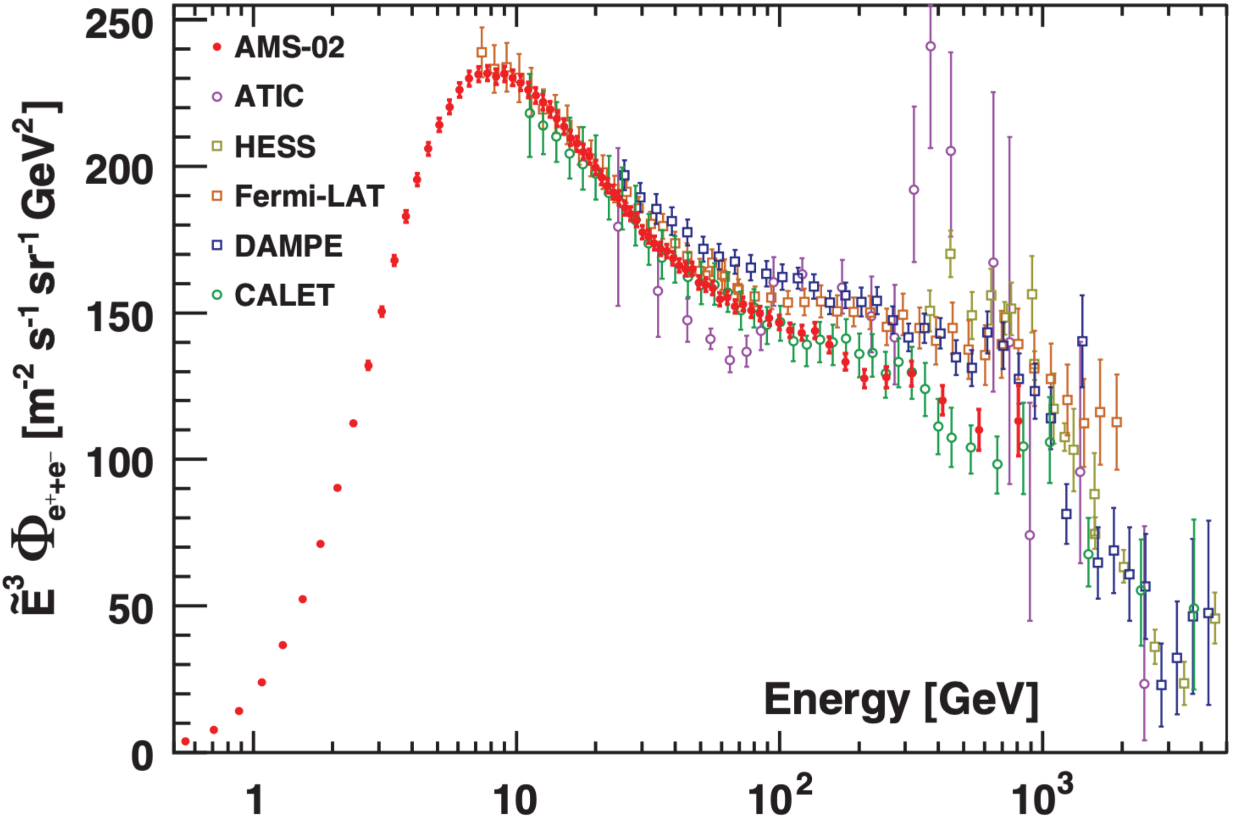

O. Adriani *et al.*, Phys. Rev. Lett. **131** (2023) 191001.

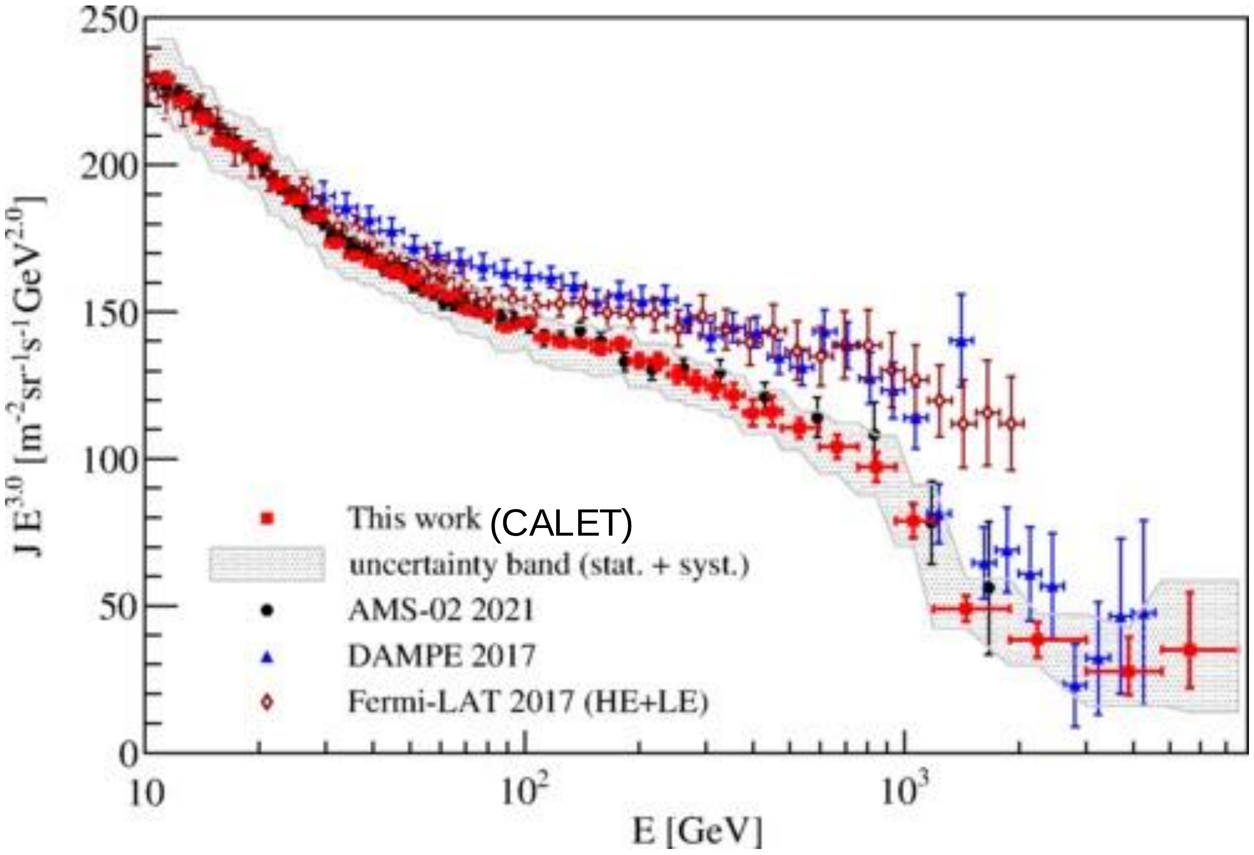

- Can be done also by calorimeters and by experiments on ground.
- Disagreements between “groups of experiment”.
- Dropoff at high energy, and a structure above 1 TeV (?).
- This channels allow to collect high statistics, and study anisotropy that is important to ascertain the origin of structures.

Antiproton Flux and the ¯/ Flux Ratio

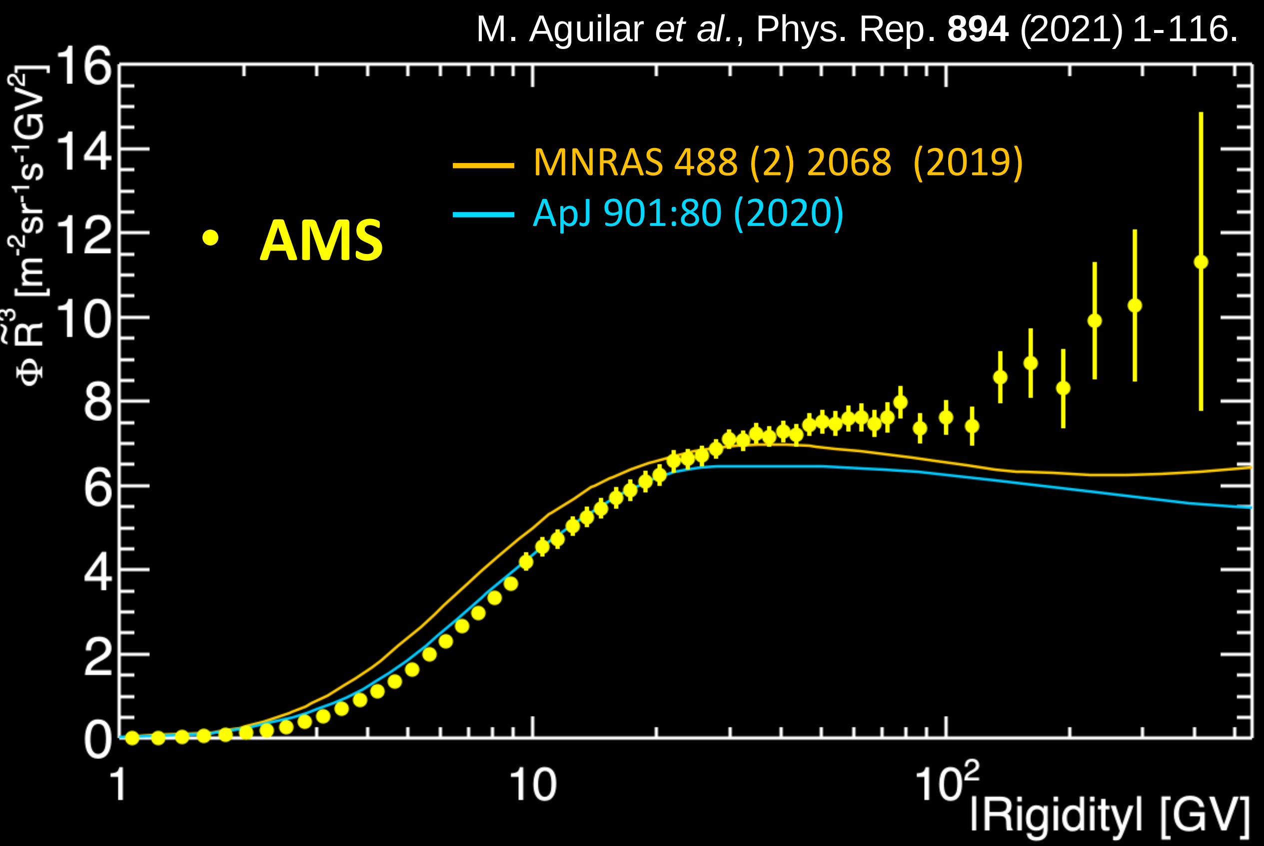

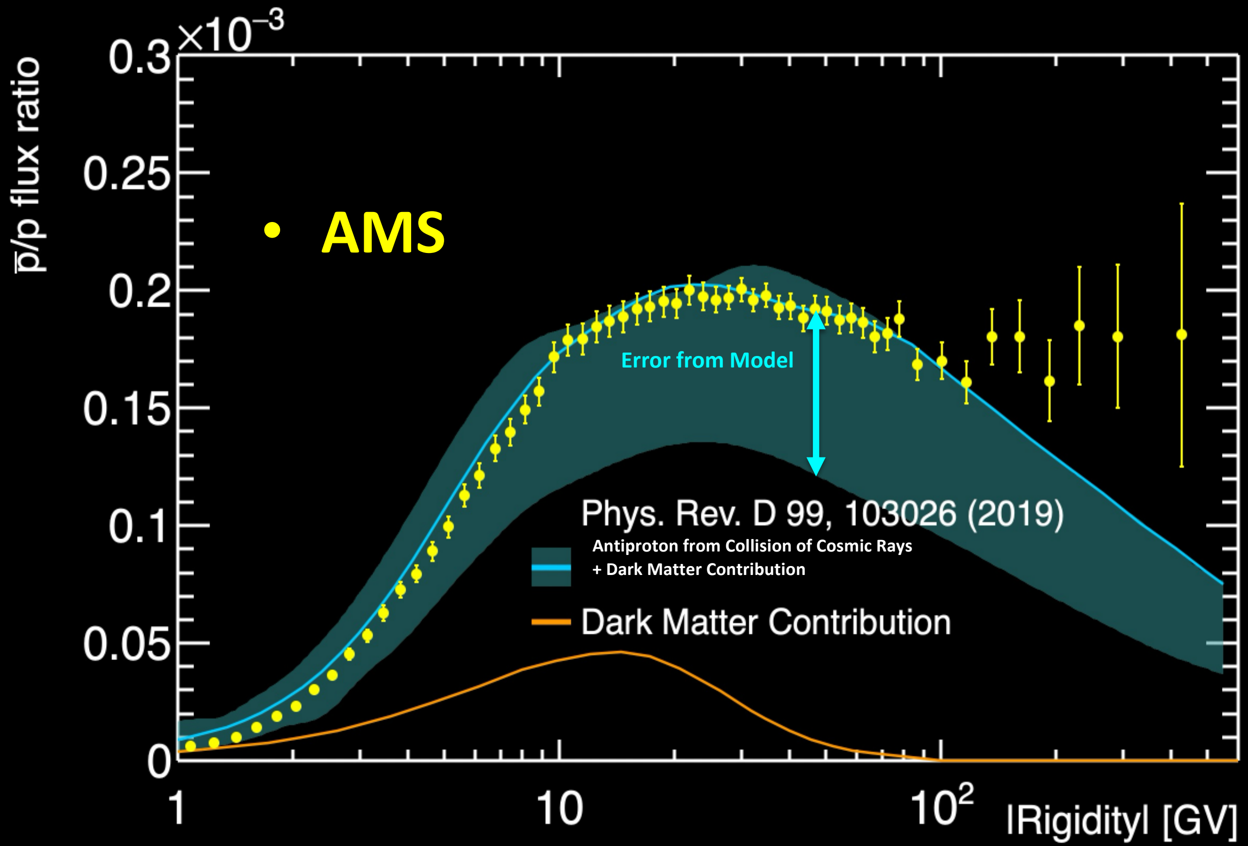

An excess at few tens of GeV has been widely discussed in literature.
The interpretation data requires precision knowledge of the **astrophysical background** (i.e., secondary production).

Uncertainty in Antiproton Astrophysical Background

Uncertainty in antiproton production:

measurements of the ¯ production cross section for + , He → ¯ are needed.

LHCb/SMOG: + He → ¯ at √¯ = 110 GeV measurement already done.

R. Aaij *et al.*, Phys. Rev. Lett. **121** (2018) 222001.

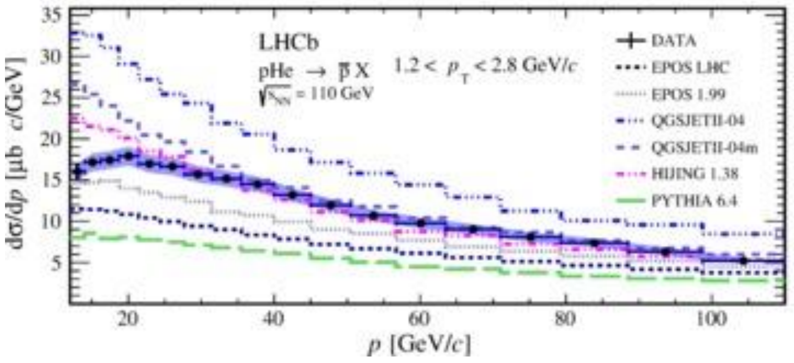

AMBER: Fixed target experiment at SPS (CERN). Data acquired for pp and pHe. Under analysis the pp at √¯ = 18.9 GeV.

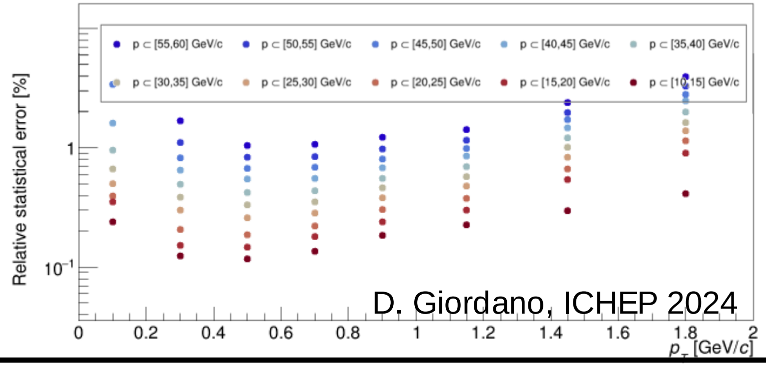

D. Giordano, ICHEP 2024

Uncertainty in galactic propagation:

parameters of the galactic propagation (diffusion coefficient, galactic halo size, …) depend on the knowledge of spallation cross section (as C + p à B):

Y. Genolini et al., Phys. Rev. C **109** (2024) 064914.

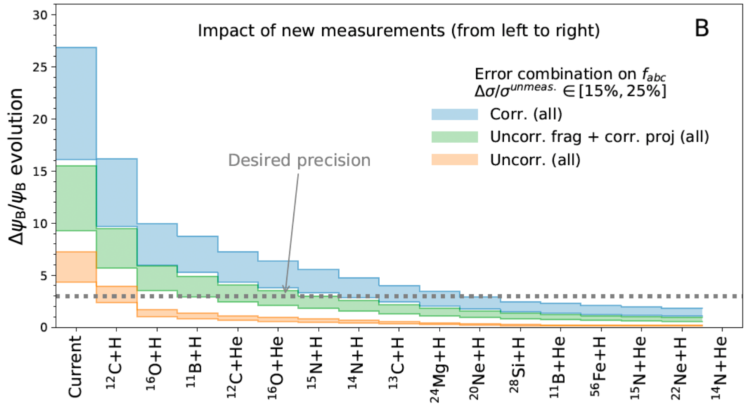

NA61/SHINE: Fixed target experiment at SPS (CERN). Pilot run in 2018.

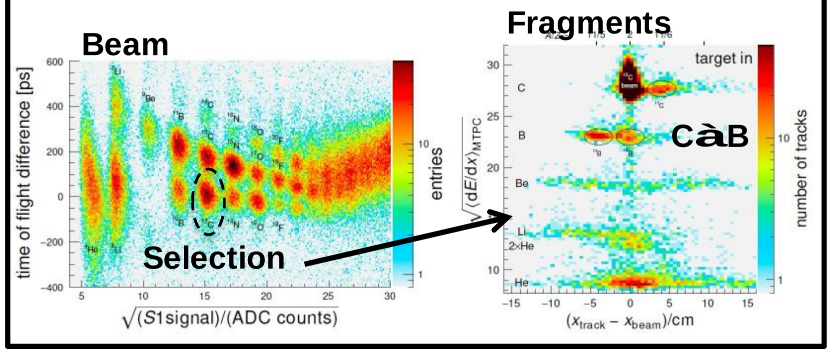

Uncertainty in solar modulation:

direct measurement of ¯ as function of time allows the accurate modelling of solar modulation.

AMS-02: measurement of all CR species over a solar cycle.

S. Lu, ICHEP 2024.

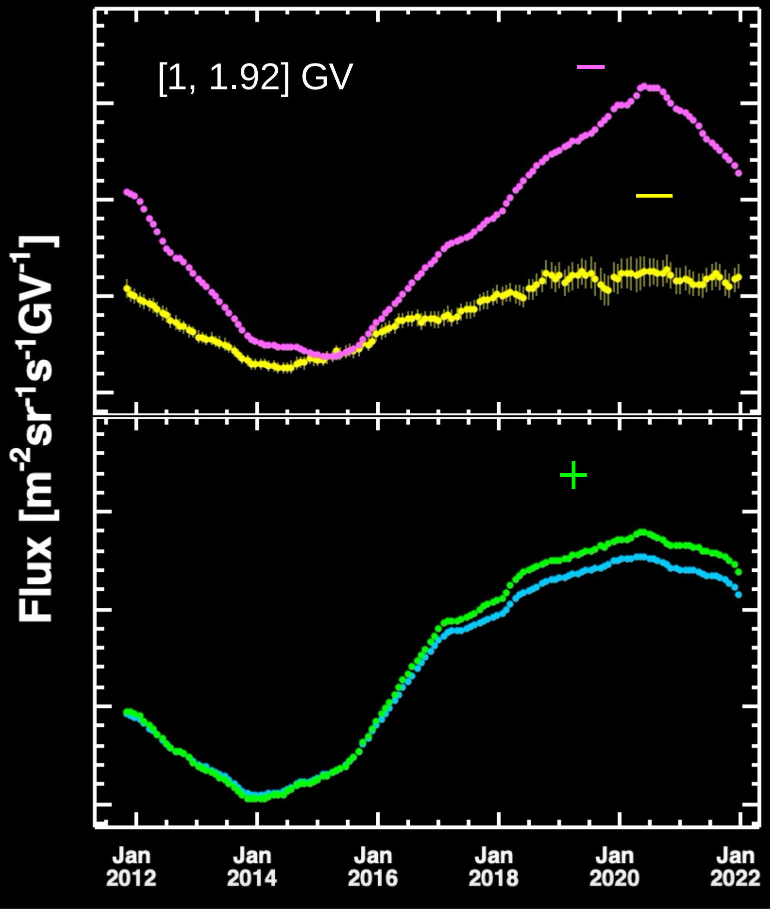

Heavy Antimatter in the Cosmos

Matter is defined by its mass *M* and charge *Z*.

Antimatter has the same mass *M* but opposite charge *–Z*.

$\overline{\mathrm{D}}$, $\overline{\mathrm{He}}$, $\overline{\mathrm{C}}$, $\overline{\mathrm{O}}$ …

Antimatter Star

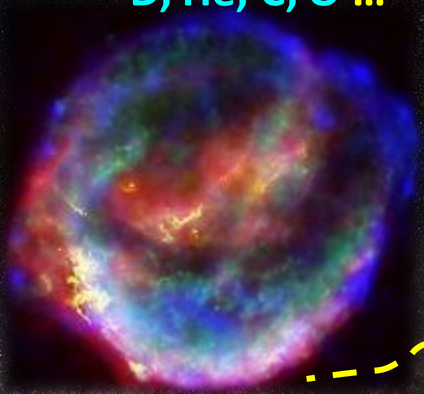

AMS on ISS

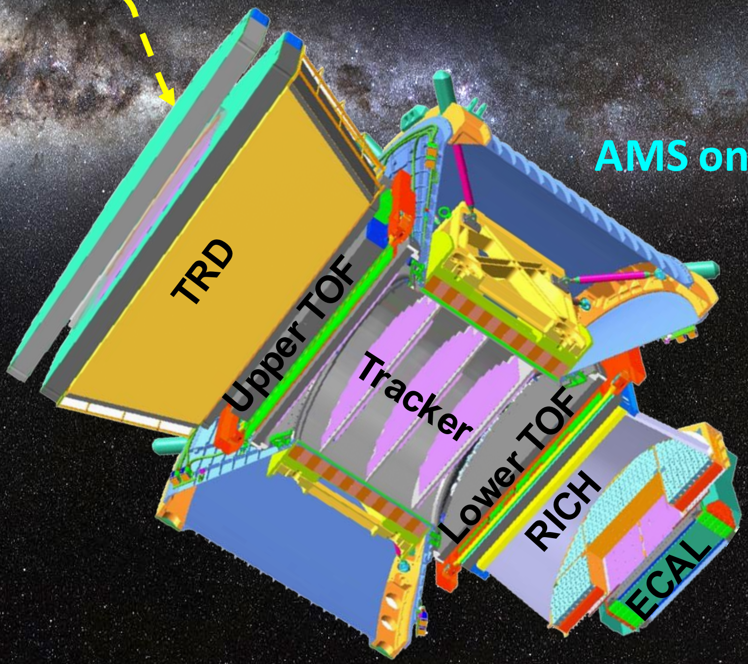

AMS is a unique antimatter spectrometer in space

Current Status of AMS Antideuteron Search

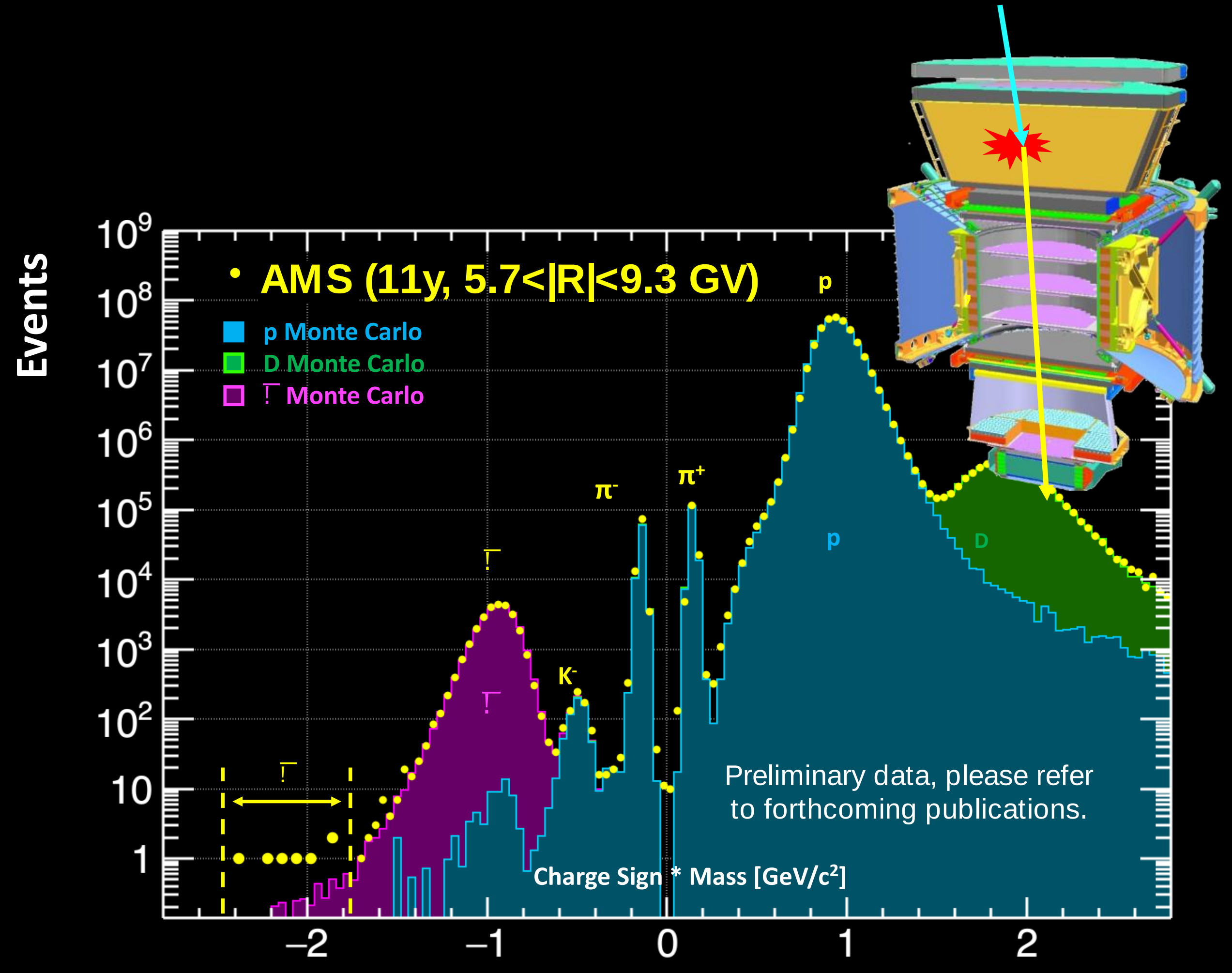

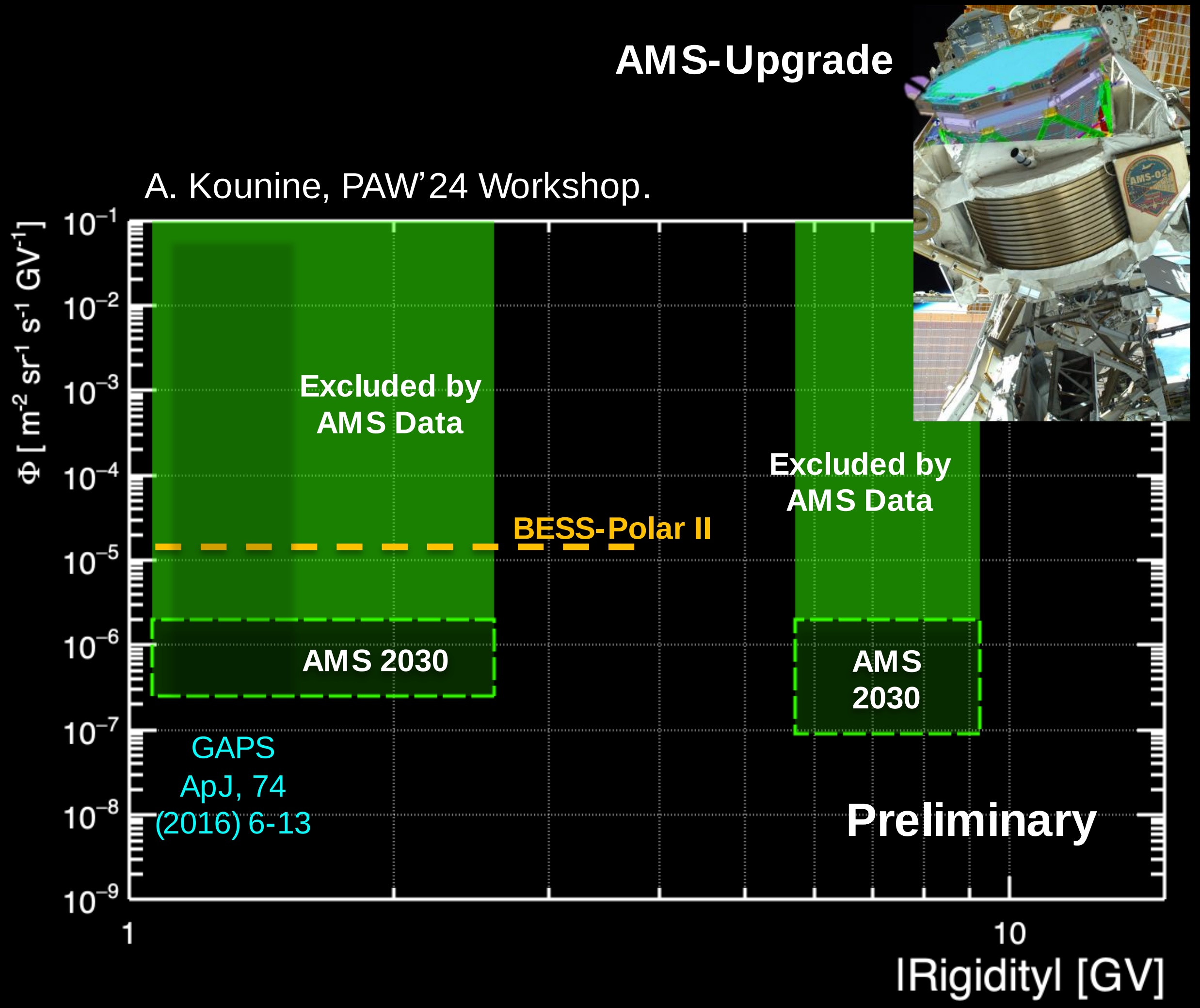

- Future AMS upgrade will provide additional measurement point to antideuterons.
- Improve analysis techniques, further MC study to better understand the background.

AMS-02

anti-He candidates

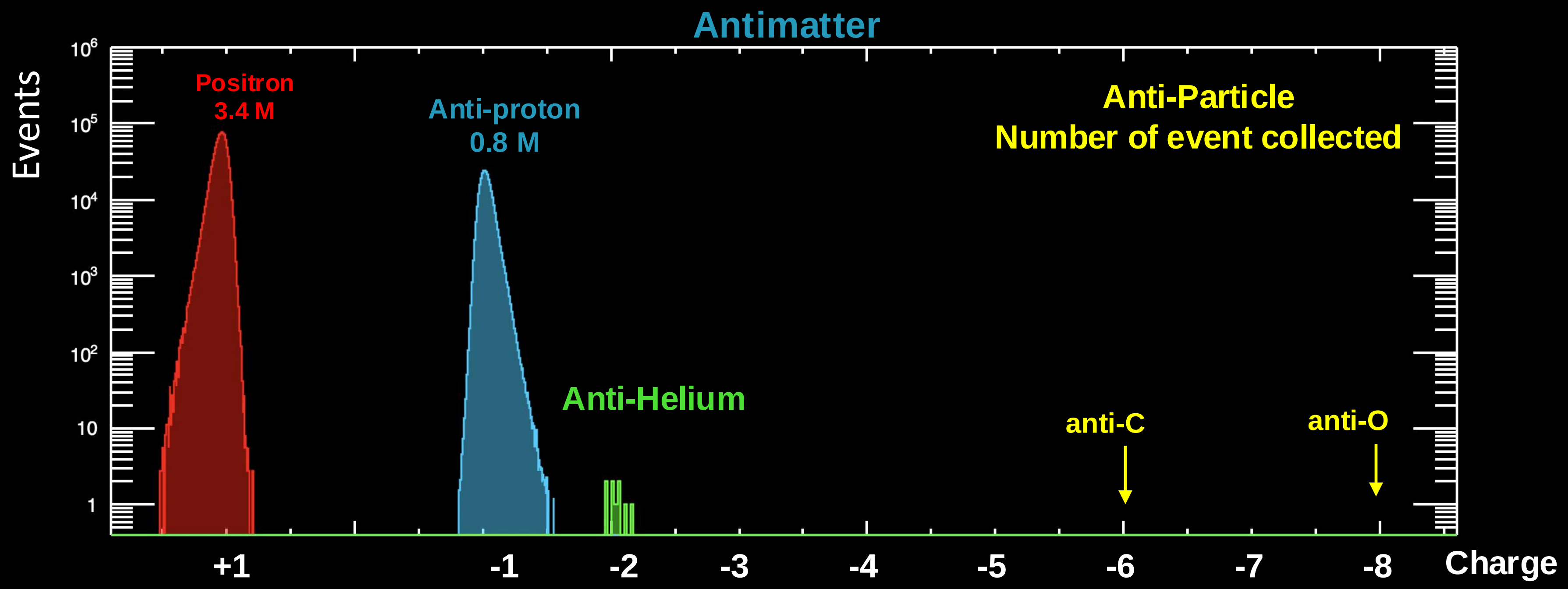

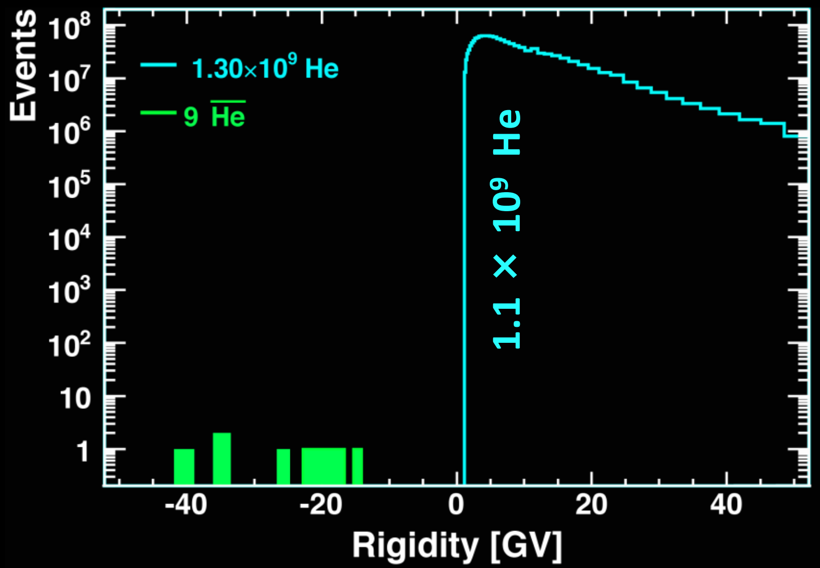

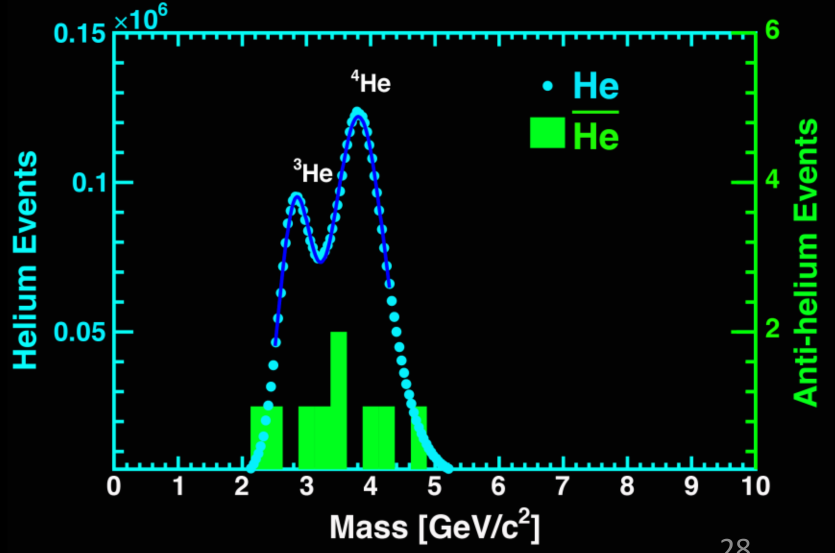

AMS-02 Upgrade: L0 Layer to Increase Acceptance (2026)

The increase of 300% in the acceptance will allow for the best use of the time left on the ISS, allowing higher rate in data collection for many analysis channels (positrons, nuclei, …).

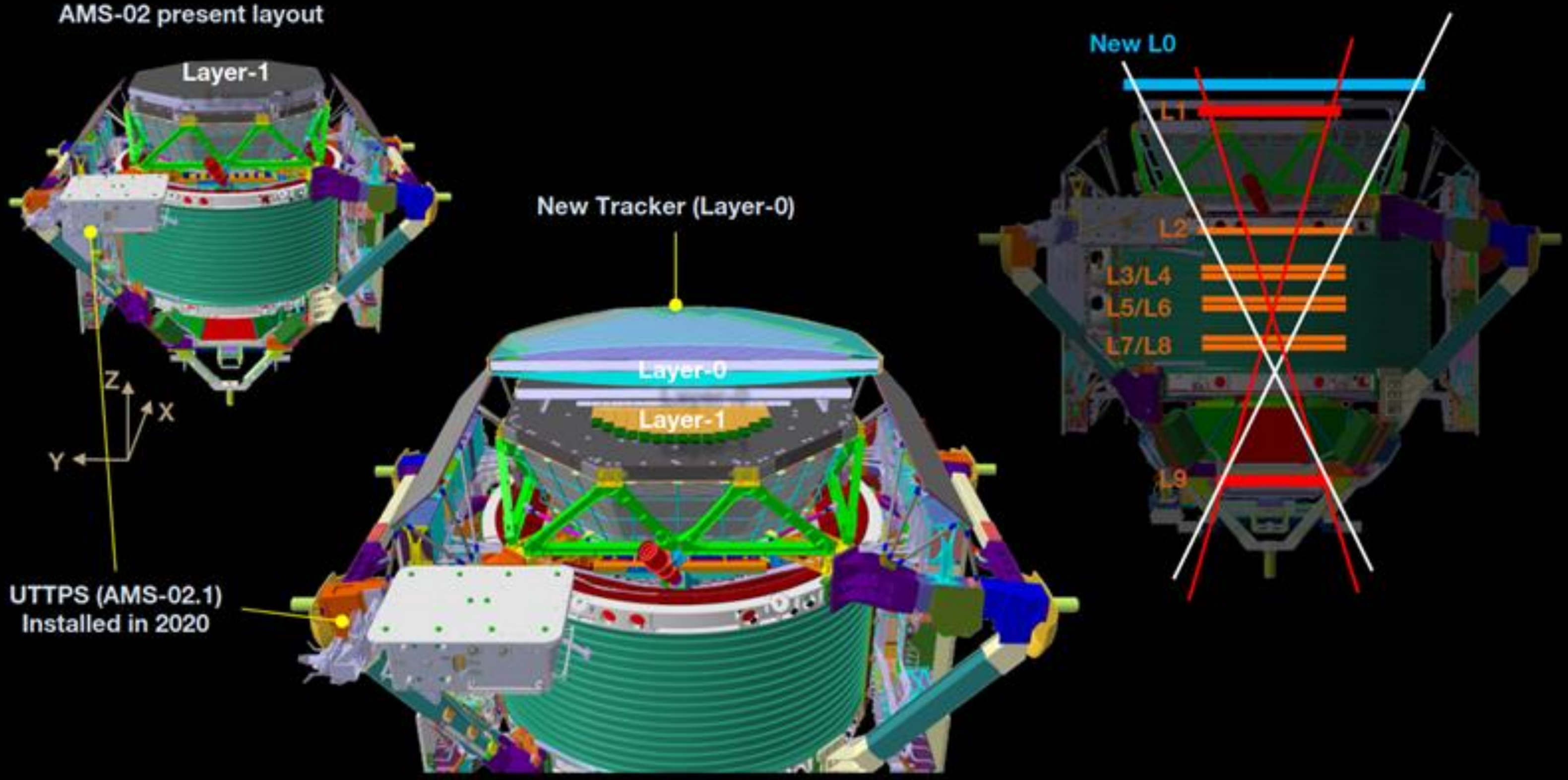

Advantages

- Extend positron spectrum measurement to 1.4 TeV
- Extend Electron spectrum measurement to 1.4 TeV
- Improve the accuracy of the anti-proton measurement
- Measure positron isotropy, to a 3.4 sigma significance with respect pulsars hypothesis
- High accuracy on Fe and sub-Fe
- Daily fluxes of heavier nuclei as C and O
- Search for rare events as anti-deuteron

AMS-02 upgrade

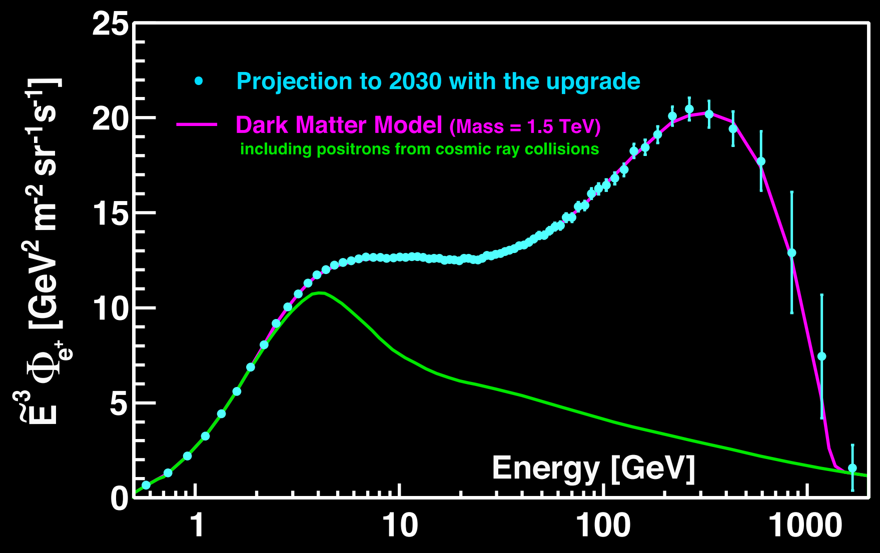

Fig 1(b): Positron studies at highest energies.

Please note that the highest energy point are from collisions only.

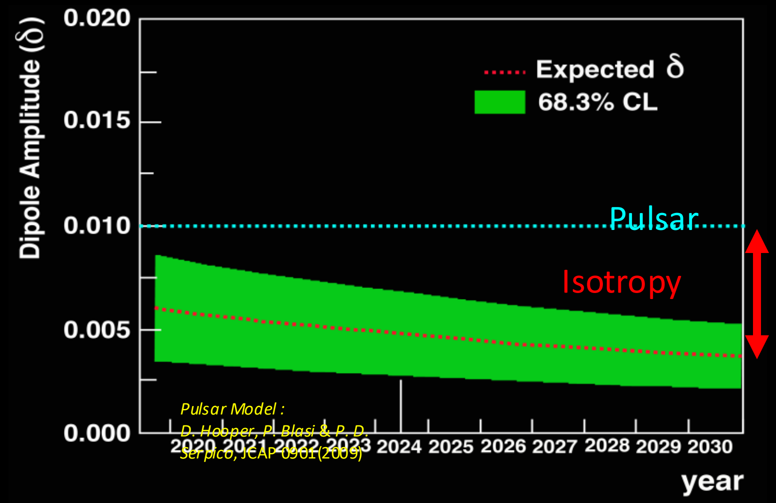

Positron anisotropy projection up to 2030 with upgrade

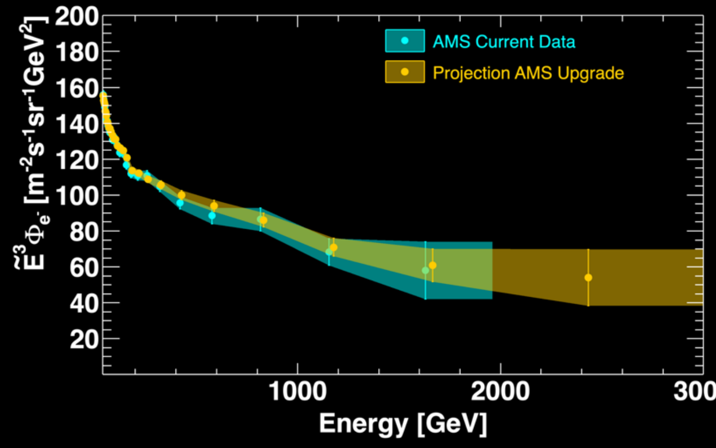

Electron Spectrum at High Energy

30

FUTURE SPECTROMETERS

AMS-100: A Next-Generation Magnetic Spectrometer

S. Shael *et al.*, Voyager 2050 White Paper (2021).

Location	**Lagrange Point L_2**
Installation	**>2030**
Dimensions	**⌀ = 4.4 m, L = 6 m**
Weight	**40 t**
Power	**10 kW**
Magnetic Field	**1 T**
Acceptance	**100 m^2 sr**
MDR	**100 TV**
Cal. thickness	**70 X_0**

A vastly larger detector than the current generation (factor of 100 in energy and Acceptance with respect AMS-02):

- Antimatter.
- $e^{\pm}$ up to 10 TeV.
- CRs composition above knee.

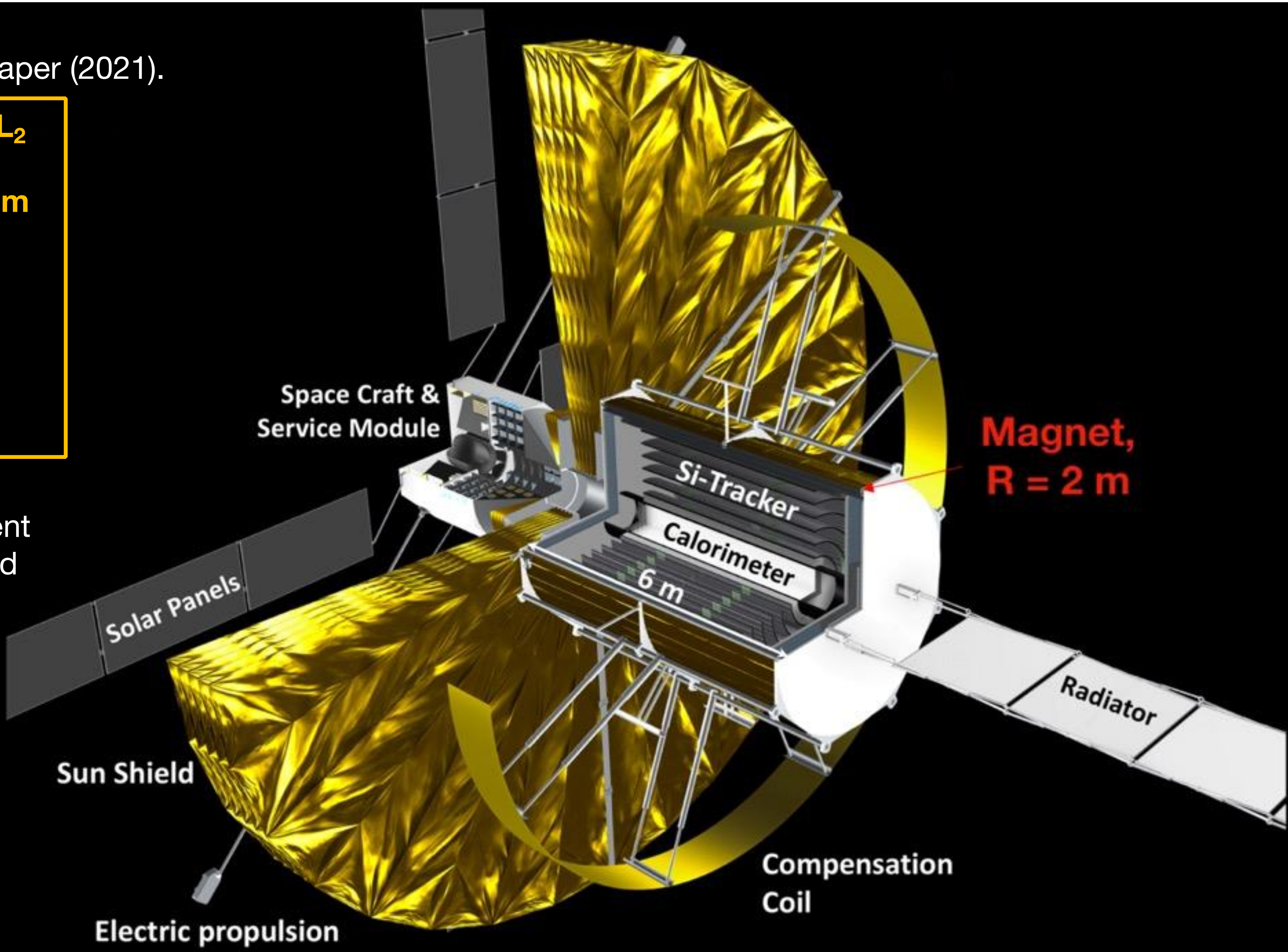

https://doi.org/10.1016/j.nima.2019.162561

ALADInO: Antimatter Large Acceptance Detector in Orbit

Location	Lagrange Point L_2
Installation	>2030
Dimensions	⌀ = 4.4 m, L = 2 m
Det. weight	6.5 t
Power	3 kW
Magnetic Field	0.8 T
Acceptance	>10 m^2sr
MDR	>20 TV
Cal. thickness	61 X_0

5-year operations in L2

https://doi.org/10.3390/instruments6020019

Physics objectives:

- Anti-nuclei;
- $e^{\pm}$ up to 10 TeV;
- Cosmic ray comp. up to *knee*.

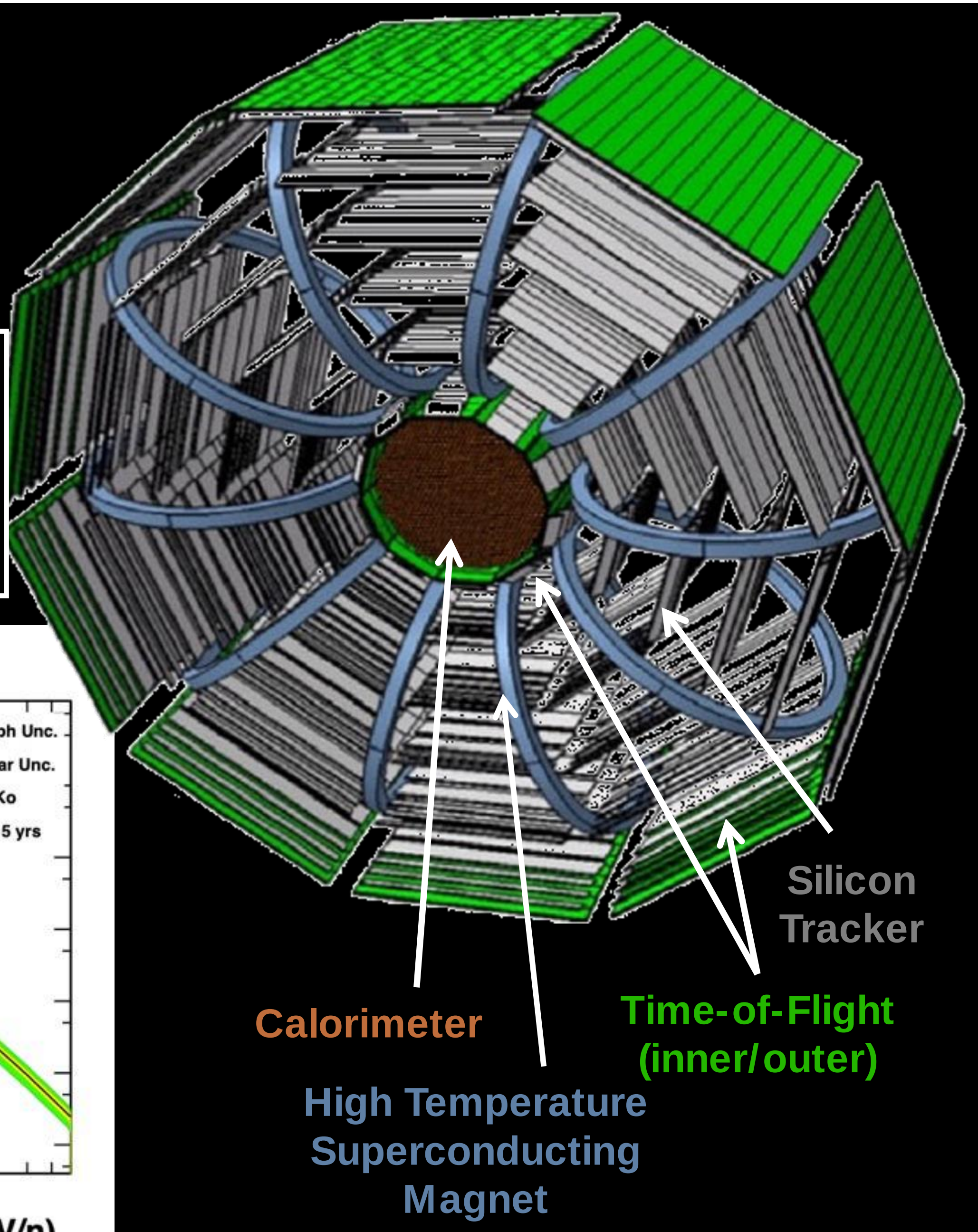

R. Battiston *et al.*, Voyager 2050 White Paper (2021).

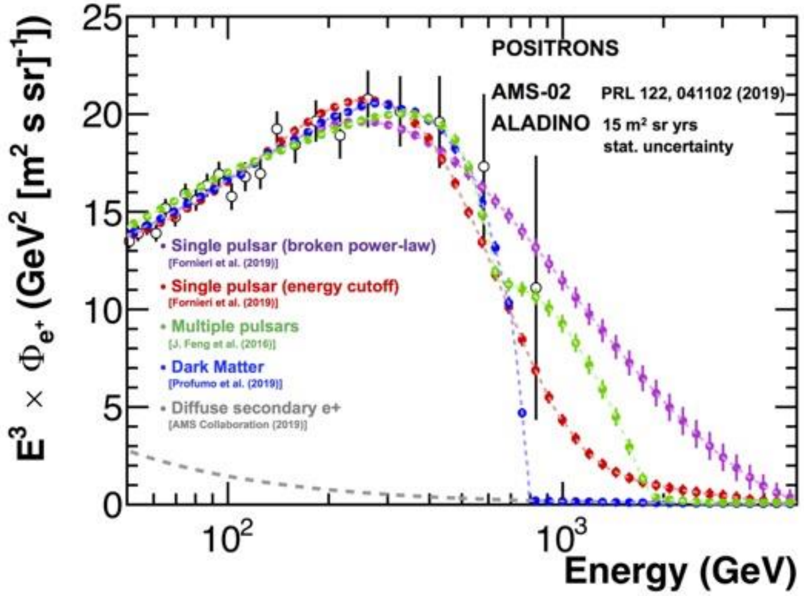

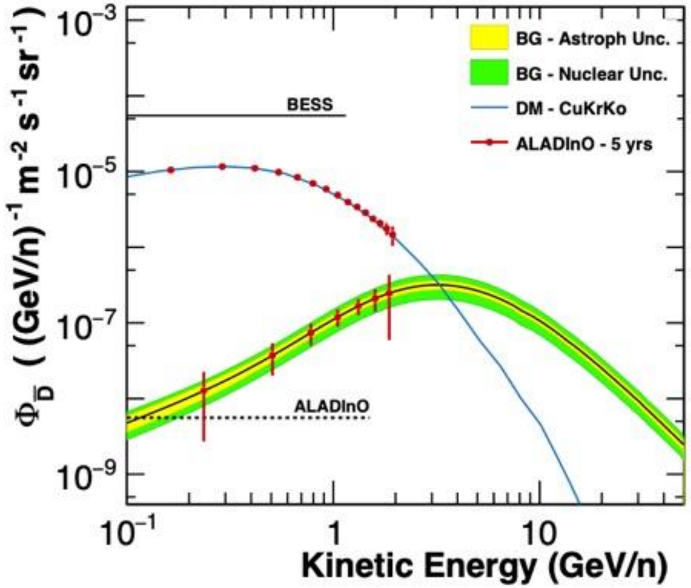

ALADInO Pathfinder: LAMP

Progressing in particle astrophysics with the
Antimatter Large Acceptance Detector In Orbit

ALADInO

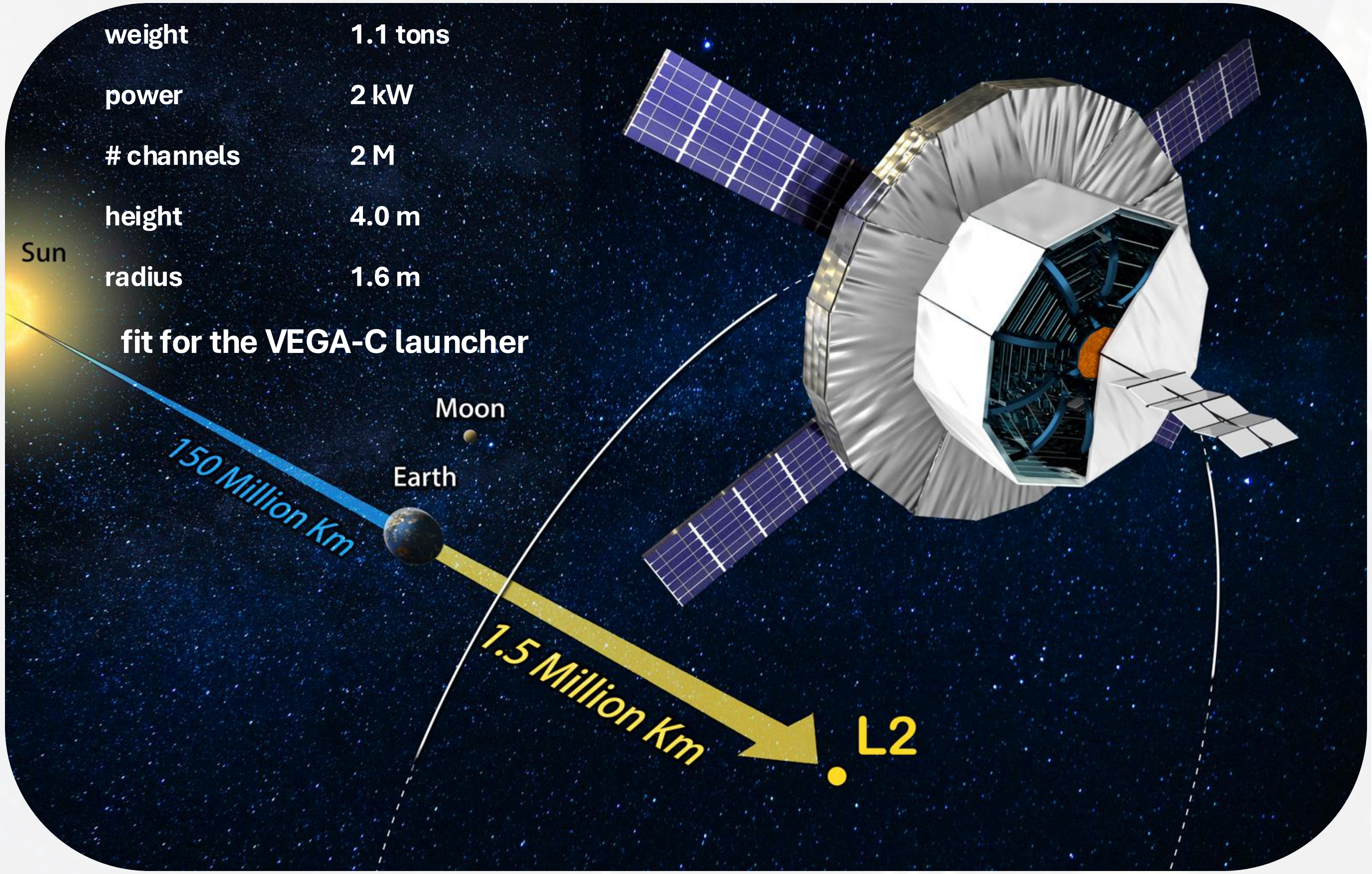

High Temperature Superconducting Magnetic Spectrometer in space
Acceptance > 10 m^2sr
Antimatter measurements up to 10 TeV
Established technologies for detection of particles in space

5-year operations in L2
Payload Weight < 6.5 t
Payload power consumption 3 kW
Compact volume (fits Ariane launcher)

Roadmap for mission opportunity
mid 2030s: ALADInO Pathfinder
mid 2040s: Operations in L2
by 2050: Unprecedented results

LAMP: Light Aladino-like Magnetic sPectrometer

ALADInO Pathfinder: LAMP

Large acceptance missions in Space

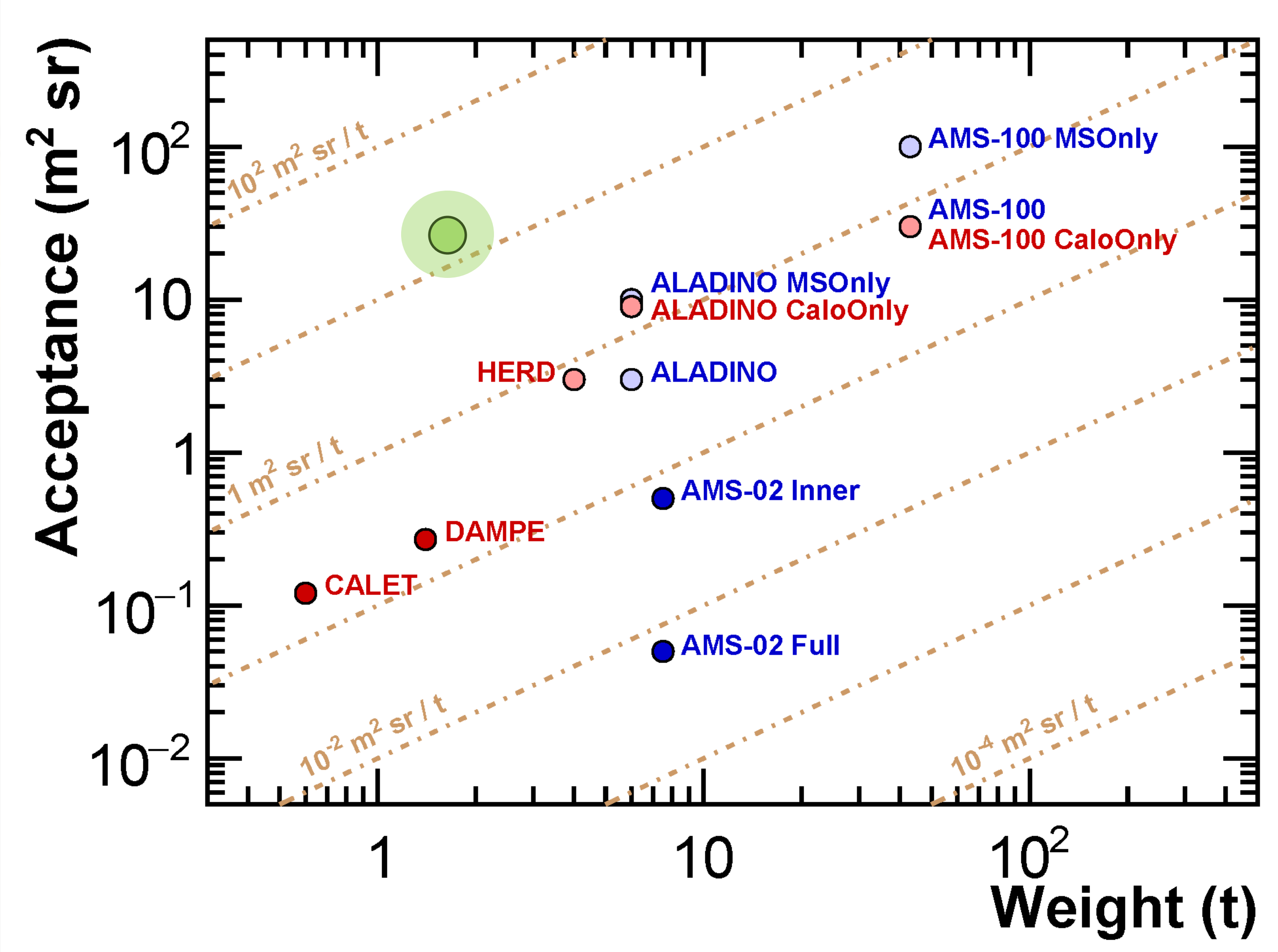

LAMP maintains the geometry of ALADInO, but **focuses on nuclear antimatter**. It features increased acceptance for the magnetic spectrometer and auxiliary detectors (TOF, Cherenkov), saving mass with a **calorimeter-free** approach.

- 2024 — Technology assessment
- 2028 — Balloon flight (validation of the HTS technology)
- 2030 — LAMP construction
- 2034 — **LAMP launch**

HTS magnet for space: the frontier

Agenzia Spaziale Italiana

UNIVERSITÀ DI TRENTO

CERN

INFN Istituto Nazionale di Fisica Nucleare

UNIVERSITÀ DEGLI STUDI DI MILANO

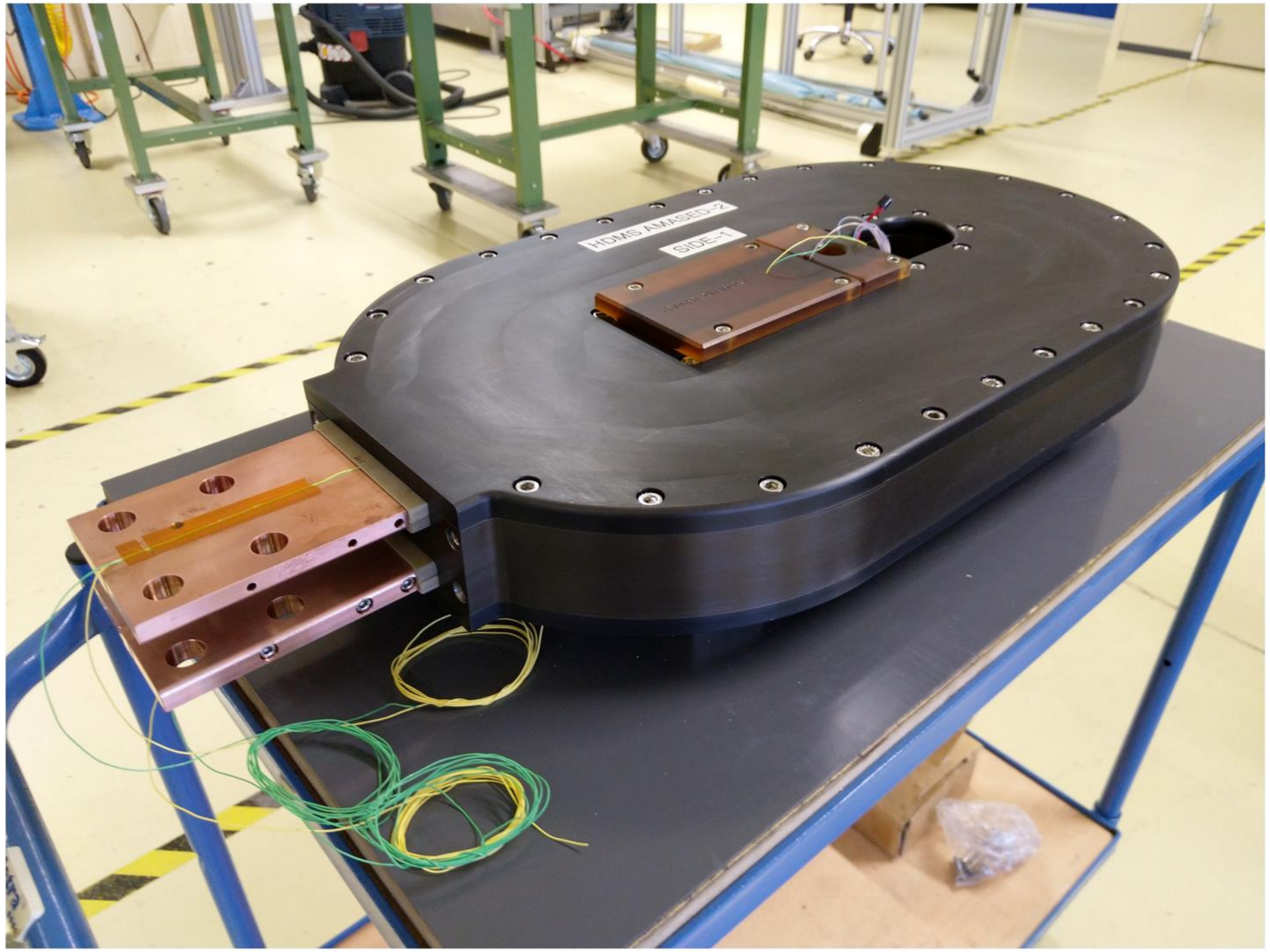

OPEN ACCESS
IOP Publishing Superconductor Science and Technology
Supercond. Sci. Technol. 33 (2020) 044012 (12pp) https://doi.org/10.1088/1361-6668/ab669b

Conceptual design of a high temperature superconducting magnet for a particle physics experiment in space

Magnus Dam[1], Roberto Battiston[2,3], William Jerome Burger[3], Rita Carpentiero[4], Enrico Chesta[1], Roberto Iuppa[2,3], Gijs de Rijk[1] and Lucio Rossi[1,5]

[1] CERN, European Organization for Nuclear Research, CH-1211 Geneva 23, Switzerland
[2] Department of Physics, University of Trento, I-38122 Trento TN, Italy
[3] TIFPA, Trento Institute for Fundamental Physics and Applications, I-38123 Povo TN, Italy
[4] ASI, Italian Space Agency, I-00133 Rome RM, Italy
[5] On leave from: Department of Physics, University of Milan, I-20133 Milano MI, Italy

E-mail: magnus.dam@cern.ch

Supercond. Sci. Technol. 33 044012 (2020)

IEEE TRANSACTIONS ON APPLIED SUPERCONDUCTIVITY, VOL. 32, NO. 4, JUNE 2022 4500105

Design and Modeling of AMaSED-2: A High Temperature Superconducting Demonstrator Coil for the Space Spectrometer ARCOS

Magnus Dam, William Jerome Burger, Rita Carpentiero, Enrico Chesta, Roberto Iuppa, Gijs de Rijk, and Lucio Rossi

IEEE TRANS. ON APPLIED SUPERCONDUCTIVITY, VOL. 32, NO. 4 (2022)

IOP Publishing Superconductor Science and Technology
Supercond. Sci. Technol. 36 (2023) 014007 (8pp) https://doi.org/10.1088/1361-6668/aca6ac

Manufacturing and testing of AMaSED-2: a no-insulation high-temperature superconducting demonstrator coil for the space spectrometer ARCOS

Magnus Dam[1,*], William Jerome Burger[2], Rita Carpentiero[3], Enrico Chesta[4], Roberto Iuppa[2,5], Glyn Kirby[4], Gijs de Rijk[6] and Lucio Rossi[1,7]

Supercond. Sci. Technol. 36, 014007 (2023)

INFN

Roberto Iuppa

Current Status of AMS Antideuteron Search

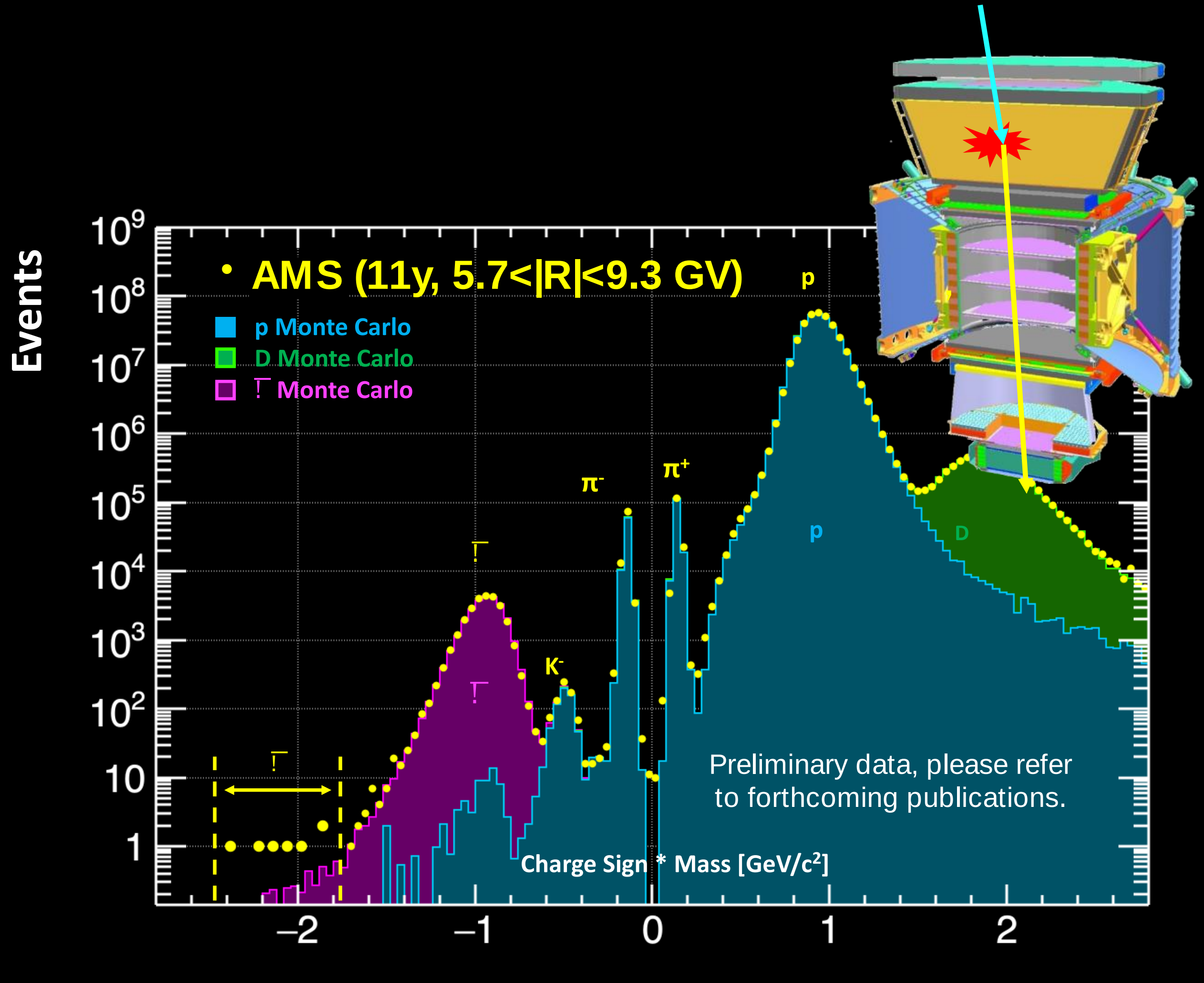

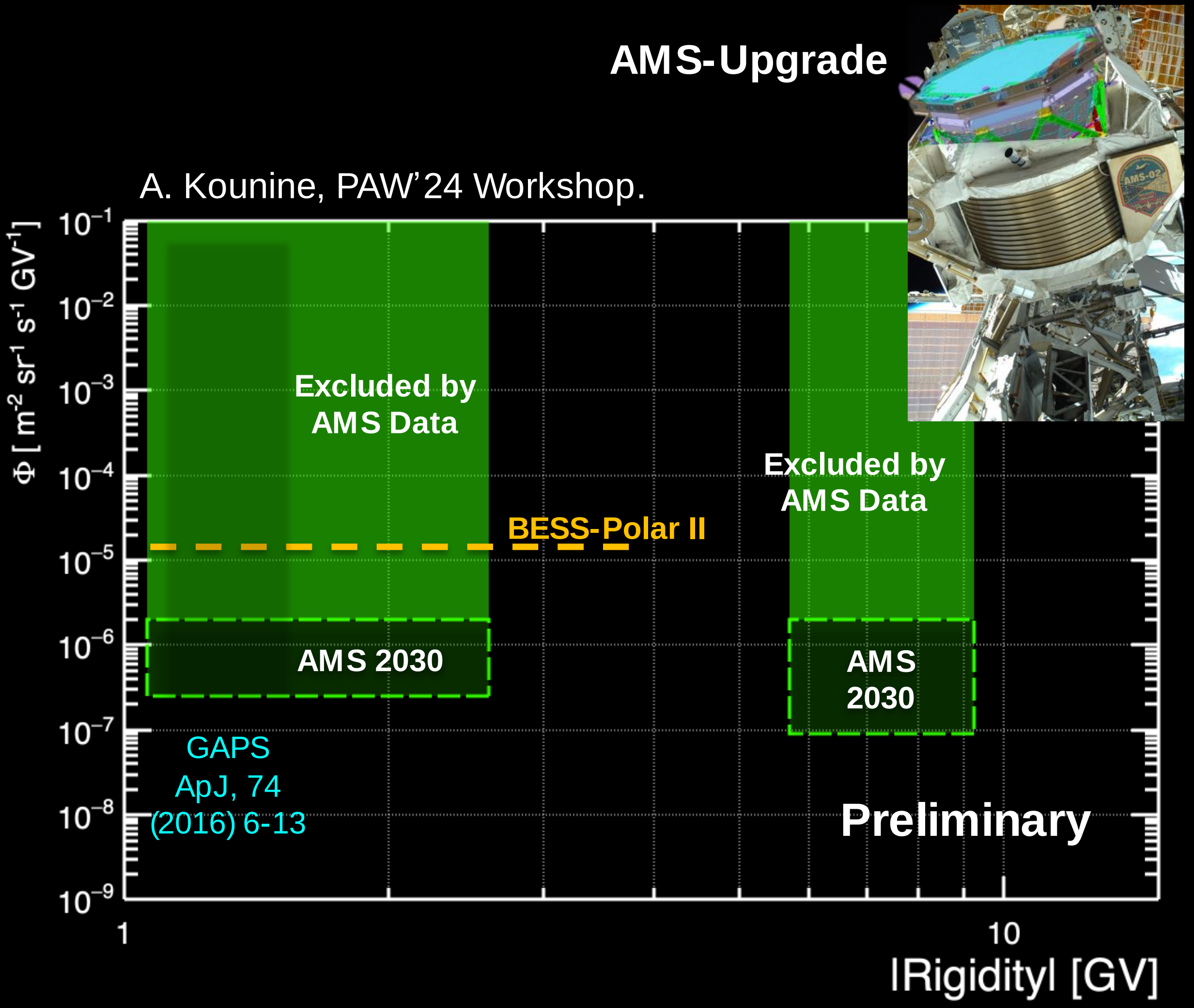

- Future AMS upgrade will provide additional measurement point to antideuterons.
- Improve analysis techniques, further MC study to better understand the background.

Anti Deuterons in Cosmic rays

Anti Deuterons have been proposed as an almost background free channel for Dark Matter indirect detection

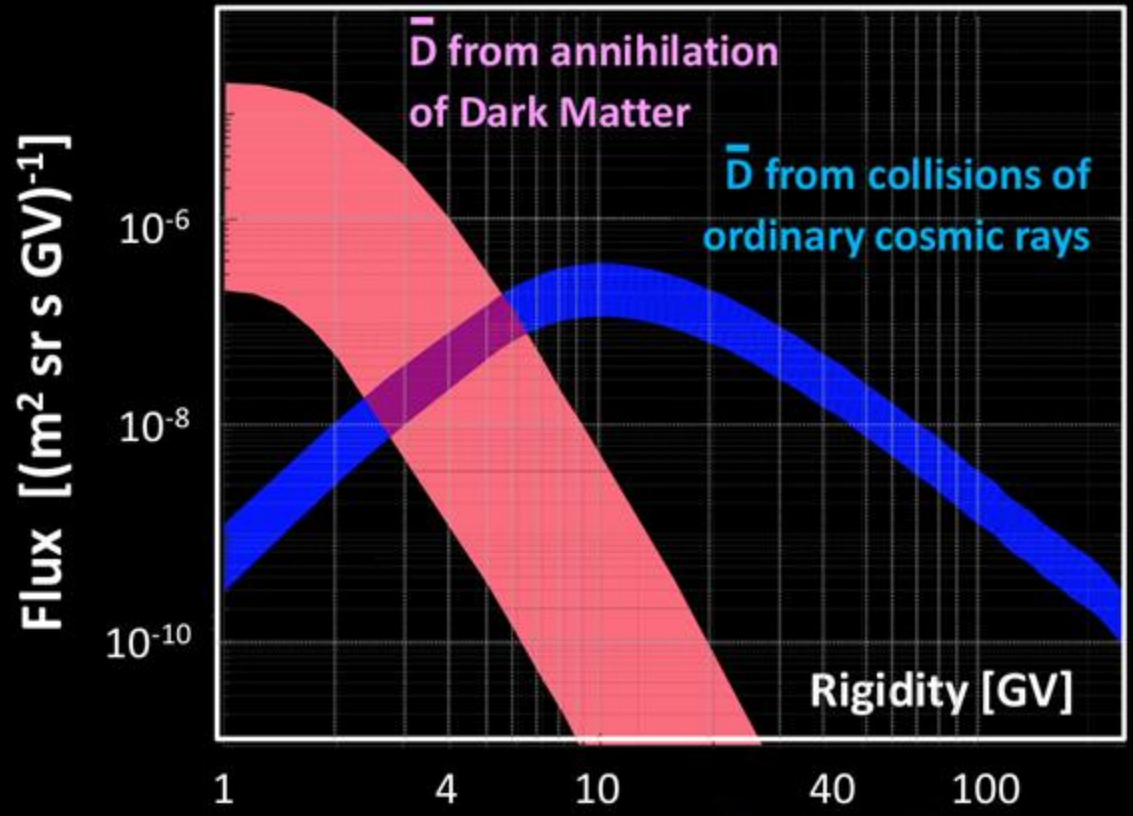

■ Dark Matter model: F. Donato et al., Phys. Rev. D, 62 (2000) 043003

■ Collisions of CR model K. Blum et al., Phys. Rev. D 96 (2017) 103021)

The Anti Deuterons Flux is $< 10^{-4}$ of the Antiproton Flux.

Additional background rejection

Established mission

GAPS

Idea for the Future

ADHD

Anti Deuteron Helium Detector

Helium metastable states

-In matter lifetime of stopped anti-p is ~ps
-In liquid/gas He delayed annihilation: few μs (~3.3% of the anti-p)(discovered @ KEK in 1991)

Observed also for K^-, π^- and expected for anti-D

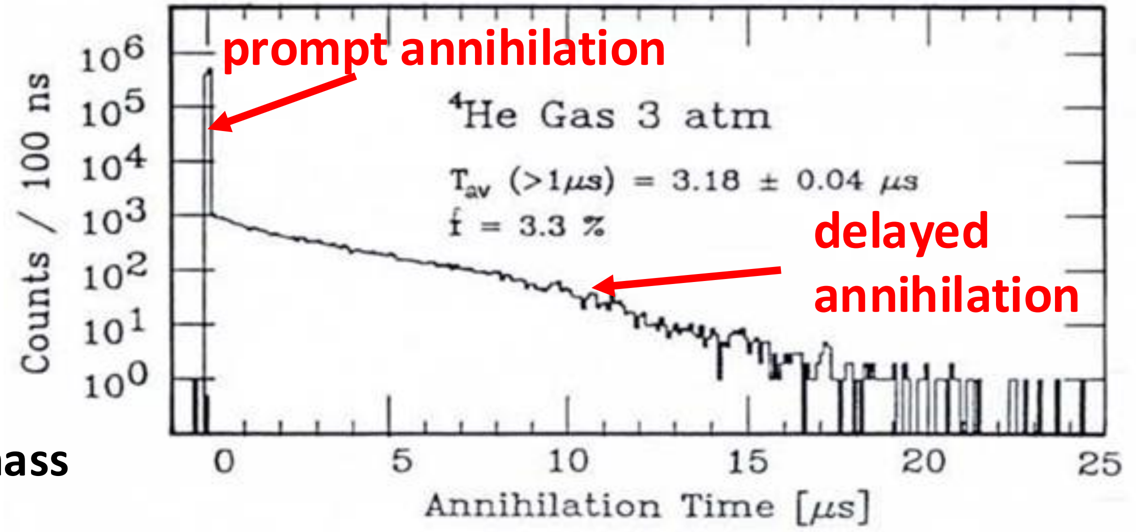

ASACUSA @ CERN use He metastable states to measure anti-P mass

K^- PRL 63 (1989) 1590

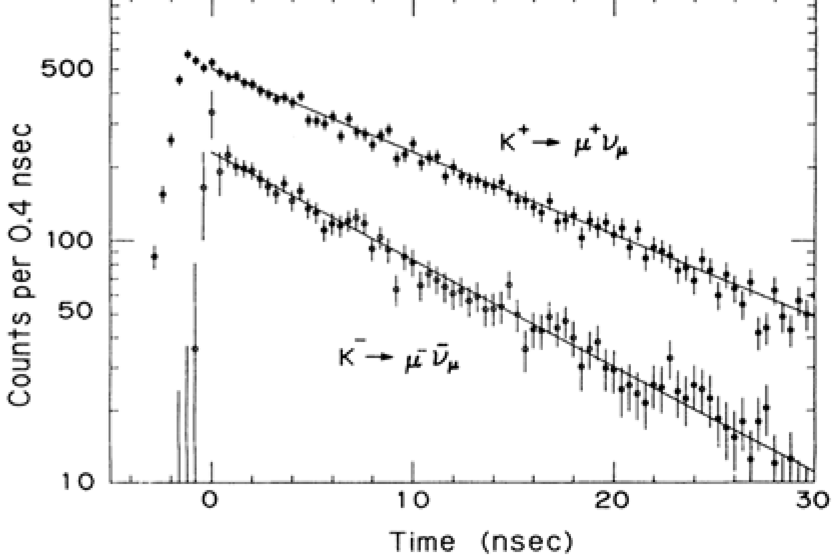

π^- PhysRevA 45(1992)6202

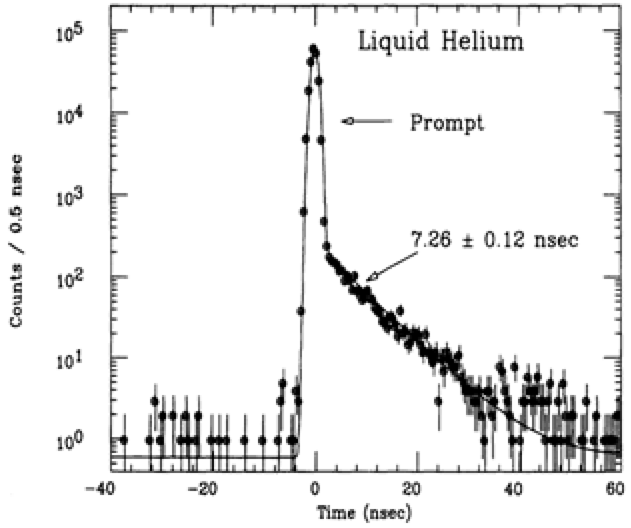

anti-P PRL 67 (1991) 1246

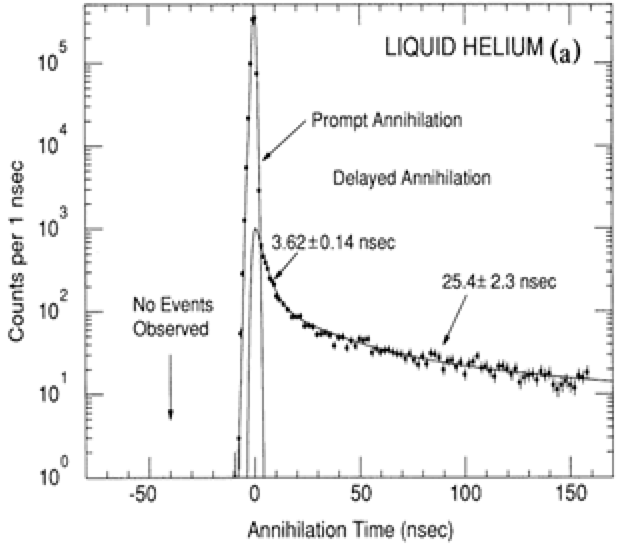

a signature for Z=-1 antimatter captures in He is a ~μs delayed energy release

Anti-Deuteron Helium Detetector (ADHD) Particle Identification

Helium pressurized vessel
Surrounded by Scintillating TOF

A particle enter ADHD and stops inside

Energetic or fragmenting particle produces additional scintillation

Anti -p forms an exotic He atom DELAYED ANNH.

Anti- D
DELAYED ANNH.
more energy and tracks

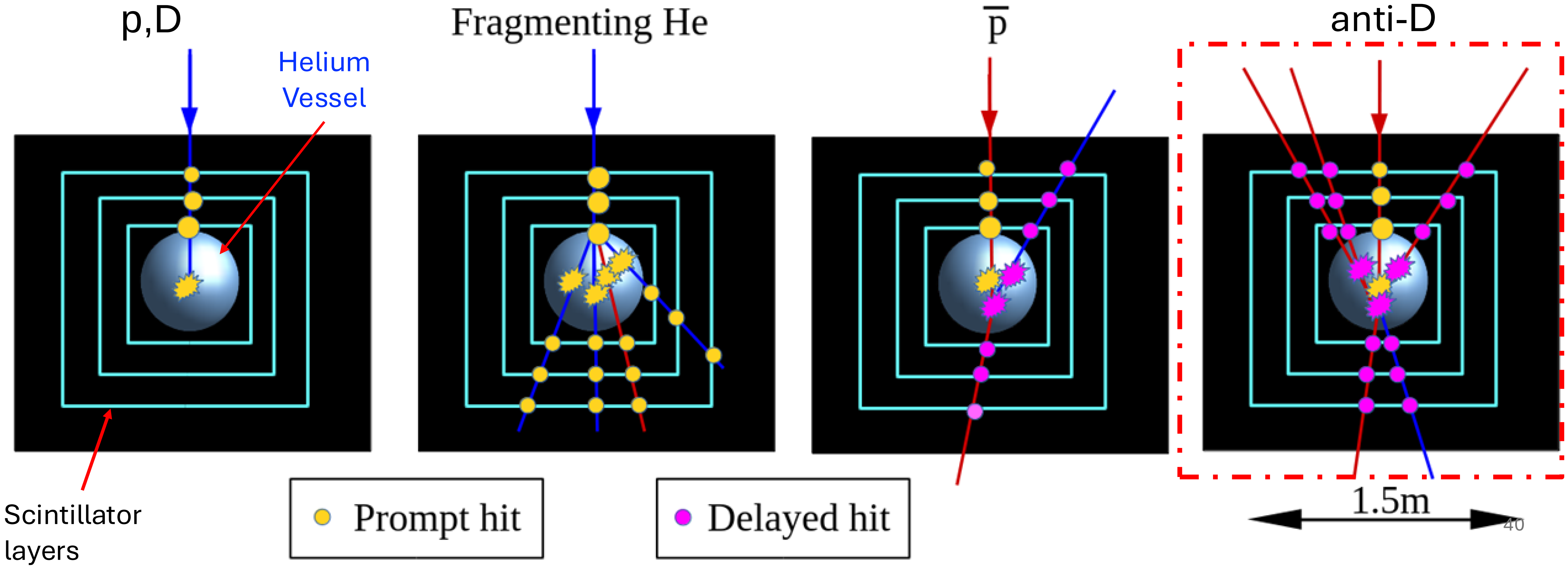

ADHD: Typical signals in Helium

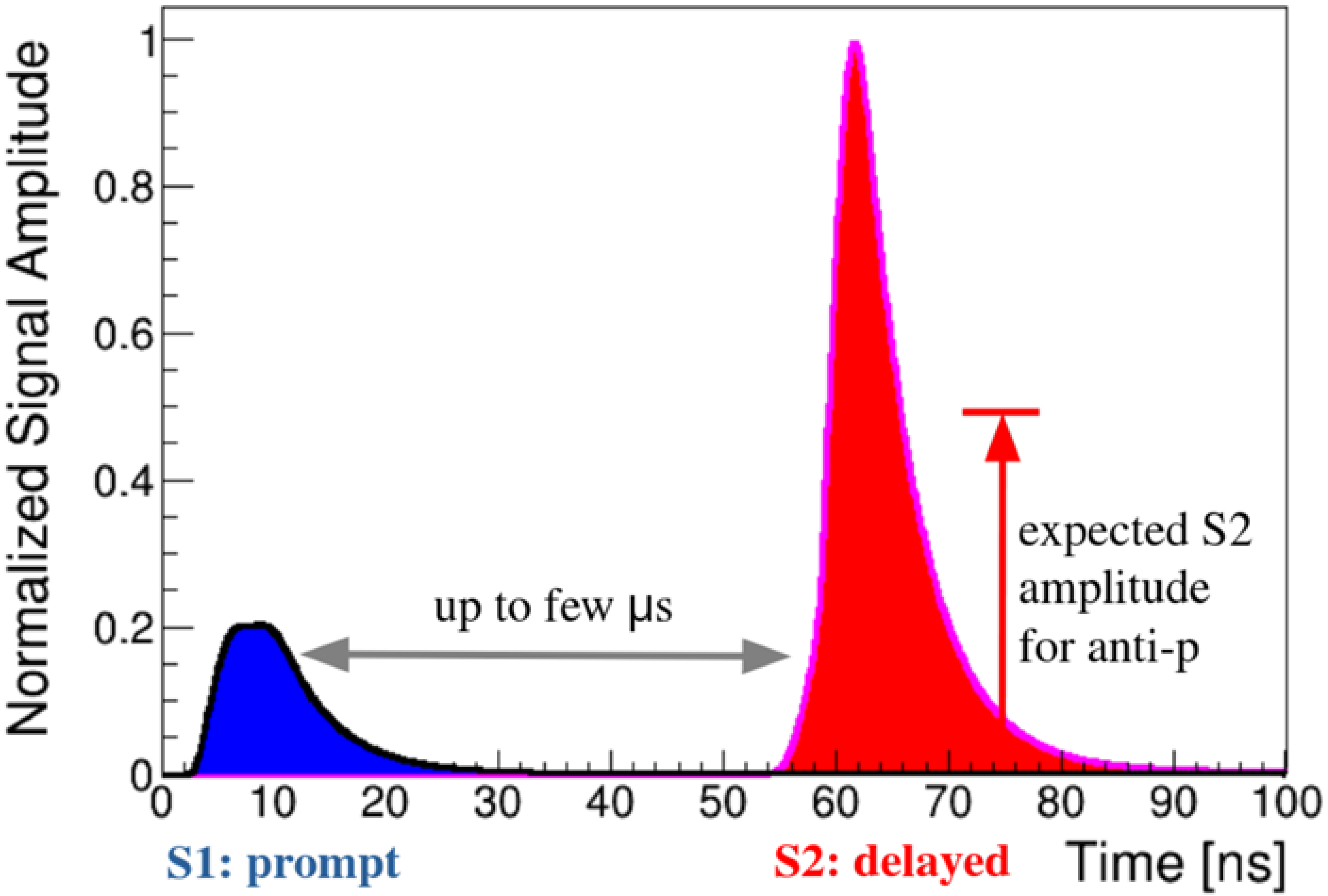

kinetic energy
(- energy loss)

Charged π
Typ. S2 > S1
S2 and Ek not related

anti-p/anti-D separation: prompt signal S1

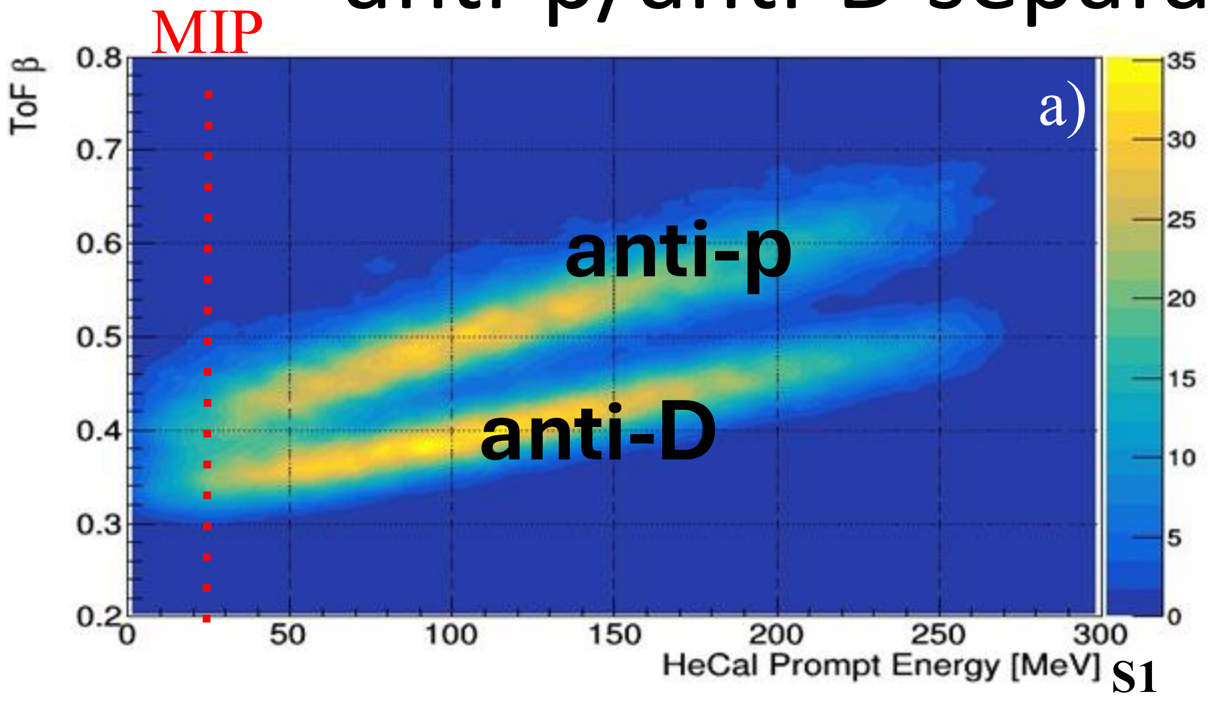

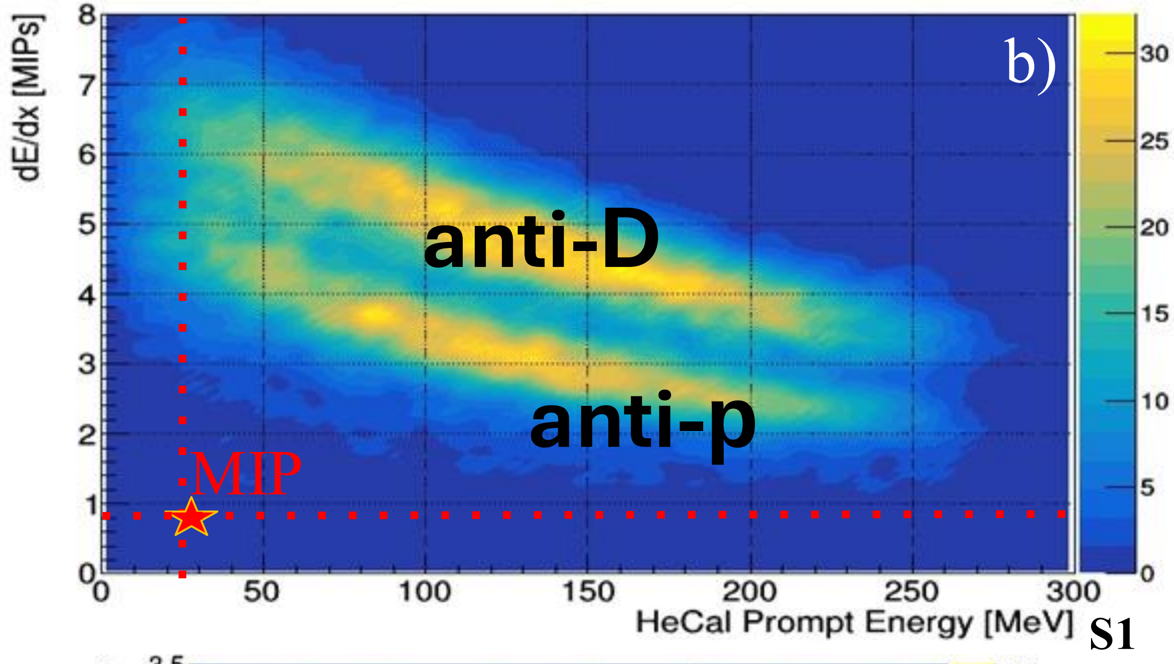

ToF (30cm baseline & 4mm thickness):
β resolution 5% => $\sigma_{x/y}$ ~few cm & σ_T<0.1ns
- ToF Energy resolution: 10%
- He Calorimeter Energy resolution: 10%

Parametrization of (**β** vs *E)* & *(dE/dx vs E)*
2 "independent" classifiers
that can be combined to obtain an overall
"Prompt signal classifier"

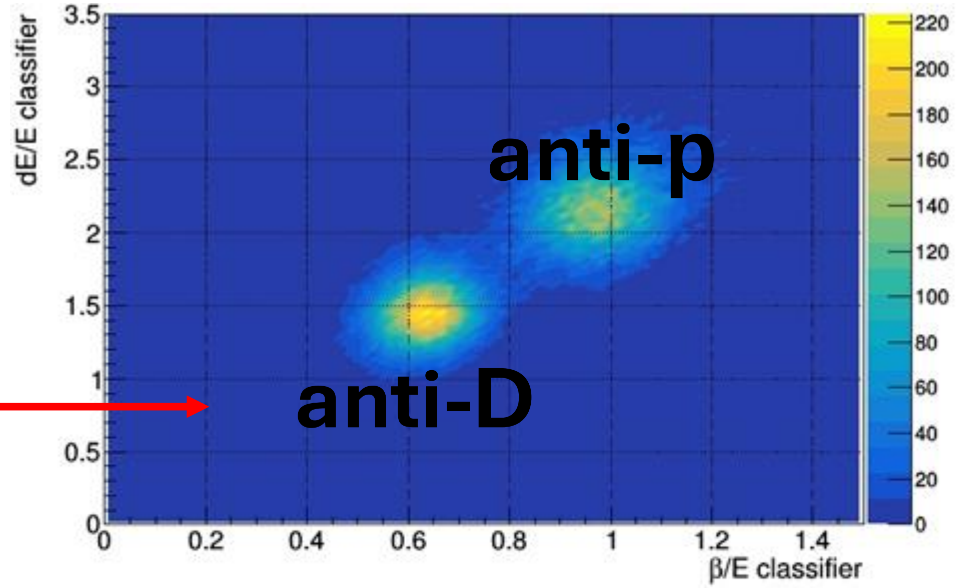

42

ADHD: anti-p/anti-D separation: delayed signal S2

delayed signal amplitude is independent from Ekin: ~3 charged pion/antinucleon

-ToF delayed activity classifier = #ToF delayed hits ⊕ ToF delayed energy

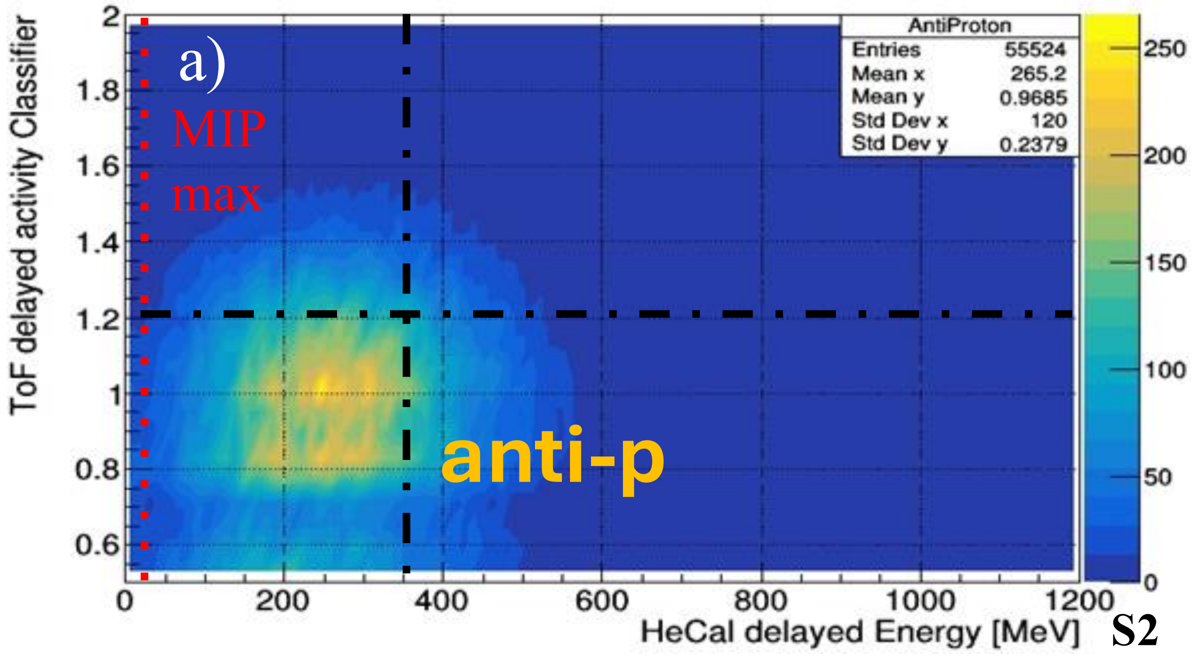

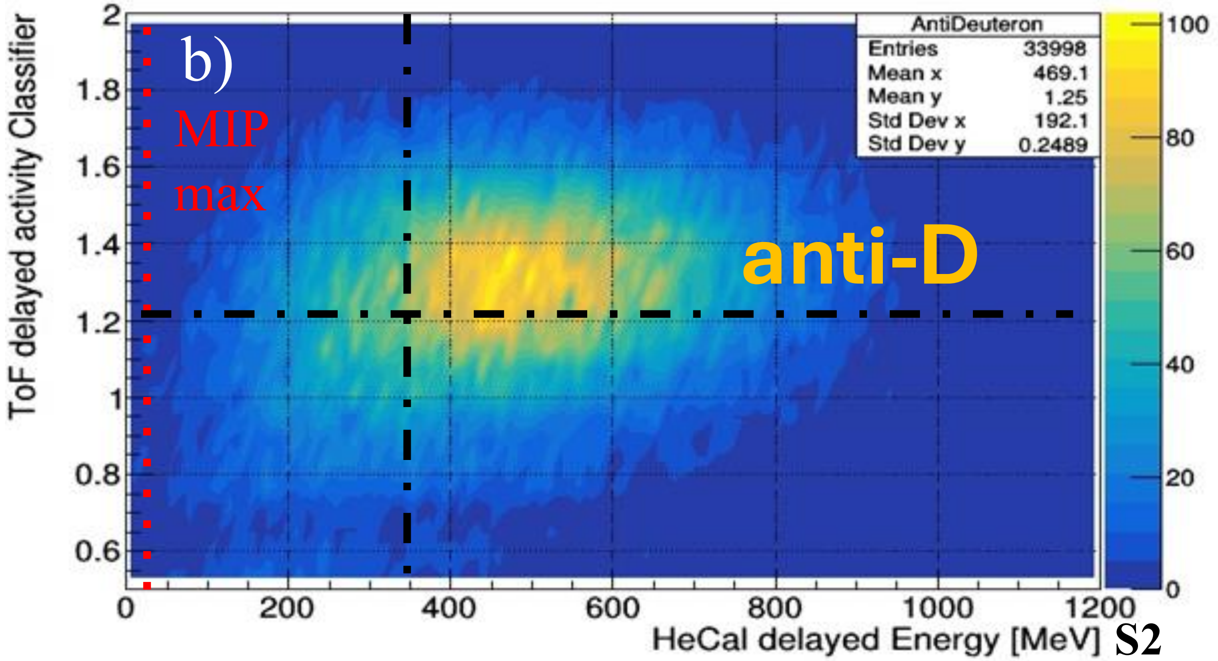

prompt signal classifier +
delayed signal classifier
possibility to detect 1anti-D/1000anti-p
(anti-p rejection 1500 @ 65% anti-D efficiency)

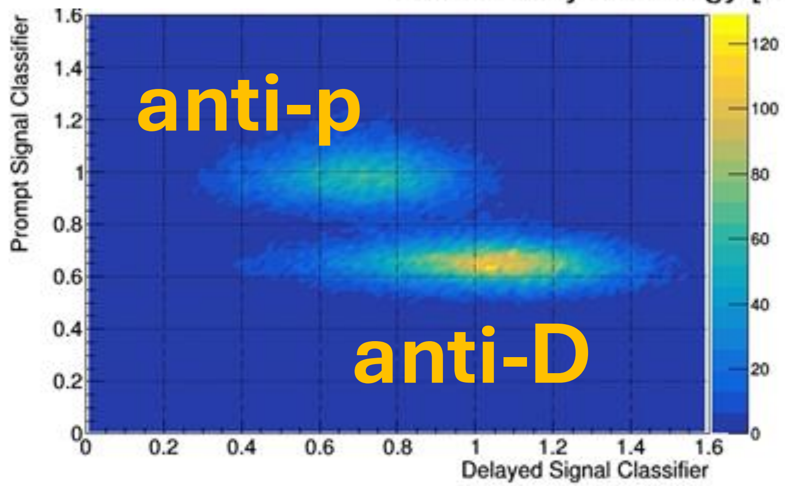

43

ADHD: Advanced prototype development status

Pressurized Helium Scintillating Calorimeter for AntiMatter Identification

F. Nozzoli, L. Ricci, F. Rossi, P. Spinnato, E.Verroi, P. Zuccon

Finanziato dall'Unione europea NextGenerationEU

Ministero dell'Università e della Ricerca

Segretariato Generale

Direzione Generale della Ricerca

PRIN: PROGETTI DI RICERCA DI RILEVANTE INTERESSE NAZIONALE – Bando 2022
Prot. 2022LLCPMH

https://www.tifpa.infn.it/projects/prin2022-phescami/

Instruments 2024, 8(1), 3;
https://doi.org/10.3390/instruments8010003

Grant to develop a ADHD prototype using a commercial COPV Type-4 tank for automotive

Finanziato dall'Unione europea NextGenerationEU | Ministero dell'Università e della Ricerca | Italiadomani PIANO NAZIONALE DI RIPRESA E RESILIENZA | UNIVERSITÀ DI TRENTO | INFN

Summary

- Cosmic rays are in a precision era
- AMS-02 will continue the measurement of all the nuclei up to Iron and isotopes at least up Nitrogen
- Calorimetric experiments like DAMPE and CALET are extending the measurement at higher energies, and possibly HERD will give in the future important new measurements
- AMS-02 with the upgrade will provide an extended and more accurate measurement of the elementary particle fluxes, especially anti-p and positrons
- New magnetic spectrometer experiments would be able to investigate the positron and anti-p spectra and search for anti-matter in the CR
- The search for low energy anti-deuterons is also a very promising channel for DM.

BACKUP SLIDES

HTS magnet for space: the frontier

Agenzia Spaziale Italiana | UNIVERSITÀ DI TRENTO | CERN | INFN Istituto Nazionale di Fisica Nucleare | UNIVERSITÀ DEGLI STUDI DI MILANO

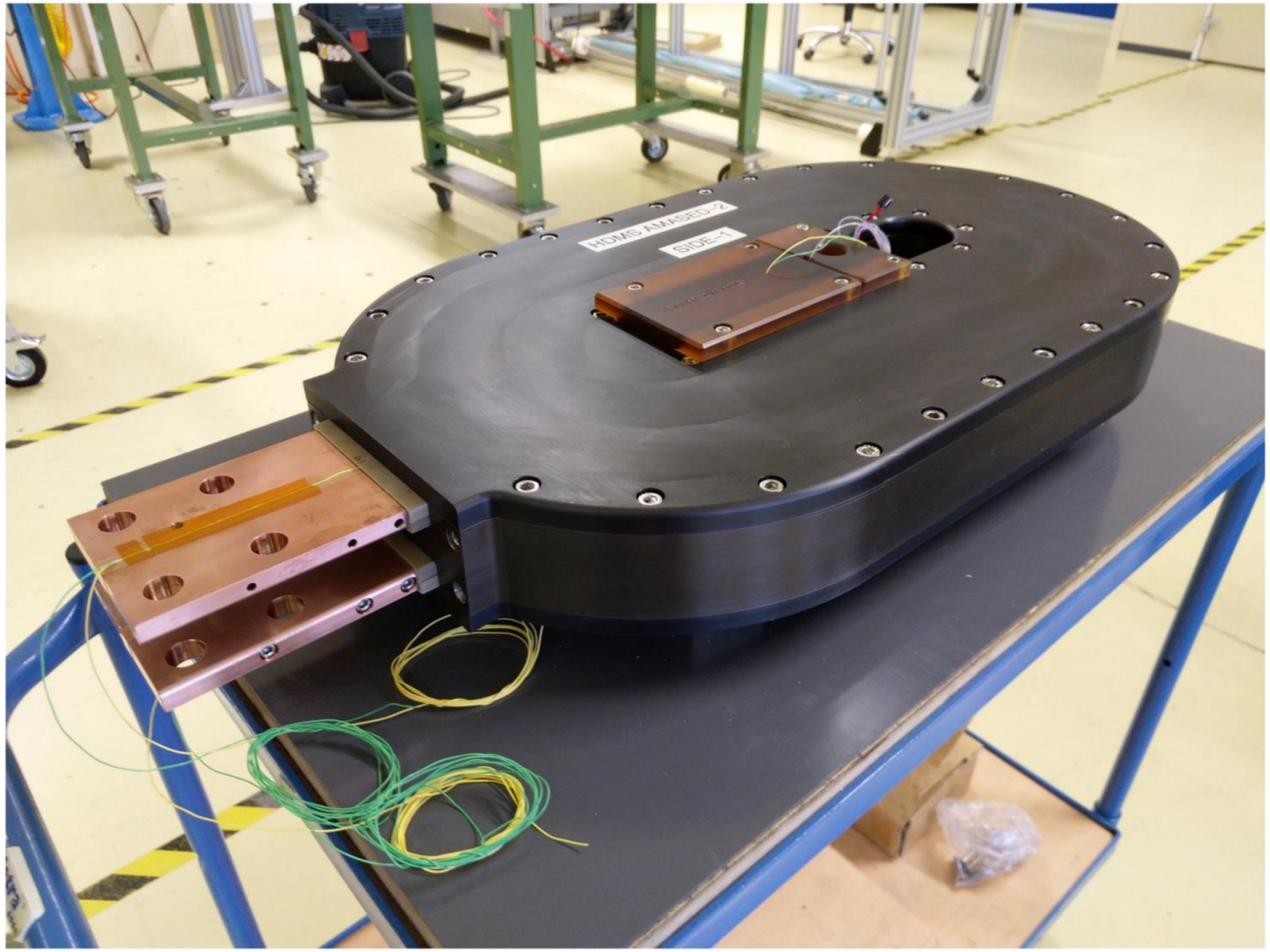

OPEN ACCESS
IOP Publishing — Superconductor Science and Technology
Supercond. Sci. Technol. 33 (2020) 044012 (12pp) — https://doi.org/10.1088/1361-6668/ab669b

Conceptual design of a high temperature superconducting magnet for a particle physics experiment in space

Magnus Dam[1], Roberto Battiston[2,3], William Jerome Burger[3], Rita Carpentiero[4], Enrico Chesta[1], Roberto Iuppa[2,3], Gijs de Rijk[1] and Lucio Rossi[1,5]

[1] CERN, European Organization for Nuclear Research, CH-1211 Geneva 23, Switzerland
[2] Department of Physics, University of Trento, I-38122 Trento TN, Italy
[3] TIFPA, Trento Institute for Fundamental Physics and Applications, I-38123 Povo TN, Italy
[4] ASI, Italian Space Agency, I-00133 Rome RM, Italy
[5] On leave from: Department of Physics, University of Milan, I-20133 Milano MI, Italy

E-mail: magnus.dam@cern.ch

Supercond. Sci. Technol. 33 044012 (2020)

IEEE TRANSACTIONS ON APPLIED SUPERCONDUCTIVITY, VOL. 32, NO. 4, JUNE 2022 — 4500105

Design and Modeling of AMaSED-2: A High Temperature Superconducting Demonstrator Coil for the Space Spectrometer ARCOS

Magnus Dam, William Jerome Burger, Rita Carpentiero, Enrico Chesta, Roberto Iuppa, Gijs de Rijk, and Lucio Rossi

IEEE TRANS. ON APPLIED SUPERCONDUCTIVITY, VOL. 32, NO. 4 (2022)

IOP Publishing — Superconductor Science and Technology
Supercond. Sci. Technol. 36 (2023) 014007 (8pp) — https://doi.org/10.1088/1361-6668/aca6ac

Manufacturing and testing of AMaSED-2: a no-insulation high-temperature superconducting demonstrator coil for the space spectrometer ARCOS

Magnus Dam[1,*], William Jerome Burger[2], Rita Carpentiero[3], Enrico Chesta[4], Roberto Iuppa[2,5], Glyn Kirby[4], Gijs de Rijk[6] and Lucio Rossi[1,7]

Supercond. Sci. Technol. 36, 014007 (2023)

UNIVERSITAS STUDIORUM ATHESINA — INFN

Roberto Iuppa

Conductor and cable configuration

Roberto Iuppa

SuperPower 2G HTS tape

Description	Value	Unit
Tape width	12	mm
Tape thickness	97	µm
Hastelloy substrate thickness	50	µm
ReBCO thickness	1.6	µm
Silver thickness	3.8	µm
Copper stabilizer thickness	40	µm
I_c at 77 K, self-field	0.4	kA

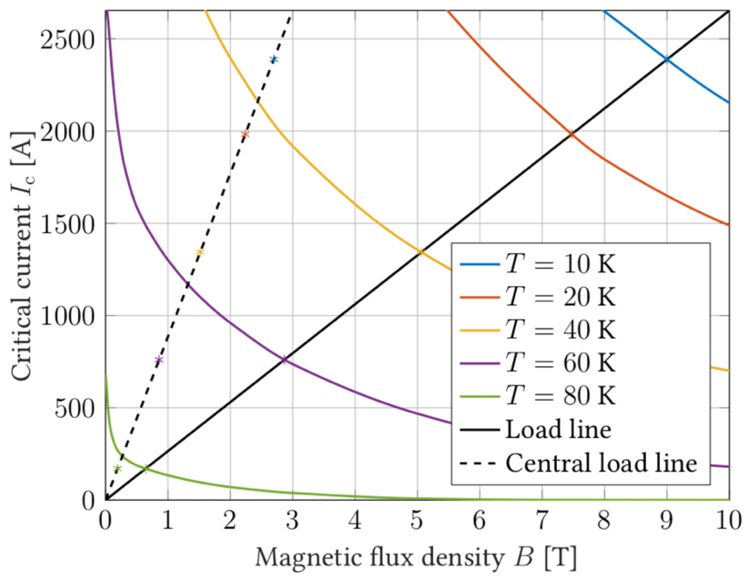

Cable configuration

- No-insulation winding technique
- Two-tape stack
- Dry wound with first and last turns soldered

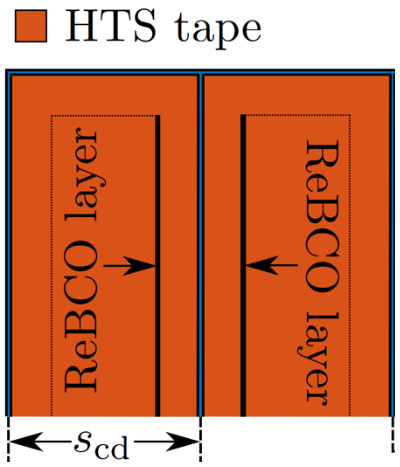

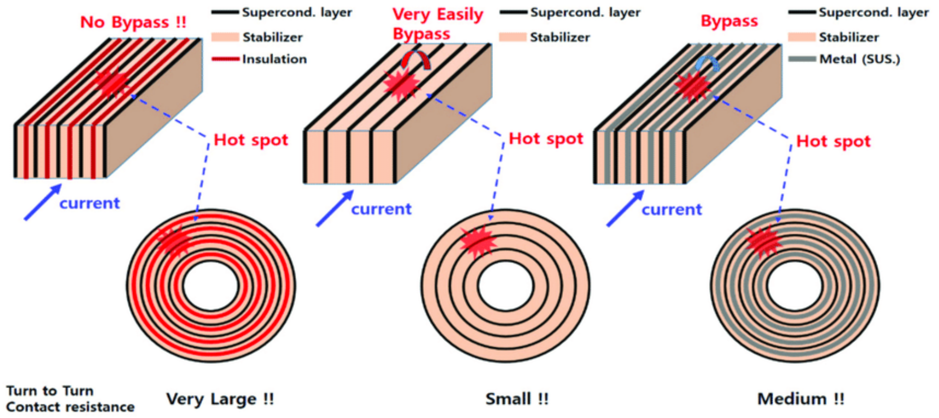

ins. winding   no ins. winding   metallic ins. winding

Appl. Sci. 2021, 11(7), 3074

Magnetic critical current measurements

[Supercond. Sci. Technol. 36 (2023) 014007]

Roberto Iuppa

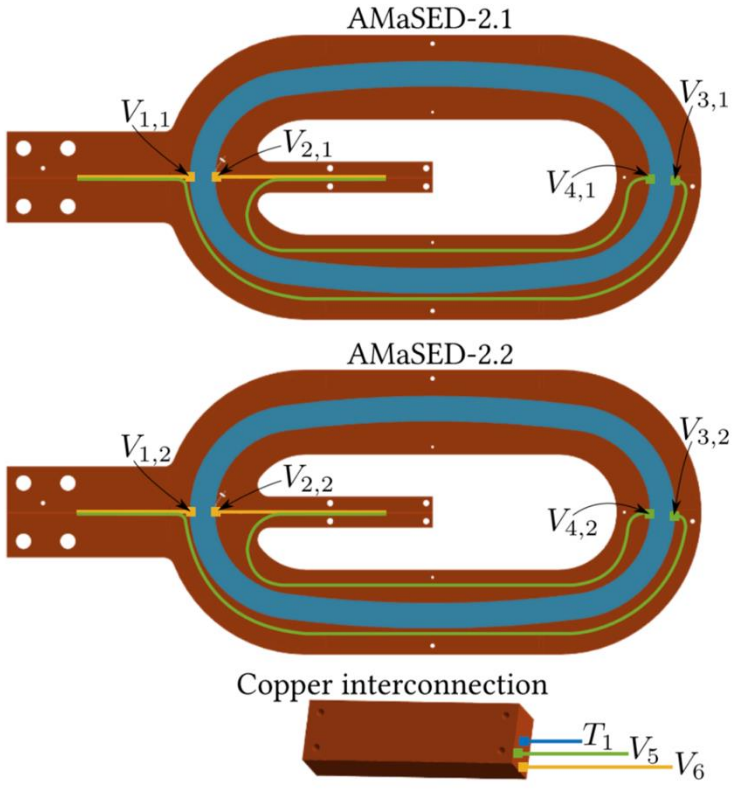

Figure 3. Locations of temperature sensor and voltage taps on coil assemblies and interconnection block.

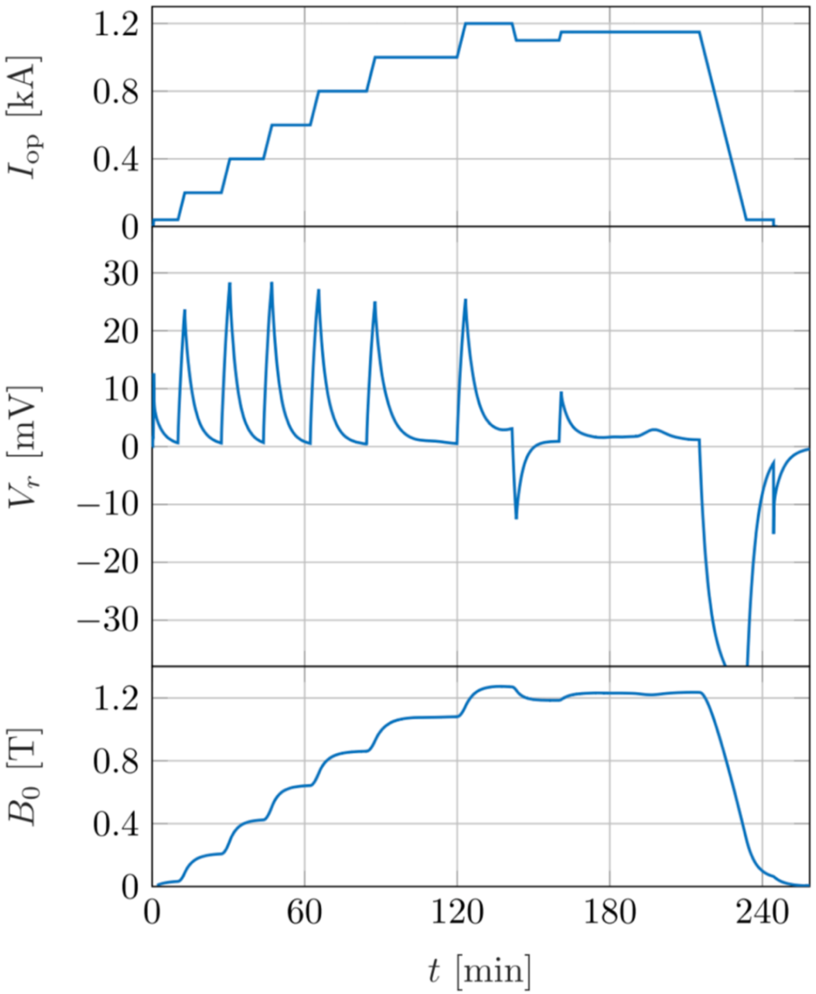

Figure 4. Measurement for $T_{op} = 40\,K$ where we increased the operating current I_{op} in steps until we approached the magnet critical current I_{mc}.

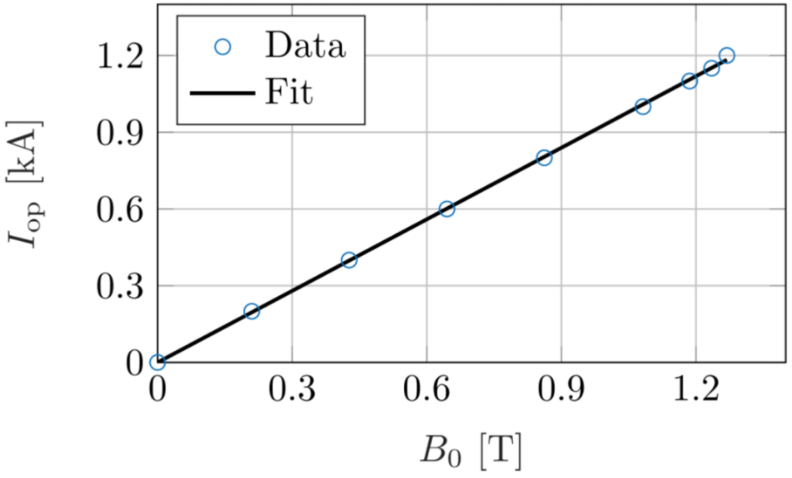

Figure 5. The operating current I_{op} as a function of the convergence value of the central magnetic flux density B_0 for $T_{op} = 40\,K$.

He VUV emission

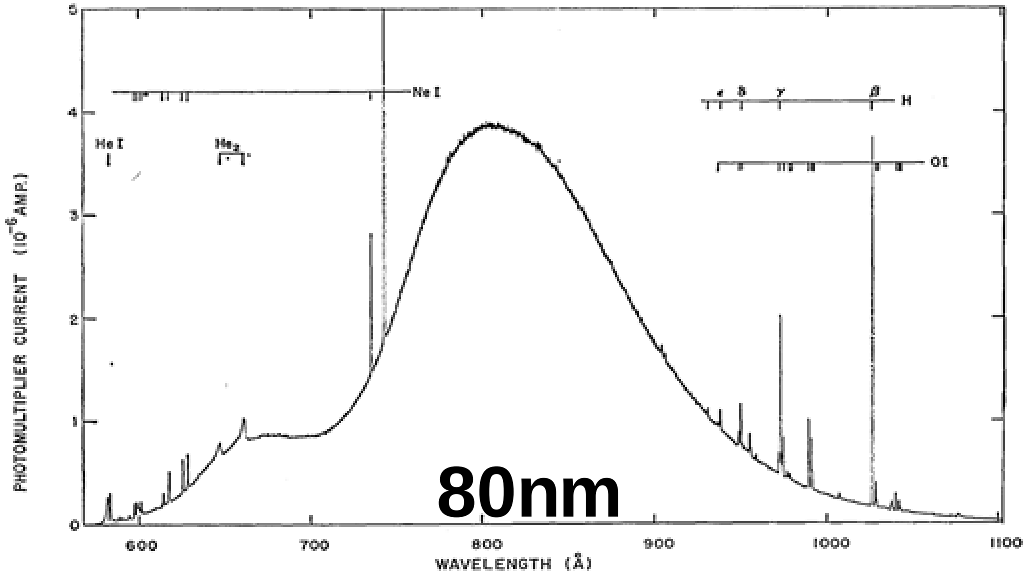

Hard to extract VUV from the tank. It is absorbed from the walls and we need an optical window for 400bar

step1: Para-TerPheny (PTP) deposited on the tank walls shift from 80 nm to 350 nm

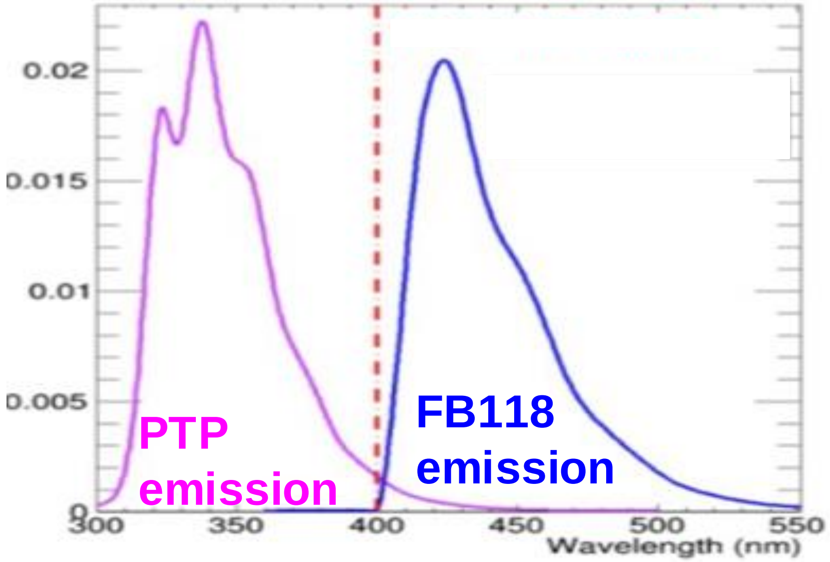

2 stages WLS: similar to the one developed for LAr (127nm) in DUNE X-Arapuca: C.Brizzolari 2021 [JINST 16 P09027]

step2: MMA central fiber doped with BBT (FB118 developed by G2P Rovereto) shift from 350 nm to 430 nm